University of Alberta

The Effects of Intercellular Adhesion Molecule (ICAM-1) Ligation on Tumor Cell MUC1 Tyrosine Phosphorylation

by

Danny Chi Ho Au

A thesis submitted to the Faculty of Graduate Studies and Research in partial fulfillment of the requirement for the degree of Master of Science

Department of Laboratory Medicine and Pathology

Edmonton, Alberta

Spring, 2005

0-494-08190-2

Library and Archives Canada

Published Heritage Branch

395 Wellington Street
Ottawa ON K1A 0N4
Canada

Bibliothèque et Archives Canada

Direction du Patrimoine de l'édition

395, rue Wellington
Ottawa ON K1A 0N4
Canada

Your file *Votre référence*
ISBN:
Our file *Notre reference*
ISBN:

NOTICE:
The author has granted a non-exclusive license allowing Library and Archives Canada to reproduce, publish, archive, preserve, conserve, communicate to the public by telecommunication or on the Internet, loan, distribute and sell theses worldwide, for commercial or non-commercial purposes, in microform, paper, electronic and/or any other formats.

The author retains copyright ownership and moral rights in this thesis. Neither the thesis nor substantial extracts from it may be printed or otherwise reproduced without the author's permission.

AVIS:
L'auteur a accordé une licence non exclusive permettant à la Bibliothèque et Archives Canada de reproduire, publier, archiver, sauvegarder, conserver, transmettre au public par télécommunication ou par l'Internet, prêter, distribuer et vendre des thèses partout dans le monde, à des fins commerciales ou autres, sur support microforme, papier, électronique et/ou autres formats.

L'auteur conserve la propriété du droit d'auteur et des droits moraux qui protège cette thèse. Ni la thèse ni des extraits substantiels de celle-ci ne doivent être imprimés ou autrement reproduits sans son autorisation.

In compliance with the Canadian Privacy Act some supporting forms may have been removed from this thesis.

While these forms may be included in the document page count, their removal does not represent any loss of content from the thesis.

Conformément à la loi canadienne sur la protection de la vie privée, quelques formulaires secondaires ont été enlevés de cette thèse.

Bien que ces formulaires aient inclus dans la pagination, il n'y aura aucun contenu manquant.

Canada

Abstract:

MUC1 is a mucin family member. Its aberrant expression in a minority of human breast cancers correlates with poor prognosis and nodal metastases. The cytoplasmic domain of MUC1 can be phosphorylated and serve as docking sites for proteins like β-catenin, Grb2, and Src, suggesting a signalling role for MUC1 during tumor progression. However, the physiological stimulus responsible for inducing MUC1 tyrosine phosphorylation is unknown. Our lab was the first to show that the MUC1 extracellular core domain could serve as a ligand for ICAM-1. Also, our lab has recently discovered that the MUC1-ICAM-1 interaction was crucial for facilitating *in vitro* tumor cell transendothelial migration and induction of tumor cell calcium ion (Ca^{2+}) oscillation. It was found in this study that both ICAM-1 and mock stimulations for 1 min with NIH3T3 transfectants could induce significant MUC1 tyrosine phosphorylation of tumor cells under experimental conditions used in tumor Ca^{2+} oscillation assays.

Table of Contents

		Page
Chapter One: Introduction		
1.1.	Background	2
1.2.	Tumor Metastasis	
1.2.1.	Introduction	5
1.2.2.	Tumor Pre-Extravasation Events	8
1.2.3.	Tumor Extravasation	11
1.3.	The Human Mucin MUC1	
1.3.1.	MUC1 Expression	16
1.3.2.	MUC1 Extracellular Domain	17
1.3.2.1.	MUC1 Extracellular Domain Function	20
1.3.3.	MUC1 Transmembrane and Cytoplasmic Domains	24
1.3.3.1.	MUC1 Cytoplasmic Domain Function	25
1.4.	The Human Intercellular Adhesion Molecule-1	
1.4.1.	ICAM-1 Expression	30
1.4.2.	ICAM-1 Structure	31
1.4.3.	ICAM-1 Function	33
1.5.	Experimental Rationale and Hypothesis	34
Chapter Two: Experimental Materials and Methods		
2.1.	Optimization of Western Blot and Immunoprecipitation	
2.1.1.	Immunoblot for MUC1 with B27.29 and α-CT2 Monoclonal Antibodies	38

2.1.2. Immunoprecipitation of MUC1 With B27.29 and α-CT2 Monoclonal Antibodies 44

2.1.3. CT2 Peptide-Block of α-CT2 Antibody 47

2.2. Optimization of Co-Culture Conditions

2.2.1. Detecting MUC1 Tyrosine Phosphorylation Under Experimental Conditions Used in Tumor Cell Transmigration Assays 50

2.2.2. Epidermal Growth Factor Stimulation and Detecting MUC1 Tyrosine Phosphorylation of Tumor Cells 55

2.2.3. Detecting MUC1 Tyrosine Phosphorylation Under Experimental Conditions Used in Tumor Cell Calcium Ion Oscillation Assays 59

2.2.4. Alkaline Phosphatase Treatment of Western Blot Membranes From MUC1-ICAM-1 Co-culturing Experiments 63

Chapter Three: Experimental Results

3.1. Optimization of Western Blot and Immunoprecipitation

3.1.1. Immunoblot for MUC1 with B27.29 and α-CT2 Monoclonal Antibodies 67

3.1.2. Immunoprecipitation of MUC1 With B27.29 and α-CT2 Monoclonal Antibodies 76

3.1.3. CT2 Peptide-Block of α-CT2 Antibody 80

3.2. Optimization of Co-Culture Conditions

3.2.1. Detecting MUC1 Tyrosine Phosphorylation Under Experimental Conditions Used in Tumor Cell Transmigration Assays 83

3.2.2. Epidermal Growth Factor Stimulation and Detecting MUC1 Tyrosine Phosphorylation of Tumor Cells 89

3.2.3. Detecting MUC1 Tyrosine Phosphorylation Under Experimental Conditions Used in Tumor Cell Calcium Ion Oscillation Assays 93

3.2.4. Alkaline Phosphatase Treatment of Western Blot Membranes From MUC1-ICAM-1 Co-culturing Experiments 99

Chapter Four: Discussion and Conclusion

4.1. Introduction 103

4.2. Review and Discussion of Experimental Data 104

4.3. Conclusion 121

Bibliography 122

Appendix A: Comparison of RIPA and Brij-97 Lysis Buffers

A.1. Objective 132

A.2. Materials and Methods 132

A.3. Results 134

A.4. Discussion and Conclusion 136

Appendix B: Differential Cell Density and MUC1 Detection

B.1. Objective 139

B.2. Materials and Methods 139

B.3. Results 141

B.4. Discussion and Conclusion 143

Appendix C: Sodium Orthovanadate Treatment of MCF-7 Cell Line

C.1. Objective 146

C.2. Materials and Methods 146

C.3. Results 149

C.4. Discussion and Conclusion 151

Appendix D: Test Specificity of HRP-Goat Anti-Mouse and HRP-Goat Anti-Armenian Hamster Monoclonal Antibodies

D.1. Objective 155

D.2. Materials and Methods 155

D.3. Results 157

D.4. Discussion and Conclusion 160

Appendix E: rhICAM-1 Stimulation on GZ.Hi and 410.4 Cell Lines

E.1. Objective 163

E.2. Materials and Methods 163

E.3. Results 166

E.4. Discussion and Conclusion 169

Appendix F: Localization of Tumor Cells at Tri-Endothelial Cellular Corners

F.1. Objective 175

F.2. Materials and Methods 175

F.3. Results 178

F.4. Discussion and Conclusion 180

Chapter 1

INTRODUCTION

1.1. Background

Although cancer is a generic term that describes more than 100 distinct types of diseases, all cancers are characterized by dysregulated cell growth and tumor manifestation[1]. A tumor is a clonal mass of cells descended from a common ancestral cell, all having inherited the characteristic of uncontrolled proliferation[2]. Despite the uniqueness of different tumor types, there are some general properties shared among them[1]. For instance, the cellular alterations common in all tumor developments include: (1) self-sustained growth, (2) immortalization, (3) sustained angiogenesis, and (4) invasion (Figure 1)[3]. Although some tumors (benign) can co-exist safely with the body, those that spread throughout the body (malignant) are usually lethal.

Despite a 19% drop in death rate, breast cancer incidence has increased by 10% from 1988 to the present[4]. In fact, breast cancer is the most frequently diagnosed cancer (excluding non-melanoma skin cancer) and the second leading cause of cancer deaths (next to lung cancer) in Canadian women[4]. According to the Canadian Cancer Society, an estimated 21,200 (one in 9) women will be diagnosed with breast cancer in 2003, and 5,300 (one in 27) will die of it. Hence, breast cancer is a very serious disease in our society (Figure 2).

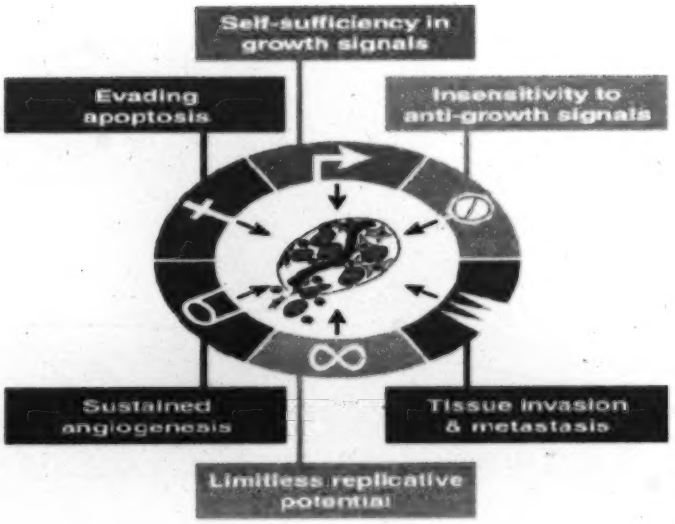

Component	Acquired Capability	Example of Mechanism
	Self-sufficiency in growth signals	Activate H-Ras oncogene
	Insensitivity to anti-growth signals	Lose retinoblastoma suppressor
	Evading apoptosis	Produce IGF survival factors
	Limitless replicative potential	Turn on telomerase
	Sustained angiogenesis	Produce VEGF inducer
	Tissue invasion & metastasis	Inactivate E-cadherin

Figure 1. The six general properties shared among different tumor types.
(Hanahan and Weinberg, 2000)

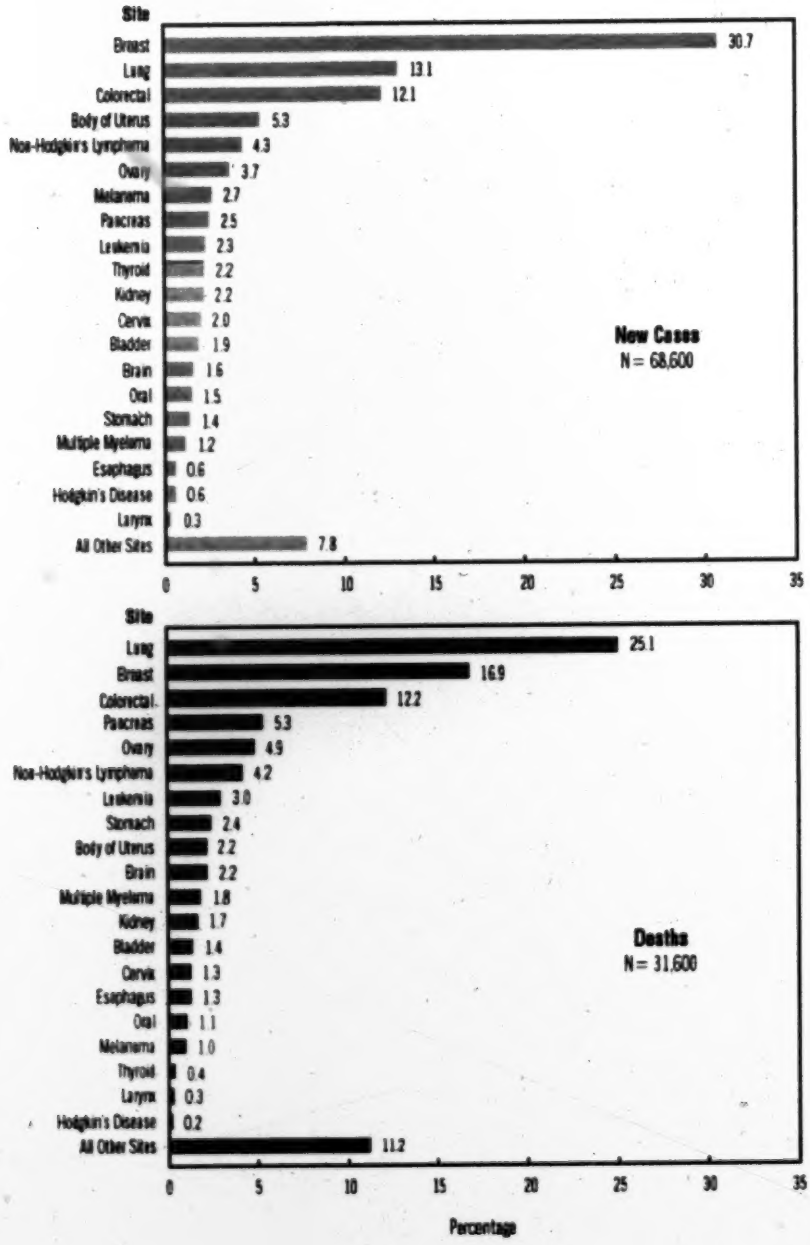

Figure 2. Canadian cancer statistics for year 2003. Breast cancer is the second leading cause of cancer deaths in Canadian women. (Canadian Cancer Society)

One of the major obstacles to offering curative cancer therapy, particularly in breast cancer is metastasis, the process by which cancer cells break through restricting boundaries to invade into surrounding tissues and vessels to establish secondary tumors at distant body sites[2]. Metastasis has traditionally been regarded as a random process, in which tumor cells adhere and subsequently proliferate in the first richly-vascularized organ they encounter[5]. However, there is increasing evidence that metastasis is more likely an outcome of a complicated series of specific tumor-host cell interactions[5, 6]. In this respect, specific adhesion molecules expressed on the surfaces of both tumor and host cells may function as an "address" system that target certain tumor types to a set of preferred organs (Figure 3). Therefore, an attractive therapeutic possibility for cancer is to selectively interfere with the tumor-host cell interaction necessary for metastasis while sparing the normal interactions between healthy cells.

1.2. Tumor Metastasis

1.2.1. Introduction

Tumor cell metastasis is a complex series of sequential events: (1) breaching physical boundaries to invade into surrounding connective tissues; (2) intravasation into blood and lymph vessels; (3) selective adhesion to endothelial cells at target organ(s) and subsequent extravasation; and finally (4) development of secondary tumor(s) accompanied by angiogenesis (Figure 4)[7].

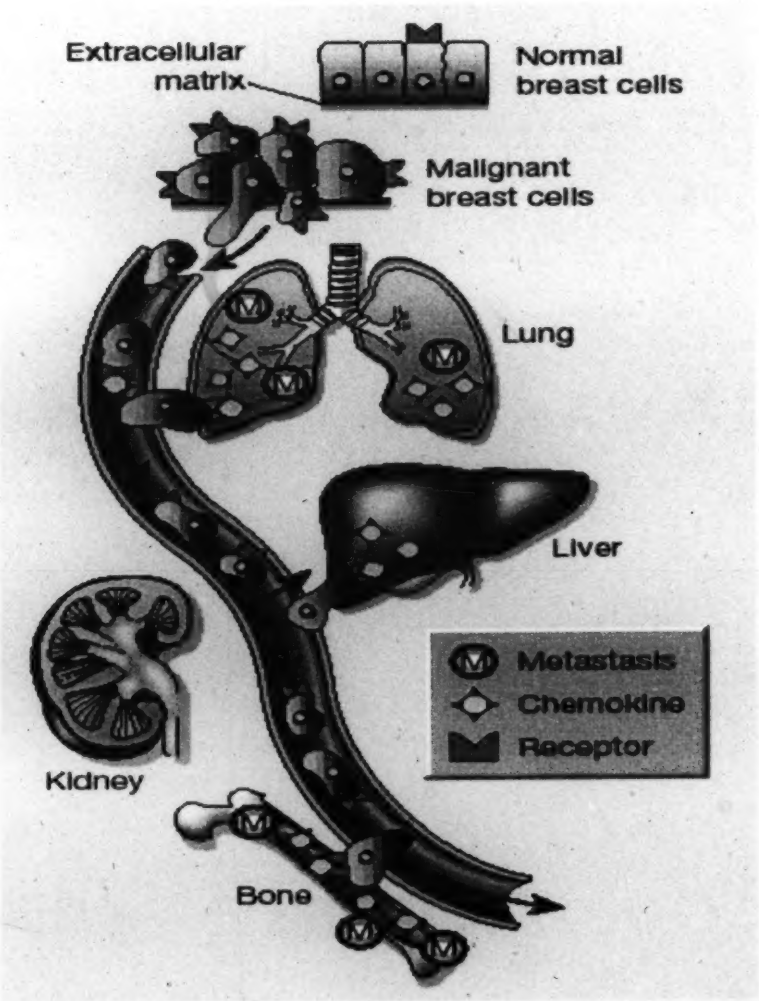

Figure 3. Preferred secondary growth sites for metastatic breast tumors. (Liotta L. A., 2001)

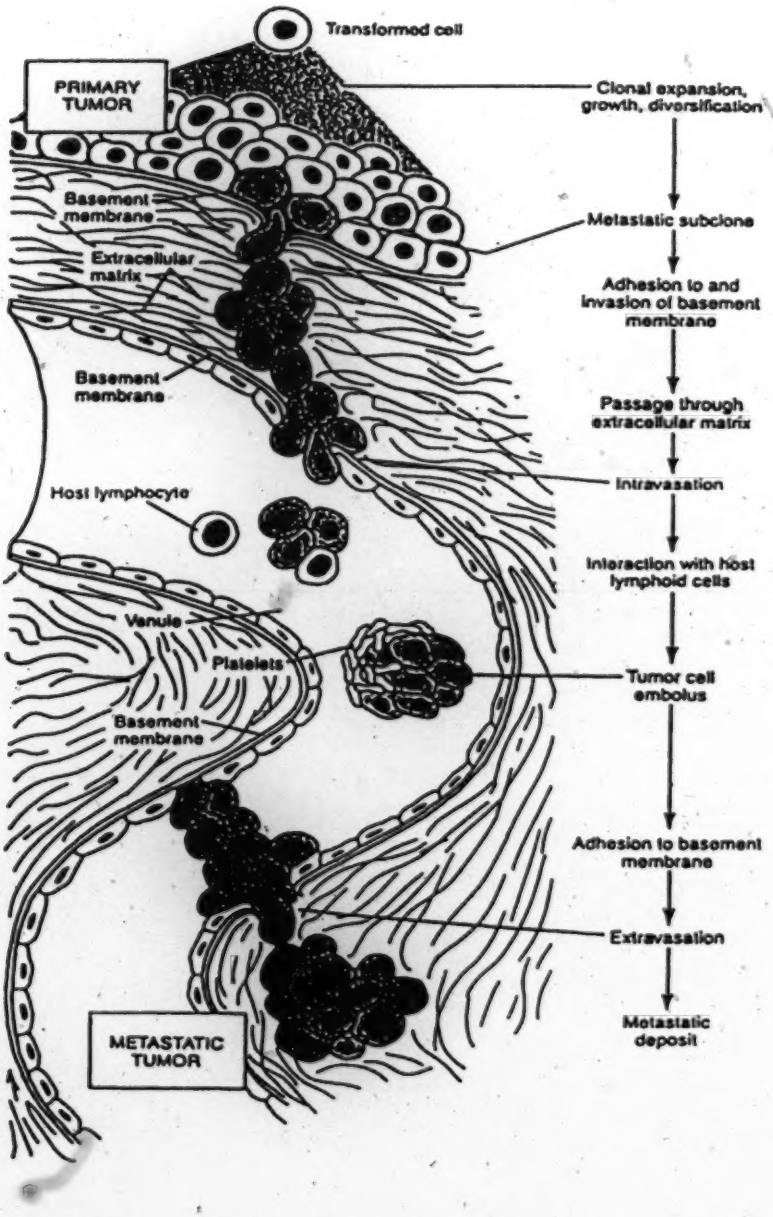

Figure 4. Blood-borne metastatic cascade. (Kam J., 1998)

1.2.2. Tumor Pre-Extravasation Events

The metastatic journey of tumor cells begins with their detachment from the primary tumor mass[8]. This phenomenon is usually facilitated by reduced expression of tumor surface cadherins, a family of calcium-dependent adhesive molecules that mediates cell-cell interactions[7]. However, detached epithelial tumor cells are initially restricted from migrating into the surrounding connective tissues by numerous physical boundaries, such as the basement membrane[7]. These barriers are breached only if tumor cells can perform two sets of coordinated actions. First, tumor cells must degrade physical boundaries via the synthesis of enzymes such as plasminogen activators[9]. These enzymes will in turn activate other proteolytic molecules including type IV collagenase, cathepsin B, and heparin sulphate endoglycosidase through the action of plasmin[9-11]. Secondly, tumor cells need to navigate through the degraded barriers by reversibly adhering to structural proteins[7, 8].

Upon successful invasion, tumor cells have to subsequently migrate through the connective tissue (also known as the extracellular matrix or ECM) before reaching the circulatory and lymphatic systems. The ECM is a complex structural entity consisting of three major classes of biomolecules: (1) structural proteins (i.e. collagen); (2) specialized proteins (i.e. fibronectin and laminin); and (3) proteoglycans (i.e. hyaluronic acid and heparan sulfate)[2]. Migration through the ECM is primarily mediated by tumor cell surface integrins, a ubiquitously expressed family of heterodimeric adhesion receptors (Figure 5A)[12]. Integrins

can facilitate metastasis in several ways depending on various α and β subunit combinations. For instance, they can aid tumor cell navigation through the connective tissue by binding to different ECM ligands like fibronectin (via $\alpha_4\beta_1$)[7], vitronectin (via $\alpha_v\beta_3$)[13], and laminin (via $\alpha_6\beta_1$)[14] (Figure 5A). Furthermore, integrin ($\alpha_2\beta_1$)-mediated signalling can induce tumor cell synthesis of matrix metalloproteinases (MMP) and serine proteases (Figure 5B)[12]. These matrix-degrading enzymes serve two crucial functions. First, they can destroy matrix components like gelatin and laminin to allow tumor cell migration through the ECM[7, 9, 12]. Secondly, MMP-2 and MMP-9 can cleave a major component of basement membranes called type IV collagen, hence, assisting tumor cell penetration into the blood and lymphatic vessels, two major routes to distant organs[7, 9, 12].

Interestingly, in breast carcinoma, it is the fibroblasts surrounding the tumor cells and not the tumor cells that contribute the most to proteolytic matrix degradation[7]. Under normal conditions, these fibroblasts produce very small quantities of matrix proteases. However, it has been suggested that soluble factors secreted by tumor cells can up-regulate their MMP synthesis[7]. In fact, *in vitro* studies have shown that tumor cell-secreted cytokines such as interleukin (IL)-1, IL-6, IL-8, tumor necrosis factor (TNF)-α, and epidermal growth factor (EGF) could induce MMP synthesis in fibroblasts[7]. These proteases will further

(A)

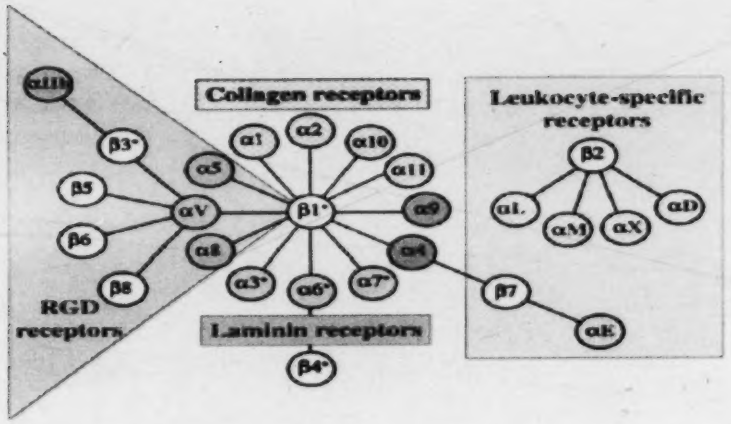

(B)

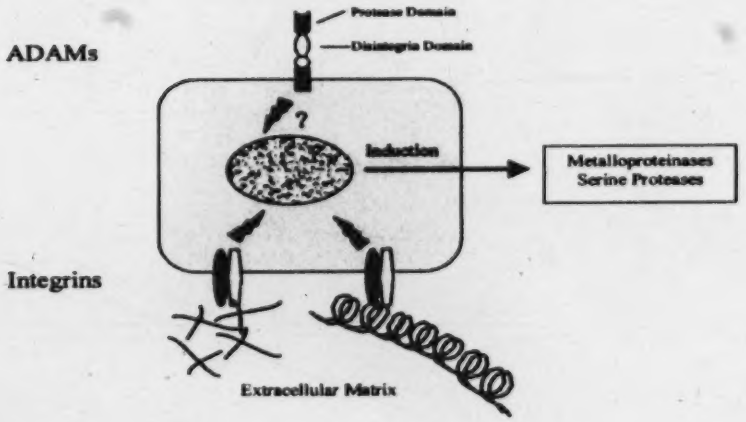

Figure 5. **(A)** The complete set of mammalian integrin subunits: 18α and 8β to make up 24 known distinct integrins (Hynes R., 2002). **(B)** Integrin-mediated signalling leading to metalloproteinase synthesis. ADAMs = A Disintegrin and A Metalloprotease domain (Kurschat and Mauch, 2000).

aid the breakdown of extracellular matrix components, hence, support tumor cell intravasation to the circulatory and lymphatic systems[7].

1.2.3. Tumor Extravasation

Successful penetration of tumor cells across the basement membranes of blood and lymph vessels marks the transition from invasion to metastasis formation[7]. Circulating metastatic cells tend to form aggregates with platelets to avoid host immunological attack[7, 15]. Subsequently, surviving aggregates will attempt to contact the endothelial lining of organ(s) targeted for secondary tumor growth[1]. However, formation of secondary tumors is often organ(s)-specific[16], a phenomenon that cannot be attributed solely to simple differential blood and lymph flow of organs[5]. There are three major alternative theories for explaining the organ-targeting mechanism of metastatic cells. The first theory suggests that although tumor cells may impact all organs equally well, they will only proliferate in those that can provide the appropriate "growth factors"[5]. The second concept known as the "chemoattraction theory", proposes that organ-specific attractant molecules are released into the circulation to signal responsive tumor cells to invade certain organs[5]. The final argument emphasizes the necessity of specific "adhesion molecules" expressed on blood vessel endothelial cells lining the target organs. These adhesion molecules can stimulate circulating tumor cells bearing the appropriate ligand to brake and invade particular organs[5, 17]. Although animal models have yet to validate which theory is superior, it is most likely that

the three targeting mechanisms along with the effects of differential body fluid flow are non-mutually exclusive in metastasis[5, 17].

Specific tumor-host cell surface molecular interactions are essential for initiating tumor extravasation - the migration of circulating tumor cells into secondary organs[5, 17]. Some of the molecular families known to govern these adhesive processes include selectins, integrins, cadherins, and immunoglobulins[17].

Interestingly, the steps involved in metastatic extravasation seem to parallel those for leukocyte extravasation during inflammation (Figure 6)[17, 18]. In an acute inflammatory reaction, circulating leukocytes first loosely adhere to and "roll" along the endothelium that lines the site of tissue injury[19]. This phenomenon is facilitated by weak interactions between selectins (possess lectin-like properties) and their carbohydrate ligands, sialylated Lewis $^{a/x}$ antigens, expressed on endothelial cells and leukocytes, respectively[19-25]. Rolling enables leukocytes to slow down within the circulation and interact with other adhesion molecules on the interacting cells. For example, leukocyte surface β_2 integrin (LFA-1) may interact with ICAM-1 on endothelial cells to initiate bi-directional signalling[24]. As a result, the expression and binding affinity of surface adhesion molecules of the two cell types are increased[21, 26]. This will lead to a series of stronger interactions allowing leukocytes to firmly attach to the endothelium[21, 27].

(A)

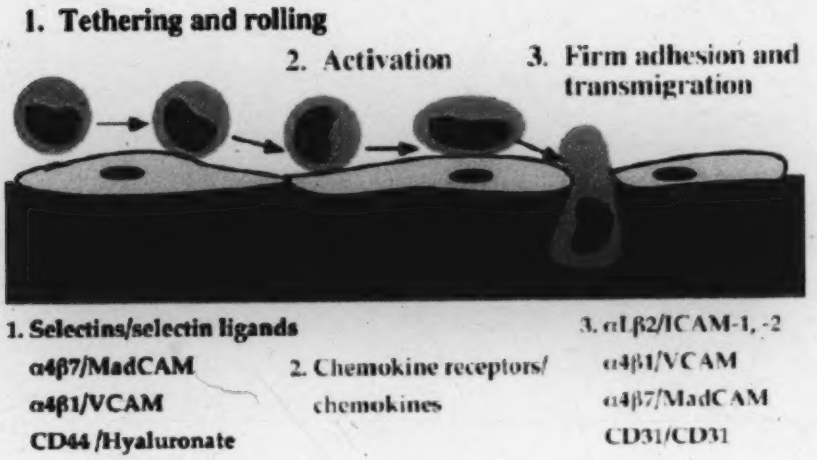

(B)

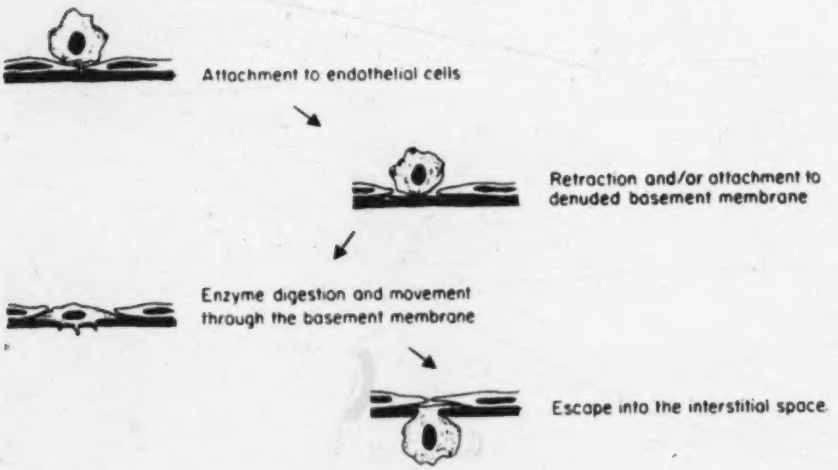
Attachment to endothelial cells
Retraction and/or attachment to denuded basement membrane
Enzyme digestion and movement through the basement membrane
Escape into the interstitial space

Figure 6. Parallels in leukocyte and tumor cell extravasation. **(A)** Inflammatory leukocyte extravasation is mediate by various adhesion molecules (Fabbri et al., 1999). **(B)** Steps in metastatic tumor cell extravasation resemble those used by leukocytes (Tannock 1998).

Arrested leukocytes will then preferentially localize to tri-endothelial cellular junctions, sites where borders of three endothelial cells meet[18]. These are also the main locations for leukocyte transendothelial migration[18]. Subsequently, junctional entry (also known as diapedesis) of leukocytes is initiated via pseudopodia formation, enabling them to 'crawl' through the endothelium to reach the injured tissue[18]. Therefore, a succession of adhesive molecular interactions between leukocytes and endothelial cells are essential for the different stages of inflammatory leukocyte extravasation.

Similarly, circulating tumor cells also commence extravasation by first binding weakly to the endothelium. These transient contacts are likely to be mediated by carbohydrate-carbohydrate interactions, involving E-selectin and sialylated Lewis a and x antigens expressed on endothelial and tumor cells, respectively[28-31]. For instance, it has been shown that colon carcinoma cells could adhere to E-selectin via their surface sialylated Lewis a and x oligosaccharides[32]. This will enable sufficient time for two processes to occur: (1) intercellular "cross-talking"; and (2) activation of the two cell types by agents like cytokines, bioactive lipids, and growth factors[17]. The latter phenomenon serves to induce the expression of adhesion molecules (i.e. selectins, integrins, and cadherins) on the surfaces of tumor and endothelial cells[17]. Again with parallels to an inflammatory response, up-regulation and interaction of adhesive proteins enable tumor cells to firmly arrest on the endothelium (Figure 6B). Following firm attachments of tumor cells, endothelial cells will retract through microfilament reorganization

and VE-cadherin and P-selectin redistribution, exposing the underlying basement membrane for degradation[17, 33]. By the process of pseudopodia formation at the basolateral surfaces, tumor cells can extravasate to a novel growth site and colonize to establish secondary tumors[33].

In molecular mimicry to leukocyte extravasation, it was first demonstrated by our lab that the extracellular domain of human mucin protein MUC1 on tumor cell surfaces could bind to ICAM-1 (intercellular adhesion molecule)[34, 35]. Hayashi *et al.* (2001) subsequently verified that a minimum of two tandem repeats of MUC1's extracellular domain were required for its binding to ICAM-1's immunoglobulin-like extracellular domain 1[158]. In subsequent work, we have found that MUC1 can mediate breast tumor cell adhesion to a simulated blood vessel wall under shear flow conditions equivalent to physiological blood flow[36] and is crucial for mediating *in vitro* tumor cell transmigration (unpublished observations)[37]. Moreover, Rahn *et al.* (2004) from our lab have recently shown through fluorescent microscopy experiments that the MUC1-ICAM-1 interaction can induce intracellular calcium ion oscillations in MUC1-positive cells[38]. Therefore, MUC1-ICAM-1 binding may play a significant part in the overall breast tumor extravasation cascade during the metastatic process.

1.3. The Human Mucin MUC1

1.3.1. MUC1 Expression

The human MUC1 is a mucin protein that was first discovered in breast milk[39, 40]. It is expressed as a type 1 transmembrane molecule on all breast epithelial cells, as well as most other secretory epithelium and some hematopoetic cells[41]. In normal breast glandular epithelium, MUC1 is heavily glycosylated and expressed only on the apical cell surface[42]. However, there are several changes that happen to MUC1 in malignant breast epithelium. Firstly, the protein is overexpressed in greater than 90% of human breast cancer[35]. This can be due to gene dosage effect (amplification of gene copies), hypomethylation (impaired gene methylation which can stem from reduced methyltransferase levels), or increased transcription of the MUC1 gene[43, 44].

Secondly, there is increased MUC1 shedding in breast cancer. Therefore, the secreted form of the mucin is commonly found in the serum of breast cancer patients[45, 46], and supernatants of cultured breast cancer cells[47, 48]. There are two possible mechanisms for soluble MUC1 generation: (1) protease cleavage of the extracellular domain from the membrane-embedded mucin[47, 49]; or (2) changes in the transmembrane domain that induce less stable membrane-embedding of the protein[42]. The properties of overexpression and increased shedding of MUC1 have led to its use as a breast tumor antigen for more than 20 years[50].

Thirdly, MUC1 is often under-glycosylated in breast tumor cells due to impaired glycosyltransferase activity, resulting in the expression of simple and truncated cancer-associated antigens (i.e. TF, Tn, and sTn)[51]. The decreased glycosylation exposes the highly immunogenic epitope (APDTRP) on the peptide backbone of the extracellular domain, which is recognizable by certain monoclonal antibodies against MUC1 (Figure 7)[52-54].

Finally, the most significant MUC1 alteration in breast cancer is that the spatial expression pattern of the protein is no longer apically-restricted. In contrast, MUC1 distribution in tumors can become circumferential and cytoplasmic in a minority of breast cancer cases[55]. This has been correlated with high metastatic frequency and poor prognosis[55].

1.3.2. MUC1 Extracellular Domain

MUC1 is a high molecular weight sialylated mucin expressed in all mammals[42]. However, it differs from classical mucins by the fact that it is an integral membrane protein[42]. The human MUC1 gene is located on chromosome 1q21-24[56]; both alleles are expressed co-dominantly[57]. The molecular structure of MUC1 is composed of three domains: (1) extracellular, (2) transmembrane, and (3) cytoplasmic (Figure 8)[42].

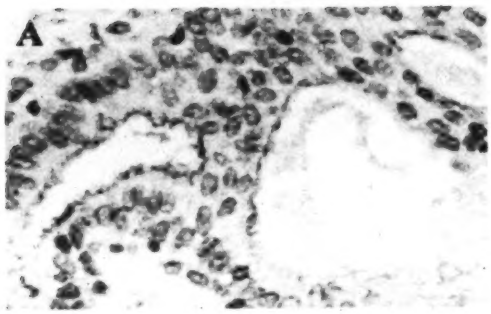

Normal glandular structures - Highly glycosylated MUC1 apically localized.

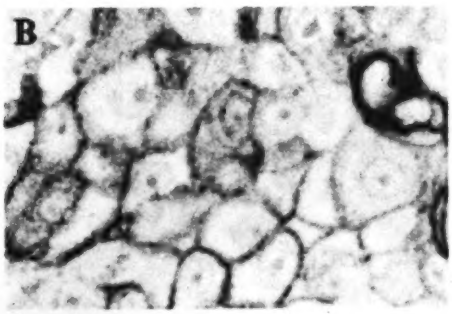

High grade in situ duct carcinoma - Under-glycosylated MUC1 with circumferential membrane distribution.

Antigenic epitope exposed to elicit an immune response

Figure 7. De-glycosylation exposes the highly immunogenic epitope (APDTRP) on the peptide backbone of MUC1's extracellular domain. (Rahn *et al.*, 2001)

MUC1 is transcribed as a pro-peptide that undergoes post-translational cleavage in the endoplasmic reticulum[49]. The larger of the two protein products is the N-terminal extracellular domain of MUC1 containing the signal sequence (a membrane-targeting signal for the protein), degenerate repeats, and tandem repeats[41, 58, 59].

The extracellular domain is composed of a variable number of tandem repeats (VNTR) encoded by the second (of the seven) exon of the MUC1 gene[42, 60-62]. The VNTR is built from a 20 amino acid motif that is tandemly repeated 30 to 90 times due to genetic polymorphism within the population (Figure 9)[42, 63]. As a result, MUC1's extracellular domain can vary in length from 1000 to 2200 amino acids[64]. The tandem repeats are abundant in threonine, serine, and proline amino acids to yield multiple effects[42]. Firstly, the ring structure of prolines can inhibit the formation of close-packed and ordered secondary protein structures[65, 66]. As a result, prolines tend to induce random coiling to promote MUC1's rigidity and extension[65, 66]. Consequently, MUC1 extends 200-500 nanometers above the plasma membrane, as compared to a maximum of 30 nm protrusion for most other membrane molecules[63, 64]. Secondly, serines and threonines are major O-linked glycosylation sites, giving a negative charge and enhancing the rigidity of MUC1[42, 54, 65, 66]. In fact, the human MUC1 is so heavily glycosylated that the galactose and N-acetylglucosamine sugars may constitute up to 50-90% of the protein mass[67]. MUC1's massive glycosylation is assisted by the presence of small-sized amino acids, glycines and alanines in the

tandem repeats, which facilitate close approach of glycosyltransferase to MUC1[42]. Due to the variable number of tandem repeats, and hence, differential MUC1 glycosylation levels within a population, MUC1 can have a mass ranging from 160 to over 400 kDa[41, 68, 69].

A recently identified component of MUC1's extracellular domain, the SEA module, has been characterized by Bork and Patthy in 1995[70]. It was named after the first three proteins in which it was identified: sperm protein, enterokinase and agrin[70, 71]. The SEA module seems to function optimally in carbohydrate-rich environments since they often coexist with O-linked carbohydrates like those found on MUC1[70]. Although the exact function of the SEA module is unknown, it has been speculated to participate in binding to extracellular matrix constituents or neighboring cell-surface molecules and mediate intracellular signalling events[70, 71].

1.3.2.1. MUC1 Extracellular Domain Function

Although the exact role(s) of MUC1 is unknown, several possible functions have been suggested. For instance, MUC1 has been thought to protect the mammary gland from mastitis, an inflammation that could adversely affect milk production[42]. In addition, secreted MUC1 mucins may serve a protective role by forming a physical barrier for organs against microorganisms and degradative

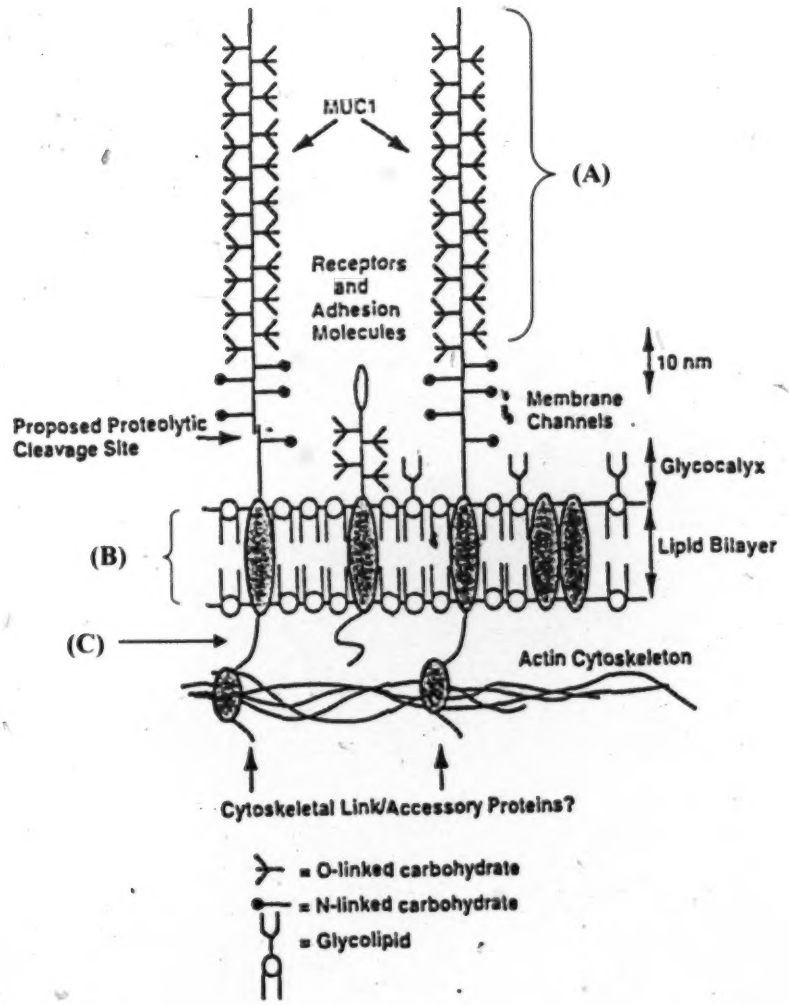

Figure 8. Molecular structure of human MUC1 consisting of the (A) extracellular, (B) transmembrane, and (C) cytoplasmic domains. (Patton *et al.*, 1995)

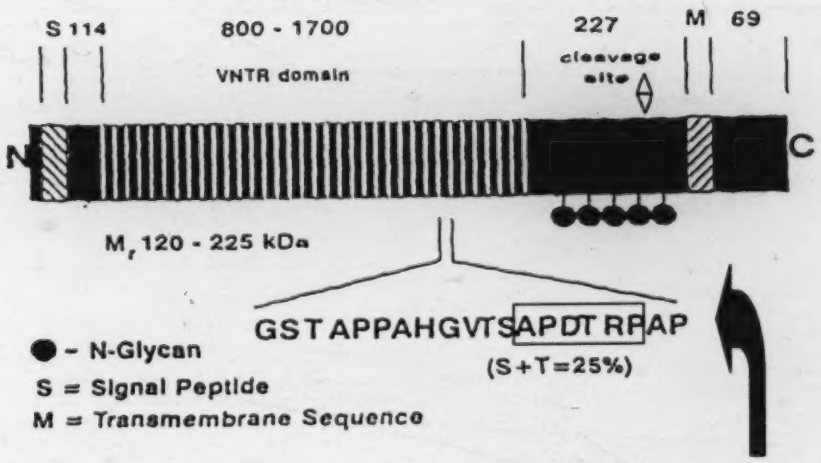

Figure 9. The short C-terminus MUC1 cytoplasmic domain, followed by the transmembrane domain (M). The next section of the molecule is the extracellular VNTR domain made of a 20 amino acid motif that may tandemly repeat from 30-90 times. This region also contains the highly immunogenic APDTRP epitope (rectangle). [Aplin *et al.*, 1995]

enzymes[72]. Furthermore, the sialic content of normal MUC1 is quite high (about 30% of the protein), making the extracellular domain very hydrophilic and negatively-charged, suggesting an anti-adhesive function[42]. This has been thought to shield the MUC1 extracellular domain from binding to other cell membrane proteins, and hence, collapsing of milk ducts[42].

With respect to cancer and metastasis, it has been suggested that MUC1 could protect tumor cells from host immune responses by blocking T cell activation[73, 74]. In fact, several groups found that soluble MUC1 purified from either cancer patients or human breast cancer cell-conditioned media could suppress cytokine secretion, proliferation, and cytotoxic capability of patients' T lymphocytes[74-77]. Moreover, there is evidence for the role of MUC1 in promoting tumor cell separation from the primary site due its anti-adhesive property, which can be attributed to the protein's overall negative charge and unusually long extracellular domain[78, 79].

Recent data from our lab have suggested the possible role of MUC1 in modulating tumor cell migration (unpublished observations)[37]. For instance, it was found that MUC1 could bind to ICAM-1 expressed on endothelial cells[34], and that such an interaction was strong enough to withstand shear stresses equivalent to physiological blood flow[36]. Since ICAM-1 normally functions to recruit circulating leukocytes, it is possible that MUC1-ICAM-1 binding may facilitate tumor cell extravasation in blood-borne metastases. In fact, our lab

showed a positive correlation between MUC1-ICAM-1 binding and transendothelial migration of tumor cells (unpublished observations)[37]. Our lab has also demonstrated that intracellular calcium oscillations of tumor cells could be triggered by MUC1-ICAM-1 interaction[38]. Therefore, it is possible that MUC1-ICAM-1 interaction is a significant event in breast tumor metastases.

1.3.3. MUC1 Transmembrane and Cytoplasmic Domains

The smaller cleaved-protein product (20-30 kDa) of the MUC1 pro-peptide consists of three C-terminal components: (1) extracellular stem, (2) transmembrane domain, and (3) cytoplasmic domain. The extracellular stem is a SDS-sensitive site, where the two protein products non-covalently heterodimerize[49]. It was recently demonstrated through site-directed mutagenesis studies that a Gly-Ser peptide bond located N-terminal to the transmembrane domain was a crucial proteolytic cleavage location, which mediated the extracellular domain shedding of membrane-bound MUC1[80]. The transmembrane domain is made of 31 highly conserved amino acids that function to hold MUC1 in the membrane[42].

The cytoplasmic domain of MUC1 contains 72 amino acids that are also highly conserved across mammalian species[42]. In fact, there is a striking 87% sequence homology between the human and mouse MUC1 cytoplasmic segment, implicating its functional significance[42]. This protein portion does not contain any known catalytic or kinase sequence motifs. As a result, it is incapable of

autophosphorylation[43], although it can be phosphorylated by kinases such as EGFR, c-Src, GSK3β, and PKCδ[41, 81, 82]. There has been increasing interest in the MUC1 cytoplasmic domain because of its ability to interact with a number of proto-oncogenic proteins like EGFR, c-*src* and β-catenin[41, 81]. Furthermore, tyrosine phosphorylation of the cytoplasmic domain in tumor cells has been shown to have downstream effects on cellular adhesion[41, 43, 81, 83, 84].

1.3.3.1. MUC1 Cytoplasmic Domain Function

The cytoplasmic domain of MUC1 contains seven tyrosine residues that are potential phosphorylation sites[85], which have been studied by several groups in the past (Tables 1 and 2). In fact, Zrihan-Licht *et al.* (1994) was one of the first groups to observe extensive phosphorylation of MUC1's cytoplasmic domain[43]. However, it was not until recently that the tyrosine kinases for MUC1 were identified to be c-Src[81] and EGFR[41]. Since many signalling molecules (i.e. EGFR, ERK1/2) are tyrosine-phosphorylated[41], the fact that MUC1 is also tyrosine- phosphorylated makes it a possible signalling candidate. Interestingly, four of the seven tyrosines are known to constitute signalling pathway motifs once phosphorylated: (1) YTNP (growth factor receptor-bound protein 2 or Grb2); (2) YHPM (phosphatidylinositol 3-kinase or PI3K); (3) YVPP (phospholipase C-γ1

Research Groups	Cell Lines	Methods of MUC1 PTyr Detection	Findings
Zrihan-Licht *et al.*, 1994	MUC1 cDNA transfected into HBL100 human mammary epithelial cells. MUC1/Y transfected into 3T3 ras transformed fibroblasts.	NP40 lysis buffer. IP with Protein A-(α-CT2) complex. 8 h incubation of cells with radioactive carrier-free inorganic phosphate. Na_3VO_4 for 30 min prior to cell lysis. SDS-PAGE → Autoradiography.	MUC1/CT PTyr at 20-30 kDa MUC1/Y PTyr at 42-45 kDa.
Pandey *et al.*, 1995	Human MCF-7 breast carcinoma cells.	Brij-96 lysis buffer with Na_3VO_4 incubation of cells for 30 min. IP with anti-DF3 antibody specific for MUC1 ECD. SDS-PAGE → IB with PTyr antibody.	MUC1 PTyr at <200 kDa. MUC1 Tyr YTNP phosphorylation led to MUC1/Grb2/Sos complex formation.
Quin and McGuckin, 2000	Human breast cancer cell lines: MCF-7, MDA-MB-231, BT-20, T-47D & ZR-75-1. Human ovarian cancer cell lines: OAW42, OVCAR-3, Caov-3 & COLO316.	Na_3VO_4 incubation 2 h prior to cell harvesting. NP40 (RIPA) and Brij-97 lysis buffers with Na_3VO_4 incubation of cells for 30 min. IP with BC2 specific for MUC1 ECD. SDS-PAGE → IB with PTyr antibody.	MUC1/CT PTyr at 25-30 kDa detected only in OAW42 & OVCAR-3 when RIPA buffer used. MUC1/CT PTyr at 25-30 kDa became detectable in MCF-7 & ZR-75-1 only when Brij-97 buffer used. Low MUC1/CT PTyr levels despite high overall MUC1 expressions.

Table 1. Review of previous studies on MUC1 tyrosine phosphorylation. CT = MUC1 cytoplasmic domain; ECD = MUC1 extracellular domain; PTyr = phosphotyrosine; IP = immunoprecipitation; IB = immunoblot; Na_3VO_4 = sodium pervanadate.

Research Groups	Cell Lines	Methods of MUC1 PTyr Detection	Findings
Li *et al.*, 1994	Human breast carcinoma cells ZR-75-1	NP40 lysis buffer. IP with anti-DF3 antibody specific for MUC1 ECD or anti-Src antibody. 15 min incubation of cells with purified c-Src and [γ^{32}P]ATP. SDS-PAGE → Autoradiography.	c-Src binds directly to MUC1/CT and phosphorylates Tyr YEKV predominately (>6.5 kDa, ~15 kDa). MUC1/CT decreased MUC1/GSK3β and increased MUC1/β-catenin associations.
Schroeder *et al.*, 2001	Human breast carcinoma cells T-47D and MDA-MB-468.	Triton X-100 lysis buffer with Na_3VO_4. IP with anti-CT1 and anti-CT2 antibodies. SDS-PAGE → IB with PTyr antibody.	EGF induces MUC1/CT Tyr-P. EGFR binds & phosphorylates MUC1/CT (~25 kDa and ~28-30 kDa), leading to ERK1/2 activation.
Meerzaman *et al.*, 2000 Meerzaman *et al.*, 2001	Monkey COS-7 cells transfected with CD8/MUC1 chimeric construct.	Na_3VO_4 incubation 15 min prior to cell harvesting. NP40 lysis buffer with Na_3VO_4 incubation of cells for 20 min. IP with CT1 antibody. SDS-PAGE → IB with PTyr antibody.	Anti-CD8 antibody induced MUC1 Tyr-P of MUC1/CD8 construct (~34 kDa). Anti-CD8 antibody also induced ERK2 phosphorylation, which was Ras- & MEK-dependent.

Table 2. Review of previous studies on MUC1 tyrosine phosphorylation. CT = MUC1 cytoplasmic domain; ECD = MUC1 extracellular domain; PTyr = phosphotyrosine; Tyr-P = Tyrosine phosphorylation; IP = immunoprecipitation; IB = immunoblot; Na_3VO_4 = sodium pervanadate.

or PLC-γ1); and (4) YEEV (c-Src family kinases)[43, 86].

MUC1 phosphorylation enables its cytoplasmic domain to interact with other signalling mediators. In 1995, Pandey *et al.* discovered that MUC1 could associate with the SH2 domain of Grb2 upon tyrosine phosphorylation[85]. This consequently led to the recruitment of Sos by the SH3 domain of Grb2, and formation of MUC1/Grb2/Sos complex[85]. This suggested a possible role of MUC1 in modulating the Ras/Raf/MAPK signal transduction pathway, and hence, the first indication of MUC1 signalling[85]. Furthermore, Li *et al.* (2001) found that c-Src-mediated tyrosine phosphorylation of MUC1 could promote the binding of MUC1 to the β-catenin signalling/adhesion protein[81]. The effects were two-fold. There was reduced GSK3β-mediated serine phosphorylation of MUC1 at the DRSPY site due to decreased GSK3β-MUC1 association[81, 87]. GSK3β-mediated phosphorylation of MUC1 is normally a negative regulator for β-catenin binding to MUC1's SAGNGGSSL motif, which is adjacent to the DRSPY site[87]. Therefore, inhibiting GSK3β-MUC1 complex formation would enhance β-catenin-MUC1 association, and depletion of β-catenin from E-cadherins[81, 87]. As a result, normal E-cadherin function was disrupted[87, 88]. Secondly, MUC1-β-catenin binding resulted in β-catenin redistribution to the invading cell margins and increased invasiveness of cancer cells[83]. These observations have supported the possible role of MUC1 in signalling tumor cell invasion during metastasis.

A more direct piece of evidence for MUC1 signalling came from Schroeder *et al.* in 2001[41]. They found heterodimerization of epidermal growth factor receptor (EGFR) with MUC1 upon stimulation of MDA-MB-468 (human breast carcinoma) cells with EGF[41]. This led to enhanced tyrosine phosphorylation of MUC1, and also increased extracellular signal-regulated kinase (ERK)1/2 phosphorylation and activity[41]. The enhanced ERK1/2 activity was not associated with increased mitogenesis as determined by unaltered proliferating cell nuclear antigen (PCNA) levels[41]. However, it is known that increased MAPK activity could negatively regulate *in vitro* tight junction formation and preservation[64, 78, 79, 89]. Moreover, the activation of MAPK/ERK pathway by EGFR has also been implicated in cellular migratory processes[90]. Therefore, it is clear that MUC1 could participate in cellular signalling events via tyrosine phosphorylation.

Meerzaman *et al.* (2000) engineered a CD8/MUC1 chimeric construct by fusing the extracellular and transmembrane domains of CD8 to the cytoplasmic domain of MUC1[91]. Following transfection of the construct into COS-7 cells, they were able to induce MUC1 tyrosine phosphorylation through anti-CD8 antibody stimulation[91]. Moreover, ERK2 activation was also observed upon induced MUC1 tyrosine phosphorylation[84]. Therefore, not only was the role of MUC1 in cellular signalling once again demonstrated, they have also shown that MUC1 tyrosine phosphorylation could be modulated by an external stimulus. However,

the physiological stimulus for regulating MUC1 tyrosine phosphorylation remains unknown.

1.4. The Human Intercellular Adhesion Molecule-1

1.4.1. ICAM-1 Expression

The monomeric/dimeric type I transmembrane glycoprotein, Intercellular Adhesion Molecule-1 (ICAM-1, also known as CD54), is a member of the immunoglobulin (Ig) supergene family[92, 93]. ICAM-1 is commonly expressed on leukocytes and endothelial cells[92]. The expression of ICAM-1 varies between different cell types and is modulated in numerous ways, mainly via transcriptional regulation and cytokine availability[92]. For instance, the human ICAM-1 gene promoter region contains a cytokine/lipopolysaccharide responsive κB element. As a result, factors such as TNF-α and IL-1 can induce ICAM-1 expression, and interferon (IFN)-γ can subsequently stabilize the mRNA[92, 94-97]. This mechanism is especially relevant in endothelial cells which constitutively express low levels of ICAM-1 due to the short mRNA half-life[98]. In contrast, glucocorticoids are responsible for repressing ICAM-1 gene transcription[94, 99]. Interestingly, angiogenic factors are also known to down-regulate ICAM-1 expression[100]. These factors tend to reduce the sensitivity of endothelial cells to inflammatory cytokines, which may serve as a mechanism to inhibit leukocyte infiltration to tumors[100].

Another regulatory mechanism for ICAM-1 expression is the activity of various signal transduction pathways[92]. For example, intracellular second messengers like cAMP[101, 102], Ca^{2+} [103], protein kinase C[104], and phospholipase A2[105] can up-regulate ICAM-1 expression in a cell type-specific manner[99]. In contrast, second messengers including cGMP[106] and tyrosine kinase can reduce ICAM-1 expression[107].

1.4.2. ICAM-1 Structure

The human ICAM-1 gene is located on chromosome 19 and is composed of seven exons that are separated by six introns[108]. It shares limited sequence homology (55-65%) with other species such as murine, rat, and canine[92].

The molecular structure of ICAM-1 contains 3 major domains: (1) extracellular, (2) transmembrane, and (3) cytoplasmic (Figure 10).

The 453 amino acid extracellular portion consists of five Ig-like domains, each of which is encoded by a different exon[108]. The tandem arrangement of these domains may have evolved to function as multiple and independent binding sites for the protein[109]. Each Ig-like domain is a composite of two antiparallel β strands capable of disulfide bridge formation via conserved cysteine residues, with the exception of domain 4[110, 111]. Moreover, there are eight N-linked glycosylation sites in the extracellular region where the extent of glycosylation

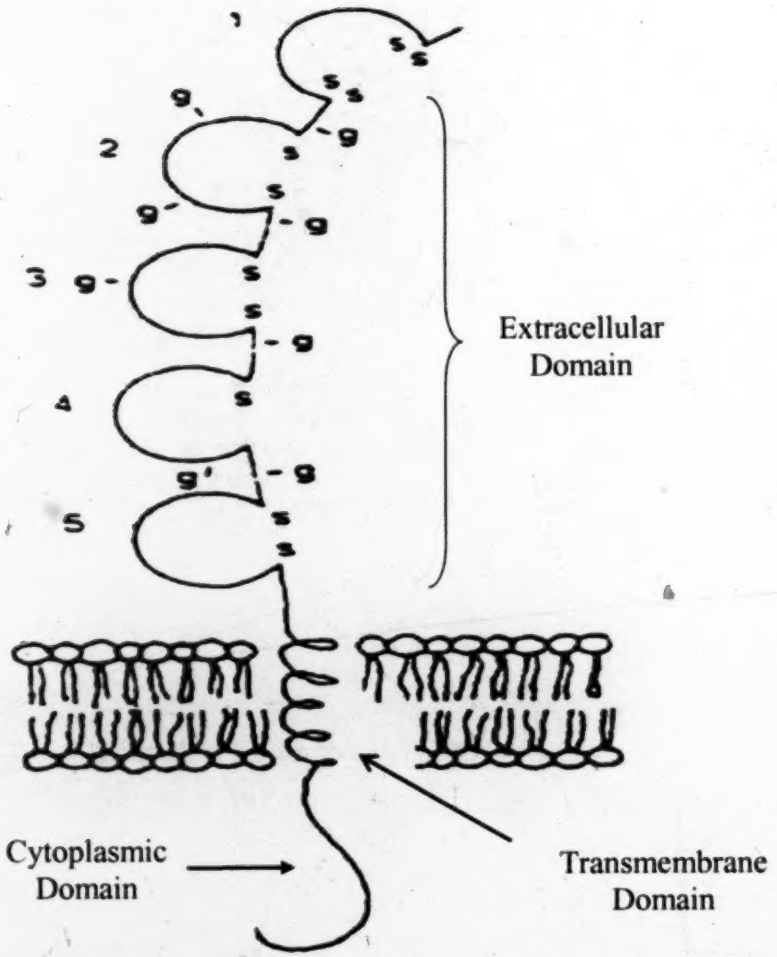

Figure 10. Molecular structure of ICAM-1 consisting of the extracellular, transmembrane, and cytoplasmic domains. (van de Stolpe and van der Saag, 1996)

varies depending on cell type[97, 111, 112]. As a result, the molecular weight of ICAM-1 ranges from 60-114 kDa[97, 111, 112].

The transmembrane domain is made of 24 hydrophobic amino acids that function to hold ICAM-1 within the plasma membrane[111]. Finally, the cytoplasmic domain of ICAM-1 contains 28 highly conserved amino acids[111]. Some of these amino acids can interact with α-actinin, the cytoskeleton-binding protein, suggesting the protein's role in mediating cell motility[113]. The cytoplasmic region has also been proposed to modulate cell-cell adhesion by mediating ICAM-1 internalization, which is directly dependent on the level of protein density on cell surface[114].

1.4.3. ICAM-1 Function

ICAM-1 is generally responsible for mediating specific and reversible cell-cell adhesion, and hence, intercellular communication[92] and signalling[115, 116]. However, ICAM-1 also plays a significant role in many host immune responses. For instance, when expressed on antigen-presenting cells (i.e. macrophages, B-lymphocytes, and plasma cells), ICAM-1 can act as a co-stimulatory molecule to activate MHC class I- and II-regulated T cells[117-120]. Therefore, ICAM-1 is a crucial modulator of T-cell mediated host immunity.

Furthermore, ICAM-1 expressed on endothelial cells of blood vessels can regulate leukocyte transmigration to sites of tissue injury and inflammation[92]. One of

the major ligands for ICAM-1 is integrins, particularly LFA-1 (CD11a/CD18) and Mac-1 (CD11b/CD18)[109, 110]. After transient rolling, leukocytes will firmly adhere to the endothelium to facilitate their subsequent spreading and locomotion. These processes are mediated by the (cation-dependent) binding of LFA-1 and Mac-1 to the amino-terminal first and third Ig-like domains of ICAM-1, respectively[109, 121-126]. Due to the active role that ICAM-1 plays in host immunity, abnormal expression of the protein has been linked with various disease manifestations, including some inflammatory disorders and malignancies[92].

1.5. Experimental Rationale and Hypothesis

The human MUC1 is a mucin protein first discovered in breast milk. It is overexpressed in more than 90% of breast cancer, hence, it has been used as a breast tumor marker for more than 20 years[45]. In fact, it has recently been identified as an oncogene, capable of inducing cellular anchorage-independent growth and tumor formation in animal models[127]. Furthermore, immunohistochemical analyses of clinical human breast cancer specimens by Rahn *et al.* (2001) revealed that aberrant (cytoplasmic or non-apical) expression of the protein correlated with poor prognosis and nodal metastases[55]. Despite the apparently obvious data implicating MUC1's importance in breast cancer, its precise pathological role remains unclear. Traditionally, MUC1 has been viewed as a passive player in tumor cell dissemination[64, 78, 79, 128]. However, more recent publications have discovered the association of MUC1 with numerous

potential signalling mediators implicated in tumorigenesis. Hence, it is possible that MUC1 may actively participate or assist tumor progression. In fact, it is known that MUC1 can be tyrosine phosphorylated and participate in cellular signalling with downstream effects on cell adhesion[41, 43, 83, 84].

Rahn *et al.* (unpublished observations) from our lab have recently discovered that MUC1-ICAM-1 interaction was crucial in mediating tumor cell transendothelial migration in a Transwell model[37]. Furthermore, the presence of fibroblasts and cytokines resulted in significantly greater extent of tumor cell transmigration than in the absence of these variables[37]. Cytokines like TNF-α and IL-1β are known to increase ICAM-1 expression on endothelial cells[92, 94-97], while fibroblasts could secrete soluble factors and proteolytic enzymes into the cellular microenvironment. Therefore, the importance of ICAM-1 and factors in the cellular microenvironment in promoting tumor cell transmigration was implicated. In addition, our lab has demonstrated that MUC1-ICAM-1 interaction could trigger intracellular calcium ion oscillations in MUC1-positive cells[38]. This calcium-based signal was later shown to be mediated through the PI3K/inositol triphosphate (IP3) pathway and Src through a series of enzyme-specific inhibitory experiments[38]. Based on our laboratory's data that point to the significance of MUC1-ICAM-1 interaction in mediating tumor cell transendothelial migration and calcium ion oscillation, it was hypothesized that the same molecular interaction could trigger subsequent tyrosine phosphorylation of tumor cell MUC1. It is known that MUC1 tyrosine phosphorylation is crucial

in facilitating the association of MUC1 with signalling molecules implicated in tumorigenesis[41, 81, 82, 85, 87, 130]. Therefore, finding MUC1 phosphorylation would suggest the significance of ICAM-1 in modulating interactions between MUC1 and signalling molecules (i.e. Grb2/Sos)[85] and signalling pathways (i.e. ERK/MAPK)[41] potentially involved in the promotion of tumor progression.

Chapter 2

EXPERIMENTAL MATERIALS AND METHODS

2.1. Optimization of Western Blot and Immunoprecipitation

2.1.1. Immunoblot for MUC1 with B27.29 and α-CT2 Monoclonal Antibodies

Objective:

The ability to detect the human mucin protein MUC1 through Western blotting was a basic prerequisite for analyzing results in this project. Two methods are commonly used in the literature for MUC1 immunoblotting. The first approach is to use antibodies specific for the extracellular tandem repeats of MUC1 (e.g. B27.29). Alternatively, antibodies (e.g. anti-CT2) that target the cytoplasmic tail segment of MUC1 can also be used. Therefore, it was attempted to detect the full-length or cytoplasmic domain of MUC1 via Western blot from ascites and the following cell lines: (1) MCF-7, (2) 410.4, (3) ZR-75-1, (4) MDA-MB-231, (5) MDA-MB-468, (6) 293T/MUC1, (7) 293T/Mock, (8) NIH3T3, (9) NIH3T3/ICAM-1, and (10) NIH3T3/Mock by using monoclonal B27.29 and anti-CT2 antibodies, respectively. The MUC1 expression pattern of these cell lines have already been determined by our lab and/or the literature. Therefore, they were useful for evaluating the effectiveness of the Western blotting techniques used in this project.

Materials and Methods:

Antibodies

Monoclonal mouse anti-MUC1 B27.29 specific for the human MUC1 extracellular domain epitope PDTRPAP (useful for detecting the full-length MUC1) was kindly donated by Biomira Inc. (Edmonton, Alberta, Canada).

Horseradish peroxidase (HRP)-conjugated goat anti-mouse as the secondary antibody was purchased from Jackson ImmunoResearch Laboratories Inc. (West Grove, PA, USA). Monoclonal Armenian Hamster anti-CT2 specific for the last 17 amino acids (SSLSYTNPAVAATSANL) of human and mouse MUC1 cytoplasmic domain was a gift from Dr. Sandra J. Gendler (Mayo Clinic Scottsdale, Arizona, USA). HRP-conjugated goat anti-Armenian Hamster as secondary was purchased from Jackson Lab Inc.

Cells and Reagents

Ascites is an excessive "acellular" fluid collected from peritoneal cavities of cancer patients that contains secreted MUC1[131]. MCF-7, a human breast adenocarcinoma cell line with moderate MUC1 expression was purchased from American Type Culture Collection (ATCC). It was maintained in DMEM supplemented with 10% (v/v) FBS and 6 μg/ml of insulin. ZR-75-1, a poorly differentiated human mammary carcinoma cell line with moderate MUC1 expression was purchased from ATCC. It was maintained in RPMI 1640 supplemented with 10% (v/v) FBS and 2 mM L-glutamine. MDA-MB-231, a human breast carcinoma cell line expressing low levels of MUC1 was purchased from ATCC. MDA-MB-468, a human breast carcinoma cell line with high levels of epidermal growth factor receptor and low levels of MUC1 expression was also purchased from ATCC. Both MDA-MB-231 and MDA-MB-468 were maintained in DMEM supplemented with 10% (v/v) FBS. 293T/MUC1 and Mock are human MUC1-negative embryonic kidney cells transfected with the

human MUC1 and an empty plasmid, respectively. These were transfected and sub-cloned by Jennifer Rahn in the lab[38], and maintained in DMEM supplemented with 10% (v/v) FBS and 200 μg/ml antibiotic G418. 410.4 is a mouse mammary adenocarcinoma line that was kindly donated by Dr. Gabrielle Zimmerman (Biomira, Canada). It was maintained in RPMI 1640 supplemented with 10% FBS (v/v) and 2 mM L-glutamine. NIH3T3 is a parental mouse fibroblast cell line maintained in DMEM supplemented with 10% (v/v) FBS. NIH3T3/ICAM-1 and NIH3T3/Mock, gifts from Dr. Ken Dimock (University of Ottawa, Ontario, Canada), are NIH3T3 transfected with the human ICAM-1 and an empty plasmid, respectively. The transfectants were maintained in DMEM supplemented with 10% (v/v) FBS and 2 μg/ml Blasticidin S HCl. All cell lines were cultured at 37°C in a humidified incubator containing 5% (v/v) CO_2 (Water-Jacketed Incubator, Forma Scientific, Marietta, OH, USA).

RPMI 1640 medium, Dulbecco's Modified Eagle's Medium (DMEM), deoxycholic acid, Phosphatase Inhibitor Cocktail 2, Protease Inhibitor Cocktail, Trizma hydrochloride (Tris-HCl), Tris Base, Polyoxyethylene-sorbitan monolaurate (Tween 20), tissue culture grade glycine, glycerol, NP40, 2-mercaptoethanol, antibiotic G418, and insulin from bovine pancreas were purchased from Sigma (Saint Louis, MO, USA). Sodium Dodecyl Sulfate (SDS) was purchased from Pierce Biotechnology, Inc. (Rockford, IL, USA). Sodium chloride (NaCl), ammonium persulfate, 40% (w/v) acrylamide stock solution and

methanol were purchased from Fisher Scientific International (Fair Lawn, NJ, USA). Sodium phosphate, dibasic (Na_2HPO_4) and potassium phosphate monobasic (KH_2PO_4) were purchased from Caledon Laboratories Ltd. (Georgetown, Ontario, Canada). Fetal Bovine Serum (FBS), Trypsin (0.5% w/v)-EDTA (5.3 mM) solution, L-glutamine, and Blasticidin S HCl were purchased from Invitrogen Corporation (Burlington, Ontario, Canada). Bromophenol blue was purchased from Bio-Rad Laboratories Ltd. (Mississauga, Ontario, Canada). ECL (enhanced chemiluminescence) Plus Western Blotting detection reagents were purchased Amersham Biosciences (Baie d'Urfe, Quebec, Canada).

Experimental Conditions and Cell Extraction

Cells were cultured on 100 mm x 20 mm tissue culture plates (Corning Inc., Corning, NY, USA) until 70-80% confluent. All cell extraction procedures were performed at 4°C or on ice. Cultured cells were held on ice and washed twice with cold PBS, then scraped into 80 µl of RIPA lysis buffer (150 mM NaCl, 1% (v/v) NP40, 0.5% (w/v) deoxycholic acid, 0.1% (w/v) SDS, 0.5% (v/v) Phosphatase Inhibitor Cocktail 2, 0.5% (v/v) Protease Inhibitor Cocktail, and 50 mM Tris, pH 7.6)[132] with a Teflon policeman. The RIPA lysis buffer was used since it was determined to be more efficient in extracting MUC1 than the Brij-97 lysis buffer in Appendix A. Subsequently, samples were collected in 1.5 ml Eppendorf tubes and lysed with 26 gauge needles (Becton Dickinson and Company, Franklin Lakes, NJ, USA). Lysates were centrifuged at 10,000 x g for 10 min (EBA 12R Hettich Zentrifugen, Rose Scientific Ltd., Edmonton, Alberta,

Canada) and the resulting supernatants were boiled in Laemmli Buffer (47.5% (v/v) dH_2O, 12.5% (v/v) 0.5 M Tris-HCl pH 6.8, 10% (v/v) glycerol, 2% (w/v) SDS, 5% (v/v) of 2-mercaptoethanol, and 0.05% (w/v) bromophenol blue)[133] for 10 min. Samples were either analyzed immediately or stored at -20°C.

SDS-PAGE and Western Blotting

Samples were subjected to Bio-Rad *DC* Protein Assay (Bio-Rad Laboratories, Hercules, CA, USA) and subsequently analyzed on SDS polyacrylamide (7.5% (w/v acrylamide), 10% (w/v acrylamide) and 12% (w/v acrylamide) with 4% (w/v acrylamide) stacking) gels. Electrophoresis was performed using Bio-Rad Mini-PROTEAN II system at 60 mA per gel, 80 V for the initial 15 min followed by 130 V (constant voltage) for the remaining time in Running Buffer (0.3% (w/v) Tris base, 1.44% (w/v) glycine, and 0.1% (w/v) SDS, pH 8.3)[133]. Proteins were then transferred to 0.45 micron Immobilon-P (Millipore Corp., Billerica, MA, USA) membranes via Bio-Rad Mini Trans-Blot system on ice for 60 min at 100 V (constant voltage) and 350 mA in Transfer Buffer (0.3% (w/v) Tris base, 1.44% (w/v) glycine, 0.1% (w/v) SDS, and 20% (v/v) methanol, pH 8.3)[133].

Prior to incubation with the B27.29 or anti-CT2 antibodies, transferred membranes were blocked with 5% (w/v) commercial milk powder in Tris-buffered saline with 0.05% (v/v) Tween-20 (TBS-T) overnight at 4°C or 1 h at room temperature. Membranes were then incubated with either 1 μg/ml of

B27.29 or 0.25 μg/ml of anti-CT2 in TBS-T for 1 h at room temperature. This was followed by three 10 min washes in TBS-T. Membranes previously blotted with B27.29 or anti-CT2 were then incubated in 120 ng/ml of secondary antibodies HRP-conjugated goat anti-mouse or 120 ng/ml of HRP-conjugated goat anti-Armenian hamster diluted in TBS-T, respectively, for 1 h at room temperature. Three 10 minute washes of membranes with TBS-T followed. ECL Plus was used for detection of reactive bands by exposing the membranes to either Fuji Super RX Medical X-ray film or Kodak Biomax ML Scientific Imaging Film (Rochester, NY, USA), and then by developing the films. Film exposure durations ranged from 10 s to 5 min, until the desired image intensity was obtained.

2.1.2. Immunoprecipitation of MUC1 With B27.29 and α-CT2 Monoclonal Antibodies

Objective:

In order to enhance the specificity of MUC1 detection on Western blots, a technique known as immunoprecipitation (IP) was tested. The procedure first utilizes a specific antibody that binds to the protein of interest. The protein-antibody complex is subsequently isolated from the cellular lysate with protein G-agarose. Two antibodies - monoclonal B27.29 and anti-CT2 - were tested for MUC1 immunoprecipitation with the following cell lines: (1) MCF-7, (2) MDA-MB-231, (3) MDA-MB-468, (4) 293T/MUC1, (5) ZR-75-1, (6) NIH3T3, (7) NIH3T3/ICAM-1, and (8) NIH3T3/Mock.

Materials and Methods:

Antibodies

Monoclonal anti-MUC1 B27.29, monoclonal anti-CT2, HRP-conjugated goat anti-mouse, and HRP-conjugated goat anti-Armenian Hamster were previously described in section 2.1.1.

Cells and Reagents

Cell lines and culturing conditions of MCF-7, ZR-75-1, MDA-MB-231, MDA-MB-468, 293T/MUC1, 293T/Mock, NIH3T3, NIH3T3/ICAM-1, and NIH3T3/Mock were previously described in section 2.1.1. All cell lines were cultured at 37°C in a humidified incubator containing 5% (v/v) CO_2.

Protein G-agarose was purchased from Roche Diagnostics Corporation (Laval, Quebec, Canada). Other reagents used were previously described in section 2.1.1.

Experimental Conditions and Cell Extraction

Cells were cultured and extracted with RIPA lysis buffer as previously described in section 2.1.1. Supernatants were subjected to immunoprecipitation (via B27.29 or CT2 antibodies) immediately. Crude samples were boiled in Laemmli Buffer, then either analyzed immediately or stored at -20°C.

Immunoprecipitation of MUC1

All immunoprecipitation procedures were performed at 4°C or on ice. Supernatants were adjusted to final volumes of 1 ml with RIPA lysis buffer. Samples intended for immunoprecipitation via CT2 antibody were first subjected to Bio-Rad *DC* Protein Assay to determine the amount of immunoprecipitating antibody required based on the protein concentrations of samples. In contrast, the quantity of B27.29 antibody needed for immunoprecipitation was based on sample volume. Hence, Protein Assay of the samples intended for immunoprecipitation with B27.29 antibody was unnecessary. Samples were gently agitated overnight with either 10 μg/ml of B27.29 antibody, or 2.5 μg of CT2 monoclonal antibody per milligram of sample proteins. Incubation continued with the addition of 60 μg/ml of protein G-agarose overnight with gentle agitation. Samples were centrifuged at 12,000 x g for 20 s, and pellets

were subsequently washed three times with 1 ml of RIPA buffer. The agarose pellets were re-suspended and boiled in 100 µl of Laemmli Buffer for 10 min, followed by centrifugation at 12,000 x g for 20 s. Supernatants were either analyzed immediately or stored at -20°C. Furthermore, the experimental condition called Mock IP, which consisted of RIPA lysis buffer, immunoprecipitating antibody (B27.29 or anti-CT2) and protein G-agarose was also included. Since this was an "acellular" controlled condition, it was effective in identifying non-specific bands associated with the reagents used in the immunoprecipitation procedure.

SDS-PAGE and Western Blotting

Samples were analyzed with Bio-Rad *DC* Protein Assay and Bio-Rad Mini-PROTEAN II gel (6% (w/v acrylamide) and 10-15% (w/v acrylamide) with 4% (w/v acrylamide) stacking) electrophoresis as described in section 2.1.1. Proteins were then transferred to 0.45 micron Immobilon-P membranes as described in section 2.1.1.

Immunoblotting procedures with the B27.29 and anti-CT2 antibodies, in addition to image development with ECL Plus were previously described in section 2.1.1.

2.1.3. CT2 Peptide-Block of α-CT2 Antibody

Objective:

The detection of non-specific protein bands was a common problem in the Western blots obtained from the MUC1 IP experiments using monoclonal B27.29 antibody (section 2.1.2). This could adversely affect the accuracy of MUC1 cytoplasmic domain identification. Thus, an attempt was made to determine the exact protein bands corresponding to MUC1's cytoplasmic domain in the MCF-7 and GZ.Hi cell lines via MUC1 Western blotting with the CT2 peptide-blocked antibody.

Materials and Methods:

Antibodies

Monoclonal anti-MUC1 B27.29, monoclonal anti-CT2, and HRP-conjugated goat anti-Armenian Hamster were previously described in section 2.1.1.

Cells and Reagents

GZ.Hi is a mouse mammary adenocarcinoma cell line (410.4) transfected with the human MUC1, donated by Dr. Gabrielle Zimmerman. This was maintained in RPMI 1640 supplemented with 10% (v/v) FBS and 2 mM L-glutamine. Cell line and culturing conditions of MCF-7 were previously described in section 2.1.1. Both GZ.Hi and MCF-7 cell lines were cultured at 37°C in a humidified incubator containing 5% (v/v) CO_2.

The purified CT2 peptide was a gift from Dr. S. Gendler. Other reagents used were previously described in sections 2.1.1 and 2.1.2.

Experimental Conditions and Cell Extraction

Cell lines were grown on 100 mm x 20 mm tissue culture plates until 70-80% confluent. Cells were extracted with RIPA lysis buffer as previously described in section 2.1.1. Supernatants were subjected to immunoprecipitation (via B27.29 antibody) immediately. Crude samples were boiled in Laemmli Buffer, then either analyzed immediately or stored at -20°C.

To prepare the CT2 peptide-blocked antibody, a small quantity of purified CT2 peptide was incubated with 7.5 µl of undiluted (0.5 mg/ml) CT2 antibody at room temperature for 15 min. The blocked antibody was then added to 15 ml of 2% (w/v) BSA in TBS-T, which was then used for immunoblotting.

Immunoprecipitation of MUC1

Supernatants were immunoprecipitated for MUC1 with monoclonal B27.29 antibody at 4°C or on ice. Detailed procedures were previously described in section 2.1.2.

SDS-PAGE and Western Blotting

Samples were analyzed with Bio-Rad *DC* Protein Assay and Bio-Rad Mini-PROTEAN II gel (15% (w/v acrylamide) with 4% (w/v acrylamide) stacking) electrophoresis. Proteins were then transferred to 0.45 micron Immobilon-P membranes. Detailed procedures can be found in section 2.1.1.

Two sets of 15% (w/v) polyacrylamide gels were used to analyze the same samples. Transferred membranes were blocked with 5% (w/v) commercial milk powder in TBS-T overnight at 4°C. One membrane was immunoblotted using monoclonal CT2 antibody, while the other with CT2 peptide-blocked antibody, both for 1 h at room temperature. After 3 washes in TBS-T, membranes were subsequently incubated with HRP-conjugated goat anti-Armenian Hamster for 1 h at room temperature. Another round of 3 washes with TBS-T took place, followed by ECL Plus detection on imaging film. Film exposure durations ranged from 10 s to 5 min, until the desired image intensity was obtained.

2.2. Optimization of Co-Culture Conditions

2.2.1. Detecting MUC1 Tyrosine Phosphorylation Under Experimental Conditions Used in Tumor Cell Transmigration Assays

Objective:

Rahn *et al.* (unpublished observations) from our lab discovered that MUC1-ICAM-1 interaction was crucial in mediating tumor cell transendothelial migration through a series of Transwell and antibody-blocking experiments[37]. Moreover, it was found that various experimental conditions had significantly different effects on migration. For instance, tumor cell transmigration was significantly higher in the presence of gelatin matrix, TNF-α and IL-1β cytokines, and fibroblasts as opposed to just gelatin alone[37]. Based on the Transwell experimental data, it was of interest to know whether experimental conditions (the use of gelatin matrix, cytokines, and fibroblast-conditioned media) known to promote tumor cell transendothelial migration would affect the status of MUC1 tyrosine phosphorylation. This was investigated with an *in vitro* MUC1-ICAM-1 co-culturing system that simulated the Transwell experimental conditions known to induce tumor cell transmigration.

Materials and Methods:

Antibodies

Monoclonal mouse anti-phosphotyrosine PY99 was purchased from Santa Cruz Biotechnology, Inc. (Santa Cruz, CA, USA). Monoclonal CT2 antibody, HRP-

conjugated goat anti-mouse, and HRP-conjugated goat anti-Armenian hamster were previously described in sections 2.1.1.

Cells and Reagents

Cell lines and culturing conditions of MCF-7, NIH3T3/ICAM-1 and NIH3T3/Mock were previously described in section 2.1.1.

MEM non-essential amino acids solution was purchased from Invitrogen Corporation. Cytokines TNF-α and Il-1β were purchased from Cedarlane Laboratories Ltd. (Hornby, Ontario, Canada). Sodium orthovanadate (a tyrosine phosphatase inhibitor), Brij-97 detergent, dithiothreitol (DTT), Gelatin (Type A from porcine skin) and Magnesium chloride ($MgCl_2$) were purchased from Sigma. Other reagents used were previously described in section 2.1.

Experimental Conditions and Cell Extraction

Cell lines MCF-7 and NIH3T3/ICAM-1 were cultured on 0.1% (w/v) gelatin-coated 100 mm x 20 mm tissue culture plates until 70-80% confluent. All of the reagents had been equilibrated to 37°C prior to usage. Prior to incubation with NIH3T3 transfectants, plates of MCF-7 were washed twice with sterile PBS. NIH3T3/ICAM-1 and NIH3T3/Mock transfectants were detached from T-150 tissue culture flasks (Corning) with 600 μl Trypsin (0.5% w/v)-EDTA. A count of 3.0×10^6 transfectants was co-cultured with MCF-7s in the presence of media

(DMEM media supplemented with 10% (v/v) FBS, 10U penicillin, 10U streptomycin, 2mM L-glutamine and 0.1mM MEM Non-Essential Amino Acids Solution) that has been used to culture human breast fibroblasts for 5 days (known as fibroblast-conditioned media), along with 20 U/ml TNF-α and Il-1β, with or without 1 mM sodium orthovanadate. Sodium orthovanadate is a tyrosine phosphatase inhibitor that helps to preserve tyrosine phosphorylation of proteins. The final volumes of all experimental conditions were adjusted to 3.5 ml with fibroblast-conditioned media containing cytokines. Co-culturing took place in a 37°C humidified incubator supplemented with 5% (v/v) CO_2 for 10 min. Non-stimulated MCF-7 and NIH3T3/ICAM-1 cell lines, in addition to MCF-7s treated with 1 mM Na_3VO_4 in DMEM + 10% (v/v) FBS media for 10 min were used as controls.

All cell extraction procedures were performed at 4°C or on ice. Cultured cells were washed twice with cold PBS, and the washes were collected in 15 ml centrifuge tubes (Corning) along with the original co-culturing media. The washes were discarded after centrifugation at 1500 RPM and 4°C for 5 min (Centra-GP8R, International Equipment Company, Needham Hits, MA, USA). Cell pellets were re-suspended in 50 µl of Brij-97 lysis buffer (150 mM NaCl, 0.5% (v/v) Brij-97, 1 mM DTT, 0.5% (v/v) Phosphatase Inhibitor Cocktail 2, 0.5% (v/v) Protease Inhibitor, and 50 mM Tris, pH 7.6)[132] and collected in 1.5 ml Eppendorf tubes. Cells that remained on culture plates were scraped into 80 µl

of Brij-97 lysis buffer with a Teflon policeman. Subsequently, samples were collected in the 1.5 ml Eppendorf tube containing the washed pellet counterpart obtained earlier, and lysed with 26 gauge needles. Lysates were centrifuged at 10,000 x g for 10 minutes, and supernatants were subjected to immunoprecipitation (via CT2 antibody) immediately. The crude lysates were boiled in Laemmli Buffer for 10 min, and were either analyzed immediately or stored at -20°C.

Immunoprecipitation of MUC1

All immunoprecipitation procedures were performed at 4°C or on ice. Supernatants adjusted to 1 ml final volumes with Brij-97 lysis buffer were assayed for protein prior to immunoprecipitation with anti-CT2 antibody. Detailed procedures were previously described in section 2.1.2. The Brij-97 lysis buffer was used for all of the washes throughout the immunoprecipitation process. Furthermore, the experimental condition called Mock IP (consisted of Brij-97 lysis buffer, CT2 antibody and protein G-agarose) was also included to identify the non-specific bands associated with the immunoprecipitation procedure.

SDS-PAGE and Western Blotting

Samples were analyzed with Bio-Rad *DC* Protein Assay and Bio-Rad Mini-PROTEAN II gel (10-15% (w/v acrylamide) with 4% (w/v acrylamide) stacking) electrophoresis. Proteins were then transferred to 0.45 micron Immobilon-P membranes. Detailed procedures can be found in section 2.1.1.

Prior to incubation with 0.13 μg/ml PY99 for 1 h at room temperature, membranes were blocked with 2% (w/v) BSA in TBS-T overnight at 4°C. Membranes were subjected to three 10 min washes with TBS-T, followed by 1 h incubation with 120 ng/ml HRP-conjugated goat anti-mouse. After three more 10-minute washes with TBS-T, ECL Plus was used for detection of reactive bands by exposing the membranes to imaging film. Film exposure durations ranged from 10 s to 5 min, until the desired image intensity was obtained. Without stripping, the same membranes were then blocked with 5% commercial milk powder in TBS-T at 4°C for at least 24 h. This served to allow sufficient time for the previous ECL Plus signals (which have a duration of 24 h) to diminish before commencing the next round of Western blotting. Membranes were subsequently incubated with 0.25 μg/ml CT2 antibody for 1 h at room temperature, followed by 3 washes with TBS-T. Then incubation with 120 ng/ml of HRP-conjugated goat anti-Armenian Hamster for 1 h took place, followed by 3 washes with TBS-T. Finally, reactive bands were detected with ECL Plus on imaging film.

The levels of phosphotyrosine and CT2 expressions in each experimental condition were quantified using the Scion Image computer software. The phosphotyrosine level in each condition was then taken as a ratio to the corresponding amount of CT2 and compared. The ANOVA test with a p value of 0.01 was performed to statistically test the null hypothesis that the phosphotyrosine/CT2 ratio of each experimental condition was the same.

2.2.2. Epidermal Growth Factor Stimulation and Detecting MUC1 Tyrosine Phosphorylation of Tumor Cells

Objective:

It was realized that a positive control for MUC1 tyrosine phosphorylation was essential for more accurate analyses of experimental data. Schroeder *et al.* (2001) was able to induce MUC1 tyrosine phosphorylation in the breast carcinoma cell line MDA-MB-468 following treatment with epidermal growth factor[41]. Therefore, the effect of epidermal growth factor stimulation on MUC1 phosphotyrosine detection was investigated with the cell line MDA-MB-468.

Materials and Methods:

Antibodies

Monoclonal anti-phosphotyrosine PY99, monoclonal anti-CT2, HRP-conjugated goat anti-mouse, and HRP-conjugated goat anti-Armenian hamster were previously described in sections 2.1-2.2.

Cells and Reagents

Cell lines and culturing conditions of MCF-7, MDA-MB-468 and NIH3T3/Mock were previously described in section 2.1.1. All cell lines were cultured at 37°C in a humidified incubator containing 5% (v/v) CO_2.

Epidermal growth factor was purchased from Sigma and reconstituted to 10 μg/ml with Nanopure water. Other reagents used were previously described in sections 2.1-2.2.

Experimental Conditions and Cell Extraction

Cell lines were cultured on 100 mm x 20 mm tissue culture plates until 70-80% confluent. They were washed twice with sterile PBS and incubated with FBS-free DMEM media overnight. After 24 h, plates of serum-starved cells were washed twice with sterile PBS and incubated with 2 ml of fresh FBS-free DMEM media for 2 h. This served to reduce the levels of any endogenously-secreted growth factors. MDA-MB-468 cells were then incubated with 100 ng/ml epidermal growth factor for 1 min at 37°C and 5% (v/v) CO_2.

All cell extraction procedures were performed at 4°C or on ice. Cultured cells were washed twice with cold PBS, and the washes were collected in 15 ml centrifuge tubes along with the original culturing media. The washes were discarded after centrifugation at 1500 RPM and 4°C for 5 min. Cell pellets were re-suspended in 50 μl of RIPA lysis buffer and collected in 1.5 ml Eppendorf tubes. Cells that remained on culture plates were scraped into 80 μl of RIPA lysis buffer with a Teflon policeman. Subsequently, samples were collected in the 1.5 milliliter Eppendorf tube containing the washed pellet counterpart obtained earlier, and lysed with 26 gauge needles. Lysates were centrifuged at 10,000 x g

for 10 minutes, and supernatants were subjected to immunoprecipitation (via CT2 antibody) immediately. The crude lysates were boiled in Laemmli Buffer for 10 minutes, which were either analyzed immediately or stored at -20°C.

Immunoprecipitation of MUC1

Supernatants were immunoprecipitated for MUC1 with monoclonal CT2 antibody at 4°C or on ice. Detailed procedures were previously described in section 2.1.2. Furthermore, the experimental condition called Mock IP (consisted of RIPA lysis buffer, CT2 antibody and protein G-agarose) was also included to identify the non-specific bands associated with the immunoprecipitation procedure.

SDS-PAGE and Western Blotting

Samples were analyzed with Bio-Rad *DC* Protein Assay and Bio-Rad Mini-PROTEAN II gel (10-15% (w/v acrylamide) with 4% (w/v acrylamide) stacking) electrophoresis. Proteins were then transferred to 0.45 micron Immobilon-P membranes. Detailed procedures can be found in section 2.1.1.

Detailed procedures for phosphotyrosine and MUC1/CT2 immunoblotting, in addition to ECL Plus detection were previously described in section 2.2.1. Protein stripping was not performed in between consecutive rounds of immunoblotting via antibodies from different species. Instead, membranes were

then blocked with 5% commercial milk powder in TBS-T at 4°C for at least 24 h, as previously described in section 2.2.1.

2.2.3. Detecting MUC1 Tyrosine Phosphorylation Under Experimental Conditions Used in Tumor Cell Calcium Ion Oscillation Assays

Objective:

In addition to promoting tumor cell transendothelial migration, Rahn *et al.* (2004) have recently discovered that MUC1-ICAM-1 interaction could also trigger calcium ion (Ca^{2+}) oscillations in tumor cells[38]. Calcium ion oscillations and protein tyrosine phosphorylations are often key components of cellular signalling events. Therefore, the effect of ICAM-1 stimulation under experimental conditions (the use of FBS matrix and Imaging Buffer) known to induce tumor cell Ca^{2+} oscillations on MUC1 tyrosine phosphorylation was investigated with the MCF-7 cell line.

Materials and Methods:

Antibodies

Monoclonal anti-CT2, monoclonal anti-phosphotyrosine PY99, HRP-conjugated goat anti-mouse, and HRP-conjugated goat anti-Armenian hamster were previously described in sections 2.1-2.2.

Cells and Reagents

Cell lines and culturing conditions of MCF-7, MDA-MB-468, NIH3T3/ICAM-1 and NIH3T3/Mock were previously described in section 2.1.1.

Potassium chloride (KCl), calcium chloride ($CaCl_2$), and 4-(2-Hydroxyethyl)piperazine-1-ethanesulfonic acid (HEPES) were purchased from Sigma. D-glucose was purchased from Fisher Scientific. Other reagents used were previously described in sections 2.1-2.2.

Experimental Conditions and Cell Extraction

Cell lines were cultured on FBS-coated 100 mm x 20 mm tissue culture plates until 70-80% confluent. All of the reagents used during the experiment had been equilibrated to 37°C prior to usage. Plates of cultured cells were washed twice with Imaging Buffer (152 mM NaCl, 5.4 mM KCl, 0.8 mM $MgCl_2$, 1.8 mM $CaCl_2$, 10 mM HEPES, 5.6 mM glucose, pH 7.2)[134]. NIH3T3/ICAM-1 and NIH3T3/Mock transfectants were detached from T-150 tissue culture flasks with 600 µl Trypsin (0.5% w/v)-EDTA (5.3 mM). A count of 2.18×10^8 transfectants (from three confluent T-150 flasks) were resuspended in 1 ml with Imaging Buffer and co-cultured with each plate of MCF-7s. Co-culturing took place in a 37°C humidified incubator supplemented with 5% (v/v) CO_2 for 1 min and 4 min. Non-stimulated MCF-7 and NIH3T3/Mock cells were used as controls. MCF-7 cells that were incubated with 1 ml of Imaging Buffer for 1 minute and 4 minutes were also used as controls. Furthermore, MDA-MB-468 cells stimulated with 100 ng/ml EGF for 1 min (as described in section 2.2.2) were used as positive controls for MUC1 phosphorylation.

Detailed cell extraction procedures with were previously described in section 2.2.1, with the exception that RIPA lysis buffer was used here instead of Brij-97.

Immunoprecipitation of MUC1

Supernatants were immunoprecipitated for MUC1 with monoclonal CT2 antibody at 4°C or on ice. Detailed procedures were previously described in section 2.1.2. Furthermore, the experimental condition called Mock IP (consisted of RIPA lysis buffer, CT2 antibody and protein G-agarose) was also included to identify the non-specific bands associated with the IP procedure.

SDS-PAGE and Western Blotting

Samples were analyzed with Bio-Rad *DC* Protein Assay and Bio-Rad Mini-PROTEAN II gel (10-15% (w/v acrylamide) with 4% (w/v acrylamide) stacking) electrophoresis. Proteins were then transferred to 0.45 micron Immobilon-P membranes. Detailed procedures can be found in section 2.1.1.

Detailed procedures for phosphotyrosine and MUC1/CT2 immunoblotting, in addition to ECL Plus detection were previously described in section 2.2.1. Protein stripping was not performed in between consecutive rounds of immunoblotting via antibodies from different species. Instead, membranes were then blocked with 5% (w/v) commercial milk powder in TBS-T at 4°C for at least 24 h, as previously described in section 2.2.1.

The levels of phosphotyrosine and CT2 expressions in each experimental condition were quantified using the Scion Image computer software. The phosphotyrosine level in each condition was then taken as a ratio to the corresponding amount of CT2 and compared. The ANOVA and Newman-Keuls tests with a p value of 0.05 were performed to statistically test the null hypothesis that the phosphotyrosine/CT2 ratio of each experimental condition was the same.

2.2.4 Alkaline Phosphatase Treatment of Western Blot Membranes From MUC1-ICAM-1 Co-Culturing Experiments

Objective:

The effect of ICAM-1 stimulation under experimental conditions known to induce tumor cell Ca^{2+} oscillations on MUC1 tyrosine phosphorylation was investigated with the MCF-7 cell line (section 2.2.3). Although the appropriate MUC1-positive and negative controls were included in the Western blots that tested for MUC1 phosphorylation, an additional test was employed in attempt to validate the phosphorylation status of the protein bands on Western blots. This was accomplished by treating Western blot membranes from the MUC1-ICAM-1 co-culturing experiments with alkaline phosphatase.

Materials and Methods

Antibodies

Monoclonal anti-phosphotyrosine PY99 and HRP-conjugated goat anti-mouse were previously described in sections 2.1-2.2.

Cells and Reagents

Cell lines and culturing conditions of MCF-7, MDA-MB-468, NIH3T3/ICAM-1 and NIH3T3/Mock were previously described in section 2.1.1.

Alkaline phosphatase in solution 20 x 10^3 units/ml (each unit is equivalent to enzyme activity that hydrolyzes 1 μmol of 4-nitrophenyl phosphate in 1 min at

37°C) was purchased from Roche Diagnostics. Other reagents used were previously described in sections 2.1-2.2.

Experimental Conditions and Cell Extraction

Please refer to section 2.2.3.

Immunoprecipitation of MUC1

Please refer to section 2.2.3.

SDS-PAGE and Western Blotting

Samples were analyzed with Bio-Rad *DC* Protein Assay and Bio-Rad Mini-PROTEAN II gel (10-15% (w/v acrylamide) with 4% (w/v acrylamide) stacking) electrophoresis. Proteins were then transferred to 0.45 micron Immobilon-P membranes. Detailed procedures can be found in section 2.1.1.

The transferred membrane was blocked with 2% BSA (w/v) in TBS-T overnight at 4°C. The membrane was removed from the blocking solution, and the lanes with the EGF-stimulated MDA-MB-468 and NIH3T3/ICAM-1-stimulated MCF-7 samples were cut into halves with a razor blade. The two cut-off halves of the membrane were incubated with 6.7 units of alkaline phosphatase in dephosphorylation buffer (0.5 M Tris-HCl and 1 mM EDTA, pH 8.5) for 6 h at 37°C and 5% CO_2.

Detailed procedures for phosphotyrosine immunoblotting and ECL Plus detection were previously described in section 2.2.1.

Chapter 3

EXPERIMENTAL RESULTS

3.1. Optimization of Western Blot and Immunoprecipitation

3.1.1. Immunoblot for MUC1 with B27.29 and α-CT2 Monoclonal Antibodies

The ability to detect the human mucin protein MUC1 through Western blotting was a basic prerequisite for analyzing results in this project. Two methods are commonly used in the literature for MUC1 immunoblotting. The first approach is to use an antibody specific for the extracellular tandem repeats of MUC1, such as the monoclonal B27.29. This antibody has been shown in the literature to be effective in detecting the full-length MUC1 protien [41, 42, 85]. Alternatively, antibodies (e.g. anti-CT2) that target the cytoplasmic tail segment of MUC1 can also be used. Therefore, it was attempted to detect the full-length or cytoplasmic domain of MUC1 via Western blot from ascites and the following cell lines: (1) MCF-7, (2) 410.4, (3) ZR-75-1, (4) MDA-MB-231, (5) MDA-MB-468, (6) 293T/MUC1, (7) 293T/Mock, (8) NIH3T3, (9) NIH3T3/ICAM-1, and (10) NIH3T3/Mock by using monoclonal B27.29 and anti-CT2 antibodies, respectively. The MUC1 expression pattern of these cell lines have already been determined by our lab and/or the literature. Therefore, they were useful for evaluating the effectiveness of the Western blotting techniques used in this project.

The mouse monoclonal B27.29 antibody is reactive against the PDTRPAP amino acid epitope located on the tandem repeats of MUC1's extracellular domain[35]. The capability to detect MUC1 with this antibody was first tested on samples of ascites, NIH3T3 and MCF-7 cells. Ascites is an excessive "acellular" fluid collected from peritoneal cavities of cancer patients that contains the secreted

(non membrane-bound) MUC1 isoform[131]. Hence, it was used as a MUC1-positive control. MCF-7 is a human breast adenocarcinoma cell line that has been used as the main experimental model throughout this project. Therefore, it was essential to determine its MUC1 expression pattern. Samples of ascites, NIH3T3 and MCF-7 were analyzed on a 7.5% (w/v) polyacrylamide gel and Western blotted for the full-length MUC1 with B27.29 antibody. Reactive protein bands were detected at greater than 200 kDa in the ascites and MCF-7s (red asterisks in lanes 1, 2, 5, 6, Figure 11), but not NIH3T3 mouse fibroblasts (lanes 3 and 4, Figure 11). Sometimes these bands were seen as a discrete doublet at lower protein concentrations (lanes 1 and 2, Figure 11). The molecular weights of the protein bands detected in Figure 11 were consistent with those reported for full-length MUC1 in the literature, which ranged from 200-500 kDa [41, 42, 85]. Therefore, the data suggested that we were capable of detecting the full-length MUC1 through Western blotting with B27.29 antibody. Also, the NIH3T3 mouse fibroblasts could be used as a MUC1-negative control for subsequent Western blots since they lacked MUC1 expression (lanes 3 and 4, Figure 11). Interestingly, additional protein bands of unknown identities located within the 127-200 kDa range were detected in the MCF-7 cells (lanes 5 and 6, Figure 11). These bands could represent degraded products of the MUC1 extracellular tandem repeats generated prior to cell lysing.

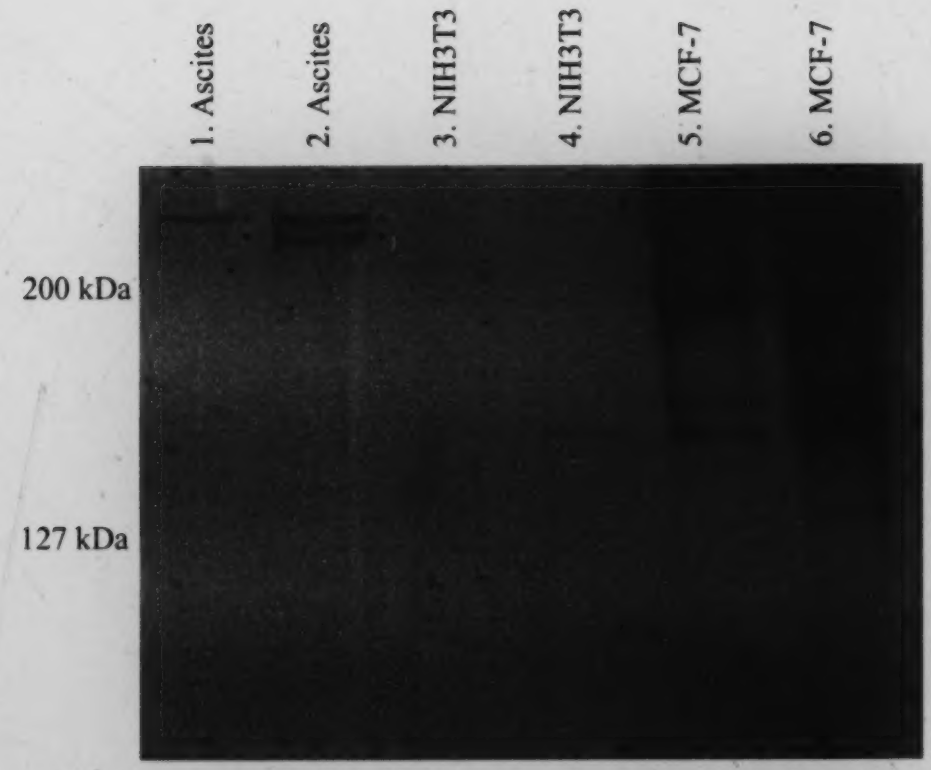

Figure 11. Full-length MUC1 detected upon Western blotting crude lysates with monoclonal B27.29 antibody on a 7.5% (w/v) polyacrylamide gel. Samples of ascites (lanes 1 and 2), mouse fibroblast NIH3T3 (lanes 3 and 4), and MCF-7 (lanes 5 and 6) were analyzed. Protein concentrations in lanes 2, 4 and 6 were double those in lanes 1, 3 and 5, respectively. Distinct protein bands (sometimes seen as a doublet at lower protein concentrations) above 200 kDa were detected in the ascites and MCF-7 samples (red asterisks), but absent in NIH3T3. Additional protein bands between 127 kDa and 200 kDa were found exclusively in MCF-7 cells.

MUC1 detection was then extended to more cell lines including the human breast carcinomas MDA-MB-231, MDA-MB-468 and ZR-75-1. The human embryonic kidney cell line 293T transfected with either human MUC1 or an empty plasmid (designated 293T/MUC1 and 293T/Mock, respectively) were also analyzed for MUC1 expression. Furthermore, mouse fibroblasts NIH3T3 transfected with either human ICAM-1 or an empty plasmid (designated NIH3T3/ICAM-1 and NIH3T3/Mock, respectively) were tested for the presence of MUC1 as well since these cell lines would be used in the later co-culture experiments. The crude lysates of these cell lines were analyzed on a 10% (w/v) polyacrylamide gel. After immunoblotting the samples with B27.29 antibody, distinct protein bands (sometimes seen as a doublet) at 250 kDa and above were detected in the MCF-7, 293T/MUC1, MDA-MB-231, MDA-MB-468 and ZR-75-1 samples (lanes 1, 2, 4, 6 and 8, Figure 12A). The molecular weights and patterns of the detected bands were consistent with those found in Figure 11. Moreover, these protein bands corresponded with the literature values of full-length MUC1[41, 42, 85], suggesting that they were most likely the full-length MUC1. Therefore, the data indicated that the B27.29 antibody and Western blotting technique used here were effective in detecting the full-length MUC1. In contrast, the same protein bands (at ≥250 kDa) were not detectable in the 293T/Mock, NIH3T3/ICAM-1 and NIH3T3/Mock transfectants (lanes 3, 5 and 7, Figure 12A). Hence, these transfectants could be used as MUC1-negative controls for future Western blots since they lack MUC1 expression.

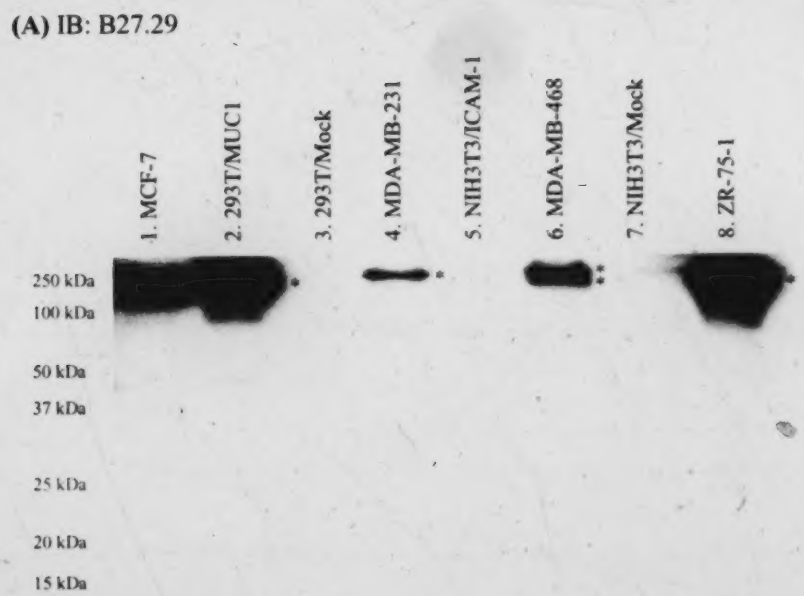

Figure 12. Full-length and cytoplasmic domains of MUC1 detected upon Western blotting crude lysates on a 10% (w/v) polyacrylamide gel. **(A)** Detection of full-length MUC1 with monoclonal B27.29 antibody. Distinct protein bands (sometimes seen as a doublet) at 250 kDa and above detected in lanes 1, 2, 4, 6 and 8 (red asterisks). **(B)** The same membrane from **(A)** was re-probed for MUC1 cytoplasmic domain with monoclonal CT2 antibody. Specific protein smears at ~21-25 kDa and ~17-19 kDa were readily detected in lanes 1, 6 and 8 (blue asterisks).

The same membrane from Figure 12A was subsequently re-probed for MUC1's cytoplasmic domain with monoclonal CT2 antibody without stripping. Unique protein smears from ~21-25 kDa and ~17-19 kDa were detected in the MUC1-positive cell lines MCF-7, MDA-MB-468 and ZR-75-1 (blue asterisks in lanes 1, 6 and 8, Figure 12B). These molecular weights were consistent with those reported in the literature for MUC1's cytoplasmic domain (usually range from 20-30 kDa)[43, 132]. Therefore, the data suggested that CT2 antibody was capable of detecting the cytoplasmic domain (CT2) of MUC1 in the Western blotting technique used. Consistent with this argument, the protein smears at ~21-25 kDa and ~17-19 kDa were absent in the 293T/Mock, NIH3T3/ICAM-1 and NIH3T3/Mock transfectants (lanes 3, 5 and 7, Figure 12B). These cells lines were also shown earlier to lack MUC1 expression via immunoblotting with B27.29 antibody (Figure 12A). Interestingly, the MUC1/CT2 bands were almost undetectable in the MUC1-positive MDA-MB-231 cell line, which has previously been reported to express low levels of the protein[83] (lane 4, Figure 12B). This was also true with the 293T/MUC1 transfectants (lane 2, Figure 12B), which was consistent with the other data from our lab (not shown). A possible reason for the obvious detection of full-length MUC1 in the MDA-MB-231 and 293T/MUC1 cell lines (Figure 12A) was most likely due to the larger number of tandem repeats in MUC1's extracellular domain, and hence, epitopes reactive against the B27.29 antibody.

Dr. Gendler's lab (donor of the monoclonal CT2 antibody used in this project) has previously detected the molecular weights of MUC1's cytoplasmic domain to range from 16-28 kDa with the CT2 antibody[83]. In order to further investigate the presence of MUC1 below 20 kDa, samples were analyzed on a higher (12% w/v) percentage polyacrylamide gel to achieve better protein separation at the lower molecular weight range. Upon Western blotting with the CT2 antibody, an intense protein smear at ~20-30 kDa and a band at ~19 kDa were detected in the MCF-7 and two of the 293T/MUC1 samples (red arrows in lanes 1, 5 and 7, Figure 13). These values were consistent with those found in Figure 12B, and the molecular weights of MUC1's cytoplasmic domain in the literature[43, 83, 132, 135]. Therefore, they were most likely to be specific MUC1/CT2 bands. Furthermore, the same protein bands were detected in the mouse mammary adenocarcinoma cell line 410.4 (red arrows in lane 2, Figure 13). This observation was expected since the CT2 antibody is reactive to the conserved sequence of the MUC1 cytoplasmic domain in both human and mouse[41]. An additional protein band at ~17 kDa was detected in two of the 293T/MUC1 transfectant clones (blue asterisks in lanes 5 and 7, Figure 13), which corresponded closely to the 17 kDa MUC1/CT2 band found by Dr. Gendler's lab [83]. Therefore, the presence of MUC1 cytoplasmic domain below 20 kDa was confirmed. However, the lower bands were much less intense than the ~20-30 kDa MUC1/CT2 smear, suggesting that not all isoforms or fragments

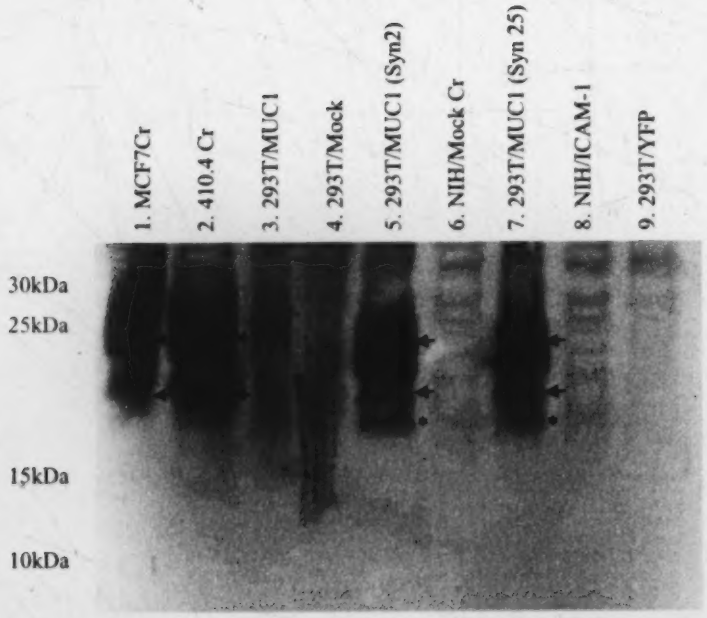

Figure 13. MUC1 cytoplasmic domains detected upon Western blotting crude lysates with monoclonoal CT2 antibody on a 12% (w/v) polyacrylamide gel. Intense protein smear at ~20-30 kDa and a band at ~19 kDa were present in lanes 1, 2, 5 and 7 (red arrows). The same smear of much lower intensity was observed in lane 3. An additional protein band at ~17 kDa was detected in lanes 5 and 7 (blue asterisks). The protein bands described above of comparable intensities were absent in lanes 4, 6, 8 and 9.

of MUC1's cytoplasmic domain were present in equal amounts. Although the 17 kDa MUC1/CT2 band was not observed in the MCF-7s, the band was detected in subsequent Western blots where even higher percentage gels were used. Therefore, the resolution of the separating gels apparently had a strong influence on the detectability of MUC1/CT2 bands below 20 kDa. The proteins at ~17 kDa, ~19 kDa and ~20-30 kDa of comparable intensities were absent in the 293T/Mock, NIH3T3/ICAM-1 and NIH3T3/Mock cell lines (lanes 4, 6, 8 and 9, Figure 13), which were previously confirmed to lack MUC1 expression (Figure 12B). This would further support that these bands were specific MUC1 cytoplasmic domains. The MUC1 cytoplasmic domain was almost undetectable in the 293T/MUC1 cells (lane 3, Figure 13), which was consistent with Figure 12B and other previous lab data (not shown). Furthermore, 293T cells transfected with the YFP plasmid were also MUC1 negative as expected (lane 9, Figure 13).

3.1.2. Immunoprecipitation of MUC1 With B27.29 and α-CT2 Monoclonal

In order to enhance the specificity of MUC1 detection on Western blots, a technique known as immunoprecipitation (IP) was tested. The procedure first utilizes a specific antibody that binds to the protein of interest. The protein-antibody complex is subsequently isolated from the cellular lysate with protein G-agarose. Two antibodies - monoclonal B27.29 and anti-CT2 - were tested for MUC1 immunoprecipitation with the following cell lines: (1) MCF-7, (2) MDA-MB-231, (3) MDA-MB-468, (4) 293T/MUC1, (5) ZR-75-1, (6) NIH3T3, (7) NIH3T3/ICAM-1, and (8) NIH3T3/Mock.

Two antibodies were tested for MUC1 immunoprecipitation, monoclonal B27.29 and anti-CT2. First, MCF-7 lysates were immunoprecipitated with B27.29 antibody and analyzed on a 6% (w/v) polyacrylamide gel. A distinct doublet of protein bands above 199 kDa were detected upon immunoblotting the samples with B27.29 antibody (red asterisks in lane 4, Figure 14A). The doublet was also present in the ascites and MCF-7 crude lysate (red asterisk in lanes 1 and 3, Figure 14A). The molecular weight of this doublet closely matched the molecular weights of full-length MUC1 found in earlier experiments (Figures 11 and 12A) and literature[41, 42, 85]. In addition, the protein doublet was absent in the NIH3T3 mouse fibroblasts (lane 2, Figure 14A), which was previously determined to lack MUC1 expression (Figure 11). Therefore, the data suggested

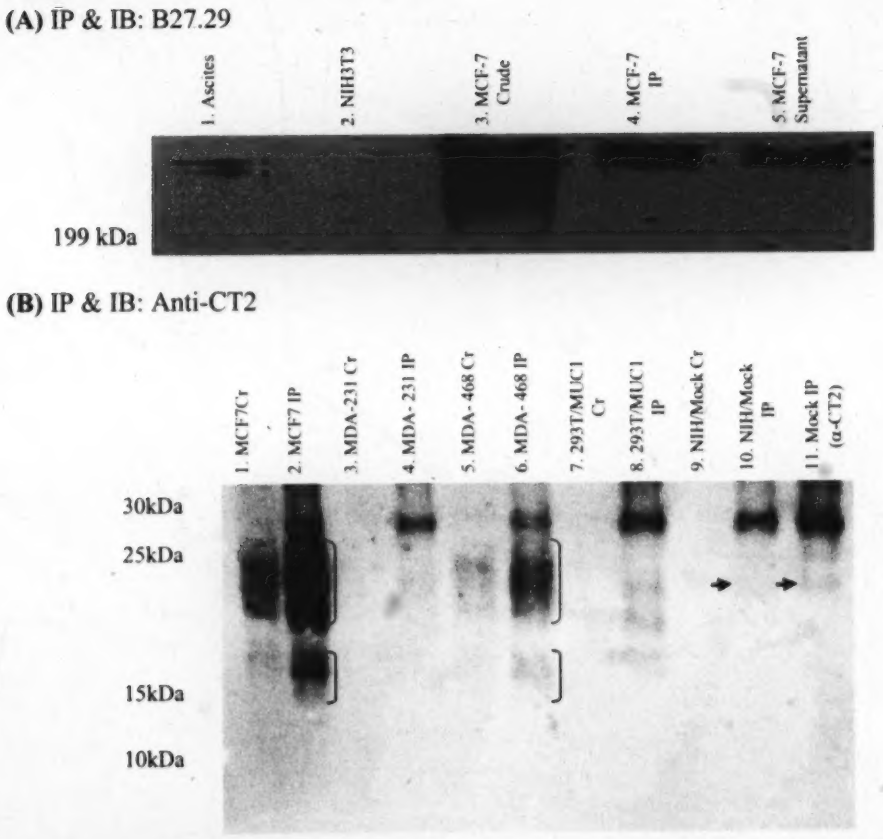

Figure 14. MUC1 immunoprecipitation with monoclonals B27.29 and anti-CT2 were effective in extracting MUC1. **(A)** Immunoprecipitation and Western blot with B27.29 antibody on a 6% (w/v) polyacrylamide gel. Lanes 1 and 2 were MUC1-positive and -negative controls, respectively. Lane 3 was MCF-7 crude lysate. Lane 4 was MCF-7 lysate immunoprecipitated with B27.29 antibody, and lane 5 was the remaining supernatant after immunoprecipitation. Distinct protein bands (usually seen as a doublet) above 199 kDa detected in lanes 1, 3 and 4 (red asterisks), but absent in lane 2. The same protein doublet was also present in the lane 5 (red arrows). **(B)** Immunoprecipitation and Western blot with CT2 antibody on a 10-15% (w/v) polyacrylamide gel. Lanes 9 and 10 were MUC1-negative controls. Lane 11 was also a MUC1-negative control since it consisted of only RIPA lysis buffer, CT2 antibody and protein G-agarose. Distinct protein smears at ~20-24 kDa and ~13-17 kDa were most readily detected in lanes 2 and 6 (red and blue brackets, respectively). The same protein bands were hardly detected in the MDA-MB-231 and 293T/MUC1 samples. A non-specific protein band at ~22 kDa band was present in lanes 10 and 11 (red arrows), which could easily be mistaken for a CT2 band.

that monoclonal B27.29 antibody was capable of isolating the full-length MUC1 isoform from cellular lysates in the immunoprecipitation procedures used here. Interestingly, the MUC1 doublet was also detected in the IP supernatant from which the protein G-agarose pellet was extracted (red arrows in lane 5, Figure 14A). This would suggest that the IP procedure was not 100% efficient in purifying MUC1 from the MCF-7 lysates.

Subsequently, immunoprecipitation of MUC1 was attempted using the monoclonal CT2 antibody. Cell lines previously determined to express MUC1 such as MCF-7, MDA-MB-231, MDA-MB-468 and 293T/MUC1 (Figure 12) were subjected to immunoprecipitation via CT2 antibody. The NIH3T3/Mock transfectants were also immunoprecipitated with CT2 antibody to be used as a MUC1-negative control. The experimental condition called Mock IP (lane 11, Figure 14B), which consisted RIPA lysis buffer, immunoprecipitation antibody (anti-CT2) and protein G-agarose was also included as a MUC1-negative control. It served to identify the non-specific protein bands associated with the immunoprecipitation procedure. The IP samples along with their corresponding crude (non-IP) counterparts were analyzed on a 10-15% (w/v) polyacrylamide gel and Western blotted for MUC1's cytoplasmic domain. Non-specific protein bands were identified with the NIH3T3/Mock crude and IP samples, as well as the Mock IP. Distinct protein smears at ~20-24 kDa were most readily detected in the MCF-7 IP and MDA-MB-468 IP samples (red brackets in lanes 2 and 6, Figure 14B). However, these bands were less intense in the MDA-MB-468 sample, and

hardly detected in the MDA-MB-231s and 293T/MUC1s due to their constitutive low MUC1 expression (Figure 14B). The molecular weights of these protein bands were consistent with the MUC1/CT2 bands found in earlier experiments (Figure 12B and 13) and the literature values of MUC1's cytoplasmic domain[43, 81, 83, 132]. Furthermore, the protein bands described above were absent in the NIH3T3/Mock samples, which were determined to lack MUC1 expression in earlier experiments. Therefore, the data suggested that monoclonal CT2 antibody was capable of isolating the cytoplasmic domain of MUC1 from cellular lysates in the immunoprecipitation procedures used here.

The MUC1/CT2 bands ranging from ~13-17 kDa were more readily detectable in the MUC1-positive MCF-7 IP, and to a lesser extent in the MDA-MB-468 IP samples (blue brackets in lanes 2 and 6, Figure 14B). Interestingly, reports on detecting the 13 kDa MUC1/CT2 band are not found in the literature. Therefore, the real identity of a possible 13 kDa band within the ~13-17 kDa protein smear remained to be determined. In addition, a non-specific protein band at ~22 kDa (red arrows in lanes 10 and 11, Figure 14B) was present in the NIH3T3/Mock IP and Mock IP, which must represent a reagent from the immunoprecipitation procedure. This non-specific band could easily be mistaken for a MUC1/CT2 band due to its location on Western blots, and hence, will be carefully noted.

3.1.3. CT2 Peptide-Block of α-CT2 Antibody

The detection of non-specific protein bands was a common problem in the Western blots obtained from the MUC1 IP experiments using monoclonal B27.29 antibody (section 3.1.2). This could adversely affect the accuracy of MUC1 cytoplasmic domain identification. Thus, an attempt was made to determine the exact protein bands corresponding to MUC1's cytoplasmic domain in the MCF-7 and GZ.Hi cell lines.

In order to identify the precise MUC1/CT2 protein bands, the CT2 peptide-block experiment was performed. Crude and IP (via B27.29 antibody) samples of MCF-7 and GZ.Hi (mammary adenocarcinoma cell line transfected with the human MUC1) were analyzed on a 15% (w/v) polyacrylamide gel. Distinct protein bands at ~24 kDa and 20 kDa were detected in all MCF-7 and GZ.Hi samples (red arrows in lanes 2-5, Figure 15A) upon immunoblotting with CT2 antibody. Two additional bands at ~17 kDa and 13 kDa were seen exclusively in MCF-7s (blue asterisks in lanes 2 and 3, Figure 15A). The protein bands described above were absent in the MUC1-negative control, which consisted of only the B27.29 antibody diluted in RIPA lysis buffer (lane 1, Figure 15A). Therefore, the protein bands at ~24 kDa, 20 kDa, 17 kDa and 13 kDa as seen in Figure 15A could represent MUC1's cytoplasmic domain.

To confirm the identities of the bands detected in Figure 15A, the same samples were analyzed on a separate 15% polyacrylamide gel. However, the CT2

(A) IB: Anti-CT2

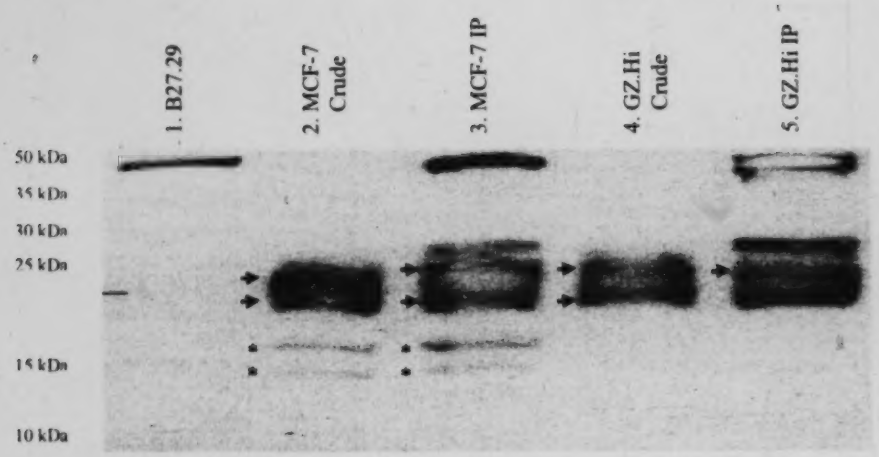

(B) IB: Pre-blocked anti-CT2

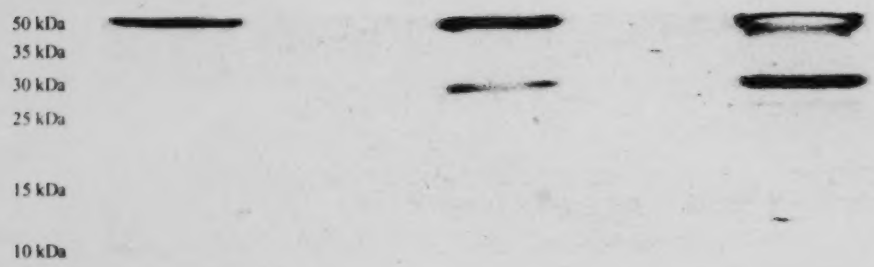

Figure 15. Molecular weights of MUC1 cytoplasmic domain identified with CT2 peptide-blocked CT2 antibody. **(A)** Western blot of crude and IP (via B27.29 antibody) samples for MUC1's cytoplasmic domain with CT2 antibody on a 15% (w/v) polyacrylamide gel. Distinct protein bands at ~24 kDa and 20 kDa detected in lanes 2-5 (red arrows). Two additional bands at ~17 kDa and 13 kDa seen exclusively in lanes 2 and 3 (blue asterisks). Protein bands at ~50 kDa and 27 kDa only present in the IP samples, most likely corresponding to the heavy and light chains of B27.29, respectively. **(B)** The same concentrations of samples from **(A)** were analyzed on a separate 15% (w/v) polyacrylamide gel and Western blotted with CT2 antibody that was pre-blocked with purfied CT2 peptides. The bands at ~24 kDa, 20 kDa, 17 kDa and 13 kDa seen in **(A)** were not detected with the pre-blocked CT2 antibody. The heavy and light chains of B27.29 antibody remained present on the membrane (~50 kDa and 27 kDa, respectively).

antibody used for immunoblotting had been pre-blocked with purfied CT2 peptides. This would prevent the antibody from binding to any MUC1 cytoplasmic domain present on the membrane. The protein bands at ~24 kDa, 20 kDa, 17 kDa and 13 kDa seen in Figure 17A were not detected with the pre-blocked CT2 antibody (Figure 15B). In contrast, the heavy and light chains of B27.29 antibody (~50 kDa and 27 kDa, respectively) remained detectable (lanes 3 and 5, Figure 15B). Therefore, the preliminary data suggested two important points. First, the peptide-blocking procedure was successful in blocking all the binding sites on the CT2 antibody as shown by the lack of MUC1 detection in Figure 15B. Secondly, the protein bands at ~24 kDa, 20 kDa, 17 kDa and 13 kDa detected by Western blotting with monoclonal anti-CT2 were most likely the MUC1 cytoplasmic domain. This also confirmed the questionable band at ~13 kDa from Figure 14B to be MUC1, which would be a novel molecular weight of MUC1/CT2 that has not been reported in the literature.

3.2. Optimization of Co-Culture Conditions

3.2.1. Detecting MUC1 Tyrosine Phosphorylation Under Experimental Conditions Used in Tumor Cell Transmigration Assays

Rahn *et al.* (unpublished observations) from our lab discovered that MUC1-ICAM-1 interaction was crucial in mediating tumor cell transendothelial migration through a series of Transwell and antibody-blocking experiments[37]. Moreover, it was found that various experimental conditions had significantly different effects on migration. For instance, tumor cell transmigration was significantly higher in the presence of gelatin matrix, TNF-α and IL-1β cytokines, and fibroblasts as opposed to just gelatin alone[37]. Based on the Transwell experimental data, it was of interest to know whether experimental conditions known to promote tumor cell transendothelial migration would affect the status of MUC1 tyrosine phosphorylation. This was investigated with an *in vitro* MUC1-ICAM-1 co-culturing system that simulated the Transwell experimental conditions known to induce tumor cell transmigration.

The human breast carcinoma cell line MCF-7 was used as the experimental model, which would be more physiologically relevant than using the GZ.Hi and 410.4 mouse cell lines. MCF-7 cells were cultured on gelatin-coated tissue culture plates until 70-80% confluent, and were then co-cultured with NIH3T3/ICAM-1 or NIH3T3/Mock transfectants with fibroblast-conditioned media and cytokines for 10 min at 37°C and 5% (v/v) CO_2, with or without sodium orthovanadate. The MCF-7 lysates were immunoprecipitated for MUC1

with CT2 antibody. Subsequently, the samples were analyzed on 10-15% (w/v) polyacrylamide gels and Western blotted with PY99 antibody for phosphotyrosines (Figures 16A, C and E). The non-specific protein bands were identified with the Mock IP condition, which consisted of Brij-97 lysis buffer, CT2 antibody and protein G-agarose (lane 9, Figures 16A, C and E). Another MUC1-negative control, NIH3T3/ICAM-1 mouse fibroblasts was also included to identify non-specific protein bands (lane 8, Figures 16A, C and E). After having taken the non-specific bands into consideration, a unique phosphotyrosine band at ~17 kDa was detected in the MUC1-positive MCF-7 samples that have been stimulated with the ICAM-1 or Mock transfectants (red asterisks in lanes 3-7, Figures 16A, C and E). The same phosphotyrosine band was also found the in the non-stimulated MCF-7s (lanes 1 and 2, Figures 16A, C and E). Therefore, this band was a potential candidate for tyrosine-phosphorylated MUC1, although it was detected in the MCF-7s regardless of the presence of ICAM-1.

In order to determine the identity of the ~17 kDa phosphotyrosine band, the same membranes from Figures 16A, C and E were re-probed with CT2 antibody after at least 24 h from the initial phosphotyrosine detection. The membranes were not stripped in between consecutive Western blotting for reasons discussed in section 4.2. After the identification of the non-specific bands with the NIH3T3/ICAM-1 IP and Mock IP (lanes 8 and 9, respectively, Figures 16B, D and F), a unique MUC1/CT2 band at ~17 kDa was detected exclusively in the MCF-7 samples

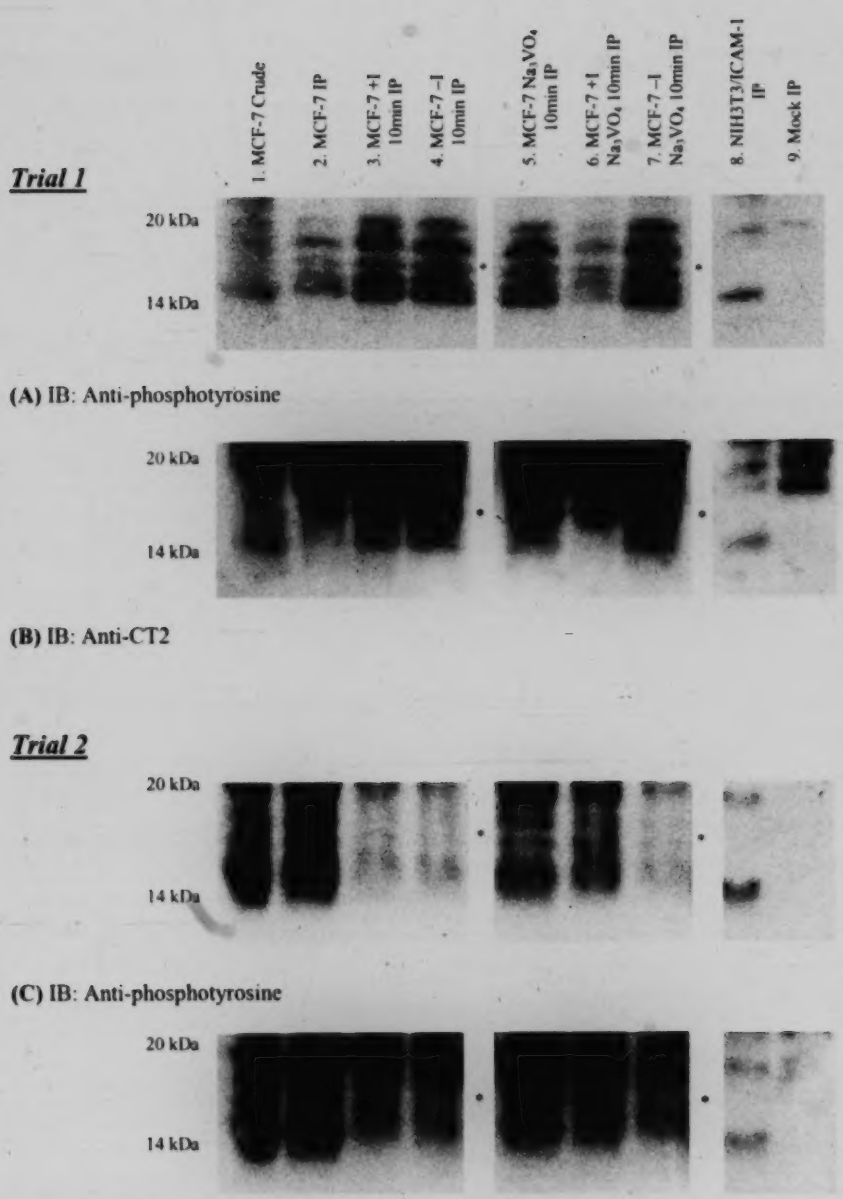

Figure 16. (To be continued on next page)

Trial 3

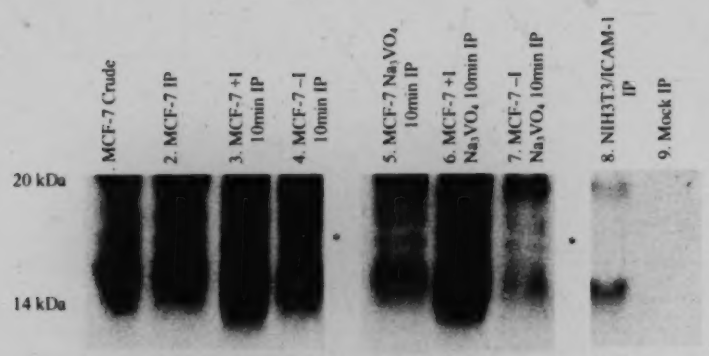

(E) IB: Anti-phosphotyrosine

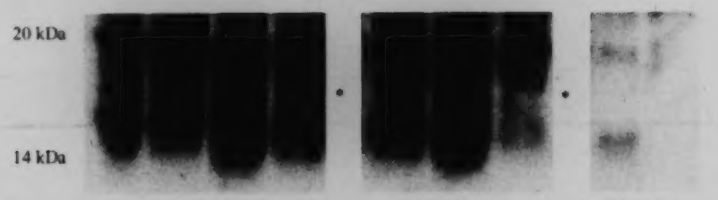

(F) IB: Anti-CT2

Figure 16. MUC1 tyrosine phosphorylation detected when MCF-7 cells cultured on gelatin-coated tissue culture plates were stimulated with (+I) or without (-I) ICAM-1 and ± sodium orthovanadate (Na_3VO_4). Samples analyzed on 10-15% (w/v) polyacrylamide gels. **(A, C and E)** Western blots for phosphotyrosines with PY99 antibody. Distinct phosphotyrosine band at ~17 kDa detected exclusively in lanes 1-7 (red asterisks). **(B, D and F)** The same membranes re-probed for MUC1's cytoplasmic domain with CT2 antibody. A specific CT2 band at ~17 kDa detected in lanes 1-7 (blue asterisks). This band also matched with the molecular weight of the ~17 kDa phosphotyrosine band detected in **(A, C and E)**.

(blue asterisks in lanes 1-7, Figures 16B, D and F). Interestingly, this ~17 kDa MUC1/CT2 band matched up with the ~17 kDa phosphotyrosine band detected earlier in Figures 16A, C and E (red asterisks) when the film images were overlaid. Therefore, the data suggested that putative tyrosine-phosphorylated MUC1 was identified at ~17 kDa, which was present when MCF-7 cells were stimulated with either NIH3T3/ICAM-1 or NIH3T3/Mock, regardless of the presence of Na_3VO_4.

In order to determine the effect of ICAM-1 stimulation on MUC1 tyrosine phosphorylation, the intensity levels of the unique protein bands from Figures 16A-F were quantified using the Scion Image computer software. The phosphotyrosine level in each lane was then taken as a ratio to the corresponding amount of CT2 and compared on a bar graph (Figure 17). Subsequently, the phosphotyrosine/CT2 ratios were analyzed with the ANOVA test using a p value of 0.01. There was no statistical difference in MUC1 phosphorylation levels among any of the experimental conditions. Therefore, the presence of ICAM-1 and/or sodium orthovanadate had no significant effect on MUC1 tyrosine phosphorylation under experimental conditions known to promote *in vitro* tumor cell transendothelial migration.

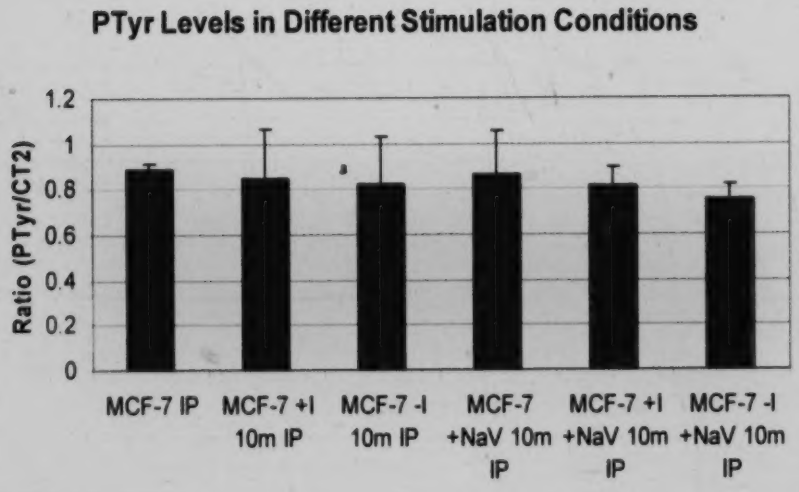

Figure 17. Based on data from three sets of experiments, MUC1 tyrosine phosphorylation levels of MCF-7 cells cultured on gelatin-coated tissue culture plates were unaffected by the presence of fibroblast-conditioned media (+ TNF-α and IL-1B), ICAM-1 (± I) or sodium orthovanadate (± NaV). The ratio of phosphotyrosine/CT2 levels for each experimental condition was quantified using the Scion Image computer software. The ratios were subsequently analyzed with the ANOVA test using a p value of 0.01. The phosphotyrosine/CT2 ratios were not significantly different between the experimental conditions. (IP = immunoprecipitation; m = minute)

3.2.2. Epidermal Growth Factor Stimulation and Detecting MUC1 Tyrosine Phosphorylation of Tumor Cells

It was realized that a positive control for MUC1 tyrosine phosphorylation was essential for more accurate analyses of experimental data. Schroeder *et al.* (2001) was able to induce MUC1 tyrosine phosphorylation in the breast carcinoma cell line MDA-MB-468 following treatment with epidermal growth factor[41]. Therefore, the effect of epidermal growth factor stimulation on MUC1 phosphotyrosine detection was investigated with the cell line MDA-MB-468.

The MUC1-positive cell line MDA-MB-468 was treated with epidermal growth factor (EGF) for 1 min, and lysates were immunoprecipitated with CT2 antibody. Subsequently, samples were analyzed on 10-15% (w/v) polyacrylamide gels and Western blotted with PY99 antibody for phosphotyrosines (Figure 18A). The non-specific protein bands were identified with the Mock IP condition, which consisted of only the RIPA lysis buffer, CT2 antibody and protein G-agarose (lane 7, Fig18A). Another MUC1-negative control, NIH3T3/Mock transfectants was also included to identify non-specific protein bands (lane 5, Fig18A). Two distinct phosphotyrosine bands at ~17 kDa and 19 KDa were detected only when MDA-MB-468 cells were stimulated with EGF (blue and red asterisks, respectively in lanes 2-4, Figure 18A). Therefore, these bands were potential candidates for tyrosine-phosphorylated MUC1.

(A) IB: Anti-phosphotyrosine

1. MDA-MB-468 IP
2. MDA-MB-468 EGF 1min IP Trial 1
3. MDA-MB-468 EGF 1min IP Trial 2
4. MDA-MB-468 EGF 1min IP Trial 3
5. NIH3T3/Mock IP
6. MCF-7 IP
7. Mock IP
20 kDa
14 kDa

(B) IB: Anti-CT2

Figure 18. MUC1 tyrosine phosphorylation detected upon treating MDA-MB-468 cells with epidermal growth factor (EGF) treatment of for 1 min. Samples were analyzed on 10-15% (w/v) polyacrylamide gels. **(A)** Western blot for phosphotyrosines with PY99 antibody. Distinct phosphotyrosine bands at ~17 kDa and 19 kDa detected in lanes 2-4 (blue and red asterisks, respectively). **(B)** The same membranes from **(A)** re-probed for MUC1's cytoplasmic domain with CT2 antibody. A non-specific protein band at ~19 kDa (red asterisks) detected in MDA-MB-468 and MCF-7 samples, as well as the Mock IP. A specific CT2 band at ~17 kDa (blue asterisks) found exclusively in MCF-7 and MDA-MB-468 samples (lanes 1-4 and 6). Hence, only the ~17 kDa phosphotyrosine band in **(A)** was MUC1.

In order to confirm identities of the ~17 kDa and 19 kDa phosphotyrosine bands, the same membranes from Figure 18A were re-probed with monoclonal CT2 antibody at least 24 hours after the initial detection reaction. The membranes were not stripped in between consecutive Western blotting for reasons discussed in section 4.2. Two protein bands at ~17 kDa and 19 kDa were readily detected in the MUC1-positive samples (blue and red asterisks, respectively, in lanes 1-4 and 6, Figure 18B). These two bands also mactched up with the phosphotyrosine bands (~17 kDa and 19 kDa) found in Figure 18A when the film images were overlaid. However, the ~19 kDa band in Figure 18B was also seen in the Mock IP (red asterisk in lane 7), and hence, was unlikely to represent the MUC1 cytoplasmic domain. This would also suggest the ~19 kDa phosphotyrosine band (red asterisk in lanes 2-4, Figure 18A) was unlikely to be tyrosine-phosphorylated MUC1. Interstingly, the ~17 kDa band (blue asterisks in lanes 1-4 and 6) in Figure 18B was exclusive to the MUC1-positive samples. Therefore, it was most likely a specific CT2 band corresponding to MUC1's cytoplasmic domain, suggesting the ~17 kDa phosphotyrosine band (blue asterisk in lanes 2-4, Figure 18A) was most likely tyrosine-phosphorylated MUC1. This was also consistent with the molecular weight of the MUC1 tyrosine phosphorylation (at ~17 kDa) found in Figure 16. Therefore, the data suggested that putative MUC1 tyrosine phosphorylation at ~17 kDa was detected in the MDA-MB-468 cell line upon EGF stimulation. This experimental condition would be a feasible positive control for MUC1 phosphorylation in subsequent experiments. However, it should be noted that the ~17 kDa MUC1 phosphorylation found in this

experiment differed in molecular weight from those found by Schroeder *et al.* (2001), which were at just below 30 kDa and 25 kDa[41].

3.2.3. Detecting MUC1 Tyrosine Phosphorylation Under Experimental Conditions Used in Tumor Cell Calcium Ion Oscillation Assays

In addition to promoting tumor cell transendothelial migration, Rahn *et al.* (2004) have recently discovered that MUC1-ICAM-1 interaction could also trigger calcium ion (Ca^{2+}) oscillations in tumor cells[38]. Calcium ion oscillations and protein tyrosine phosphorylations are often key components of cellular signalling events. Therefore, the effect of ICAM-1 stimulation under experimental conditions (the use of FBS matrix and Imaging Buffer) known to induce tumor cell Ca^{2+} oscillations on MUC1 tyrosine phosphorylation was investigated with the MCF-7 cell line.

MCF-7 tumor cells were cultured on FBS-coated tissue culture plates until 70-80% confluent, which were then co-cultured with NIH3T3/ICAM-1 or NIH3T3/Mock transfectants for 1 and 4 min at 37°C and 5% (w/v) CO_2. The lysates were immunoprecipitated for MUC1 with monoclonal CT2 antibody. Subsequently, samples were analyzed on 10-15% (w/v) polyacrylamide gels and Western blotted with PY99 for phosphotyrosines (Figures 19A, C and E). The non-specific protein bands were identified with the Mock IP condition, which consisted of only RIPA lysis buffer, monoclonal CT2 antibody and protein G-agarose (lane 11, Figures 19A, C and E). Another MUC1-negative control, NIH3T3/Mock transfectants was also included to identify the non-specific protein bands (lane 10, Figures 19A, C and E). After taking the non-specific bands into

Trial 1

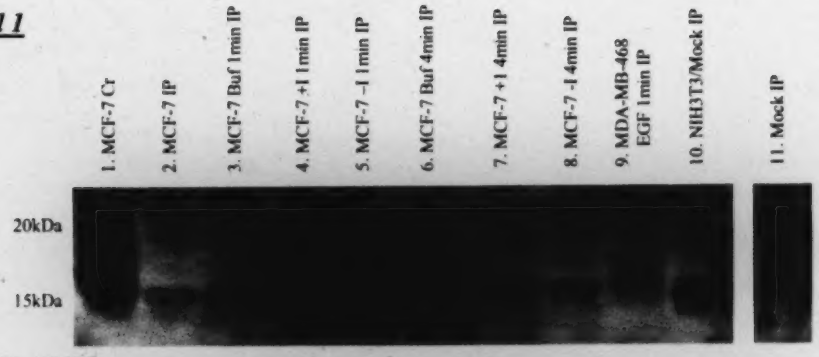

(A) IB: PY99

(B) IB: Anti-CT2

Trial 2

(C) IB: PY99

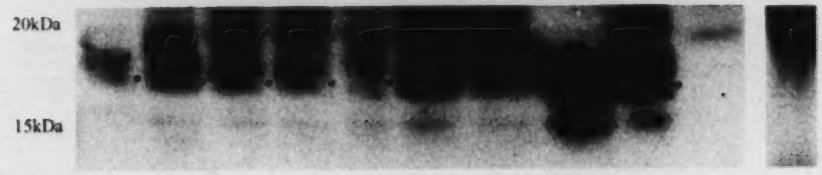

(D) IB: CT2

Figure 19. (To be continued on next page)

Trial 3

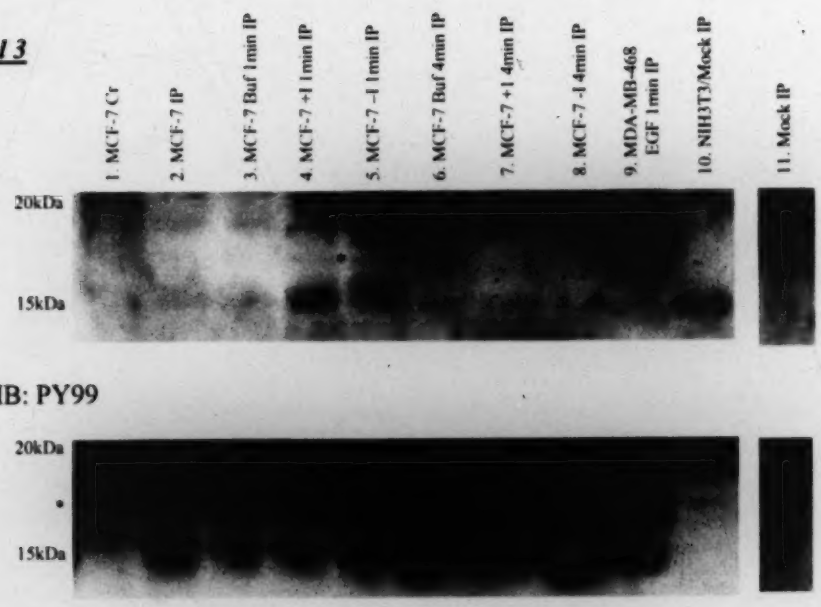

Figure 19. MUC1 tyrosine phosphorylation detected only after 1 min of stimulation. MCF-7 cells cultured on FBS-coated tissue culture plates were stimulated with (+I) or without (-I) ICAM-1. Non-stimulated MCF-7 cells were incubated in Imaging Buffer (Buf). Samples were immunoprecipitated with CT2 antibody and analyzed on 10-15% (w/v) polyacrylamide gels. **(A, C and E)** Western blots for phosphotyrosines with PY99 antibody. Distinct phosphotyrosine band at ~17 kDa most readily detected in lanes 4, 5 and 9 (red asterisks). **(B, D and F)** The same membranes re-probed for MUC1 cytoplasmic domain with CT2 antibody. A specific CT2 band at ~17 kDa detected in lanes 1-9 (blue asterisks). This band also matched with the molecular weight of the ~17 kDa phosphotyrosine band detected in **(A, C and E)**.

consideration, a unique phosphotyrosine band at ~17 kDa was most readily detected when MCF-7 cells were stimulated with NIH3T3/ICAM-1 or NIH3T3/Mock for 1 min (red asterisks in lanes 4 and 5, Figures 19A, C and E). The same band was also detected in the MDA-MB-468s that were treated with EGF for 1min (red asterisk in lane 9, Figures 19A, C and E). This condition has previously been shown to be a feasible positive control for MUC1 tyrosine phosphorylation (Figure 18). Therefore, the ~17kDa phosphotyrosine band was a potential candidate for the tyrosine-phosphorylated MUC1. However, the phosphotyrosine band was noticeably less detectable in the MCF-7s when co-culturing was extended to 4 min (lanes 7 and 8, Figures 19A, C and E). Furthermore, the band was absent in the non-stimulated MCF-7 cells that were incubated with Imaging Buffer for 1 min and 4 min (lanes 3 and 6, respectively, Figures 19A, C and E).

In order to determine the identity of the ~17 kDa phosphotyrosine band, the same membranes from Figures 19A, C and E were re-probed with CT2 antibody at least 24 hours after the initial detection reaction (Figures 19B, D and F). The membranes were not stripped in between consecutive Western blotting for reasons discussed in section 4.2. A unique MUC1/CT2 band at ~17 kDa was detected exclusively in all of the MUC1-positive samples (blue asterisks in lanes 1-9, Figures 19B, D and F). The band also mactched up with the ~17 kDa phosphotyrosine band found in Figure 19A, C and E when the film images were overlaid. Therefore, the data suggested that putative MUC1 tyrosine

phosphorylation was detected at ~17 kDa, consistent with the findings from Figures 16 and 18.

In order to determine the effect of ICAM-1 stimulation on MUC1 tyrosine phosphorylation, the intensity levels of the unique protein bands from Figures 19A-F were quantified using the Scion Image computer software. The phosphotyrosine level in each lane was then taken as a ratio to the corresponding amount of CT2 and compared on a bar graph (Figure 20). The phosphotyrosine/CT2 ratios were first analyzed with the test of ANOVA using a p value of 0.05, which led to rejection of the null hypothesis. Subsequently, the data were analyzed with the Newman-Keuls test using a p value of 0.05. It was found that only ICAM-1 and Mock co-culturing for 1 min had significantly increased the extent of MUC1 tyrosine phosphorylation (asterisks in Figure 20). Furthermore, phosphorylations attenuated to basal levels (MCF-7s incubated with only Imaging Buffer for 1 min and 4 min) after 4 min of co-culturing with the NIH3T3 transfectants.

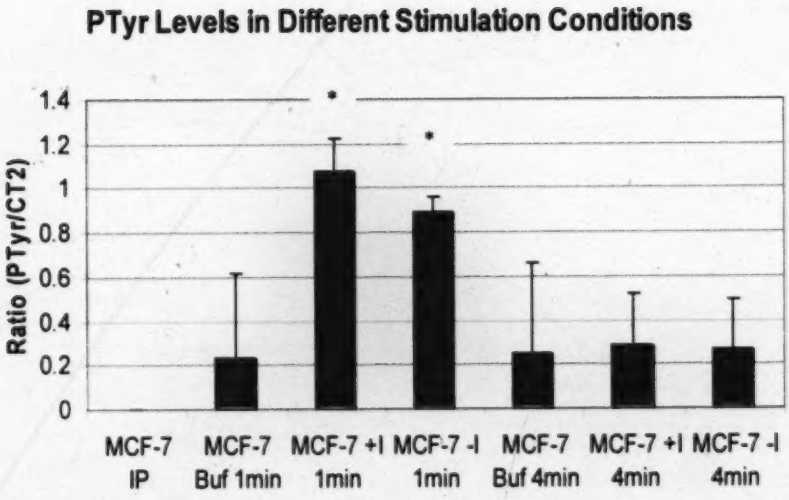

Figure 20. Based on data from three sets of experiments, significant induction of MUC1 tyrosine phosphorylation observed only when MCF-7 cells cultured on FBS-coated tissue culture plates were either stimulated with (+I) or without (-I) ICAM-1 for 1 min. The ratio of phosphotyrosine/CT2 levels for each experimental condition was quantified using the Scion Image computer software. The ratios were subsequently analyzed with the ANOVA and Newman-Keuls tests using a p value of 0.05. The phosphotyrosine/CT2 ratio was significantly higher when MCF-7 cells were stimulated for 1 min with either ICAM-1 or Mock transfectants. However, these two conditions were not significantly different from each other.

3.2.4. Alkaline Phosphatase Treatment of Western Blot Membranes From MUC1-ICAM-1 Co-Culturing Experiments

The effect of ICAM-1 stimulation under experimental conditions known to induce tumor cell Ca^{2+} oscillations on MUC1 tyrosine phosphorylation was investigated with the MCF-7 cell line (section 2.2.3). Although the appropriate MUC1-positive and negative controls were included in the Western blots that tested for MUC1 phosphorylation, an additional test was employed in attempt to validate the phosphorylation status of the protein bands on Western blots. This was accomplished by treating Western blot membranes from the MUC1-ICAM-1 co-culturing experiments with alkaline phosphatase.

Three samples from a MUC1/ICAM-1 co-culturing experiment under Ca^{2+} oscillation assay conditions (section 3.2.3) were analyzed on a 10-15% (w/v) polyacrylamide gel. They were (1) MDA-MB-468s stimulated with EGF for 1 minute, (2) MCF-7s incubated with imaging buffer for 1 min, and (3) MCF-7s co-cultured with NIH3T3/ICAM-1 for 1 min (lanes 1-3, respectively, Figure 21). Sections of the membrane consisted of halves of lanes 1 and 3 were cut off and incubated with alkaline phosphatase for 6 h at 37°C and 5% (v/v) CO_2. Subsequently, all sections of the membrane were Western blotted for phosphotyrosines with monoclonal PY99 antibody. A distinct phosphotyrosine band at ~17 kDa (red asterisks) was detected exclusively in the MDA-MB-468/EGF 1 min and MCF-7/ICAM-1 1 min conditions regardless of prior

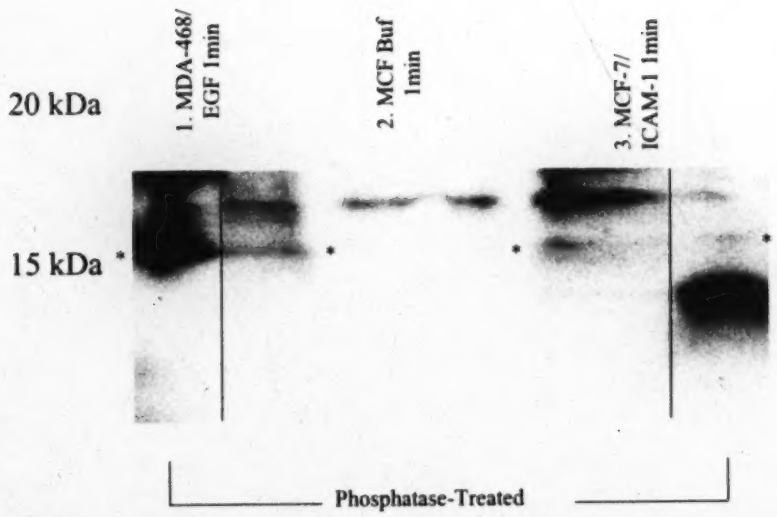

Figure 21. Phosphatase treatment on sections of the membrane was ineffective in removing phosphotyrosines bands. Samples from a MUC1/ICAM-1 co-culturing experiment (section 2.2.3) were analyzed on a 10-15% (w/v) polyacrylamide gel. Sections of the membrane consisted of halves of lanes 1 and 3 were cut off and incubated with alkaline phosphatase for 6 h at 37°C and 5% (v/v) CO_2. All sections of the membrane were then Western blotted for phosphotyrosines with monoclonal PY99 antibody. A distinct phosphotyrosine band at ~17 kDa (red asterisks) was detected exclusively in lanes 1 and 3, regardless of treatment with alkaline phosphatase.

treatment with alkaline phosphatase (lanes 1 and 3, Figure 21). The molecular weight of this band was previously found to be tyrosine-phosphorylated MUC1 in earlier experiments (Figures 16, 18 and 19). The same protein band was not detected in the MCF-7 cells incubated with imaging buffer for 1 min (lane 2, Figure 21). This condition was also shown earlier to lack MUC1 tyrosine phosphorylation in section 3.2.3 (Figure 19). Unfortunately, there was insufficient lysate to repeat this experiment. Also, there was no control utilized so that confirmation of the ability of this technique to remove phosphorylated residues is lacking. Given these shortcomings, the preliminary data suggested that the protocol used here for treating Western blot membrane with alkaline phosphatase was ineffective in removing tyrosine phosphorylation of protein bands.

Chapter 4

DISCUSSION AND CONCLUSION

4.1. Introduction

Breast cancer is the most frequently diagnosed cancer and the second leading cause of cancer deaths in Canadian women[4]. Tumor metastasis is the major cause of death in these patients. MUC1 is overexpressed and under-glycosylated in greater than 90% of human breast cancer. In a minority of cases, the expression of this oncogene becomes cytoplasmic or circumferential (non-apical) and is correlated with higher nodal metastatic frequency and poor prognosis[55]. Regimbald *et al.* (1996) discovered that MUC1 could bind to ICAM-1, and subsequent work from our lab has demonstrated that such interaction was more than just simple binding[34]. It was found that MUC1-ICAM-1 interaction was crucial in mediating *in vitro* tumor cell transmigration (unpublished observations)[37], and the induction of intracellular calcium ion oscillations in tumor cells[38]. Therefore, it seems like MUC1-ICAM-1 interaction may be an important event in facilitating tumor metastasis.

The cytoplasmic domain of MUC1 contains seven tyrosine residues, some of which when phosphorylated, can associate with signalling molecules (i.e. β-catenin, Grb2/Sos, PKCδ, GSK3β, Src, and EGFR) implicated in tumorigenesis[41, 81, 85, 87, 130]. Thus, there is strong evidence supporting the signalling role of MUC1 in promoting tumor progression. Although the modulation of MUC1 tyrosine phosphorylation was shown to be possible via artificial stimuli (i.e. EGF and CD-8 antibody)[41, 91], the physiological modulator remains unknown. Since ICAM-1 is capable of triggering both

transmigration and calcium ion oscillation of MUC1-positive tumor cells, it is of interest to determine whether ICAM-1 can also induce MUC1 tyrosine phosphorylation. The objective of this thesis was to investigate whether MUC1-ICAM-1 interaction can trigger subsequent phosphorylation of tumor cell MUC1 under experimental conditions known to induce tumor cell transendothelial migration and calcium ion oscillation. Therefore, finding MUC1 phosphorylation would suggest the significance of ICAM-1 in modulating interactions between MUC1 and signalling molecules (i.e. Grb2/Sos)[85] and signalling pathways (i.e. ERK/MAPK)[41] potentially involved in the promotion of tumor progression.

4.2. Review and Discussion of Experimental Data

The ability to detect the human mucin protein MUC1 through Western blotting was one of the most basic prerequisites for analyzing results in this project. MUC1 immunoblotting can be accomplished by using antibodies that either target the extracellular tandem repeats or the cytoplasmic tail segment of MUC1. The mouse monoclonal B27.29 antibody is reactive against the PDTRPAP amino acid epitope located on the tandem repeats of MUC1's extracellular domain[35]. As demonstrated in section 3.1.1, B27.29 antibody could consistently detect the full-length MUC1, which was usually seen as a smear. This could be due to differential glycosylation of MUC1 in the extracellular VNTR region[42, 68, 69], although experiments involving deglycosylation of MUC1 would be necessary for verification. Sometimes the full-length MUC1 was detected as a protein doublet at lower protein concentrations. The heavier protein band of the doublet most

likely represented MUCX, a more glycosylated form of MUC1 due to higher threonine content[42]. The fact that MUCX migrates less readily down SDS-gel systems than MUC1 can be attributed to its greater mass, less sialylation or both[42]. The molecular weights of the reactive protein bands were greater than 200 kDa (Figure 11 and 12A), consistent with the literature values (200-500 kDa) for the full-length MUC1[41, 42, 85]. Interestingly, additional protein bands of unknown identities were also detected within the 127-200 kDa range (Figure 11) with the B27.29 antibody. Although these bands have not been reported in the literature, they could be degradation products of MUC1 (still consisting of the extracellular tandem repeats) that were generated prior to cell lysing. This could explain why they were lighter in molecular weights than the full-length MUC1, but yet, still detected by the B27.29 antibody.

Subsequently, we tested the monoclonal CT2 antibody for its MUC1-detecting capability. The antibody is specific for the last 17 amino acids (SSLSYTNPAVAATSANL) of the human and mouse MUC1 cytoplasmic domains[41]. A unique protein smear at ~20-30 kDa, and additional bands at ~17 kDa and 19 kDa were detected in the MUC1-positive cell lines of both human and mouse origins (Figure 12B and 13). These molecular weights were consistent with those reported in the literature for MUC1's cytoplasmic domain, which usually ranged from 16-30 kDa[43, 83, 135]. However, MUC1/CT2 bands below 20 kDa were often less readily detected than those of greater molecular weights. The reason for this discrepency is unknown, although cross-reactivity of the CT2

antibody was unlikely as determined later in the CT2 peptide-block experiment (section 3.1.3). Perhaps the MUC1/CT2 bands below 20 kDa were degradation products of MUC1's cytoplasmic domain, and that these protein fragments were only a small fraction of the total MUC1 population. Hence, the relatively lower quantities of these proteins would reduce their detectability on Western blots.

MUC1's cytoplasmic domain was hardly detectable in the MUC1-positive MDA-MB-231 cell line (Figure 12B). This was consistent with the findings from Schroeder *et al.* (2003), who have also reported low MUC1 expression in this cell line[83]. In addtion, low MUC1/CT2 detection was observed with the 293T/MUC1 transfectants (Figure 12B and 13), which was consistent with other data from our lab (not shown). However, the full-length MUC1 was readily identified in the MDA-MB-231 and 293T/MUC1 cell lines (Figure 12A). This was most likely due to the larger number of tandem repeats in MUC1's extracellular domain, and hence, epitopes reactive against the B27.29 antibody. Consequently, the full-length MUC1 would be much easier to detect than the cytoplasmic domain, which consists of only a single epitope for the CT2 antibody. A final comment was that cell lines NIH3T3, NIH3T3/ICAM-1, NIH3T3/Mock and 293T/Mock were shown to lack MUC1 expression (Figure 12 and 13). Therefore, these cell lines are suitable MUC1-negative controls for Western blots. The data from section 3.1.1 suggested that the Western blotting protocol was effective for both monoclonal B27.29 and CT2 antibodies to detect the full-length and cytoplasmic domains of MUC1, respectively.

In order to enhance the specificity of MUC1 detection on Western blots, a technique known as immunoprecipitation (IP) was tested in section 3.1.2. The procedure first utilizes a specific antibody that binds to the protein of interest. The protein-antibody complex is subsequently isolated from the cellular lysate with protein G-agarose. Protein G is a component of the bacteria cell wall that is covalently coupled to cross-linked agarose beads. It has the capability of binding to the Fc-parts of most mammalian IgGs with high affinity[136]. Two antibodies - monoclonal B27.29 and anti-CT2 - were tested for MUC1 immunoprecipitation. Monoclonal B27.29 antibody was effective in immunoprecipitating the full-length MUC1 exclusively from MUC1-positive cellular lysates. The immunoprecipitated MUC1 was greater than 199 kDa (Figure 14A), which closely matched the molecular weights of the full-length MUC1 found in earlier experiments (Figures 11 and 12A) and the literature[41, 42, 85]. However, MUC1 extraction was not 100% efficient as the protein remained detectable in the IP supernatants from which the protein G-agarose pellets were extracted (Figure 14A). This inefficiency was expected since complete protein extraction often requires multiple rounds of immunoprecipitation.

Although we have shown the feasibility of using B27.29 antibody for MUC1 IP, the findings of Quin *et al.* (2000) suggested a potential pitfall in this approach[132]. The two protein segments comprising the mature MUC1 are non-covalently joined at the SEA domain[58, 71]. However, the site of association is SDS detergent-sensitive, which would cause the dissociation of MUC1's

extracellular domain from the rest of the membrane-embedded protein[58]. The RIPA lysis buffer used for cell lysis and immunoprecipitation procedures contained SDS detergent. In an immunoprecipitation reaction, B27.29 antibody binds to the epitope located in MUC1's extracellular domain. The subsequent addition of protein G-agarose serves to extract B27.29-MUC1 complexes from the other unbound proteins. However, the presence of SDS in an immunoprecipitation reaction would present the risk of dissociating MUC1's two segments. If this were true, then only MUC1's extracellular domain would remain bound to B27.29, and hence, extracted by the protein G-agarose. This would be problematic since tyrosine phosphorylation occurs on the cytoplasmic domain of MUC1, which could potentially be lost during an immunoprecipitation procedure. Therefore, it would be more advantageous to immunoprecipitate with anti-CT2 antibody to maximize MUC1 cytoplasmic domain extraction.

To test our hypothesis, we used monoclonal CT2 antibody to immunoprecipitate MUC1 from cellular lysates. The MUC1 cytoplasmic domain bands obtained from immunoprecipitation weighed ~20-24 kDa and 13-17 kDa (Figure 14B). These molecular weights were consistent with those found in earlier experiments (Figure 12B and 13) and the literature[43, 83, 132, 135]. The MUC1/CT2 bands at ~13-17 kDa were most readily detected in the MCF-7 cell line (Figure 14B). Interestingly, the 13 kDa MUC1/CT2 band has not been reported in the literature, and hence, its identity was questionable. Furthermore, MUC1/CT2 detection was difficult in cell lines MDA-MB-231, MDA-MB-468 and 293T/MUC1, apparently

due to their low constitutive MUC1 expression (Figure 14B). These findings were consistent with our lab's data (Figure 12B and 13; and other data not shown) and the literature[83]. It should be noted that a non-specific protein band at ~22 kDa was identified in the NIH3T3/Mock IP and Mock IP (Figure 14B). This non-specific band most likely arose from the immunoprecipitation procedure and could easily be mistaken as a CT2 band on Western blots. Therefore, special attention was necessary for Western blot analyses. The data from section 3.1.2 suggested that both monoclonal B27.29 and CT2 antibodies were effective in MUC1 extraction in the immunoprecipitation procedures used here.

The detection of non-specific protein bands on Western blots was a common problem, especially for IP samples obtained with B27.29 antibody (section 3.1.2). This could adversely affect the accuracy of MUC1 cytoplasmic domain identification in subsequent experiments. Thus, it was necessary to identify the precise CT2 protein bands corresponding to MUC1 on Western blots. Western blotting the crude and immunoprecipitated (via B27.29 antibody) samples of MCF-7 and GZ.Hi with CT2 antibody revealed distinct MUC1 bands at ~24 kDa, 20 kDa, 17 kDa and 13 kDa (Figure 15A). In contrast, these protein bands were undetected when the same samples were immunoblotted with the pre-blocked CT2 antibody (Figure 15B). However, the heavy and light chains of B27.29 antibody (~50 kDa and 27 kDa, respectively) remained detectable (lanes 3 and 5, Figure 15B). The lack of MUC1 detection (Figure 15B) showed that the peptide-blocking procedure was effective in blocking all the binding sites on the CT2

antibody. Therefore, the preliminary data from section 3.1.3 suggested that protein bands at ~24 kDa, 20 kDa, 17 kDa and 13 kDa identified by Western blotting with the CT2 antibody were most likely MUC1's cytoplasmic domains. This also confirmed the questionable band at ~13 kDa from Figure 14B to be MUC1, which would be a novel moleuclar weight fragment of MUC1's cytoplasmic domain previously unreported in the literature.

It was realized that a positive control for MUC1 tyrosine phosphorylation was essential for more accurate analyses of experimental data. Schroeder *et al.* (2001) was able to induce MUC1 tyrosine phosphorylation in the breast carcinoma cell line MDA-MB-468 with epidermal growth factor (EGF) stimulation [41]. Therefore, it was attempted to repeat their findings in section 3.2.2. The MDA-MB-468 cells were treated with EGF for 1 min and Western blotted with PY99 antibody for phosphotyrosines (Figure 18A). Two distinct phosphotyrosine bands at ~17 kDa and 19 KDa were detected only in the stimulated MDA-MB-468 cells (Figure 18A). A common protocol used for consecutive Western blotting in the literature is to strip membranes with Stripping Buffer in order to remove any bound antibodies. This approach was tried but no longer employed in this project after several attempts due to some undesirable side-effects. In addition to the removal of bound antibodies, the stripping process often resulted in the loss of proteins from membranes. Also, protein properties on membranes were frequently altered, sometimes resulting in the crossing-over of protein lanes and very messy blots that made interpretation very difficult. Therefore, consecutive

Western blotting done throughout this project was to simply allow sufficient time for the previous ECL Plus signals (which have a duration of 24 hours) to diminish before commencing the next round of antibody staining. The same membranes from Figure 20A were then re-probed with CT2 antibody and a specific MUC1/CT2 band at ~17 kDa was identified in the MDA-MB-468s (Figure 18B). This CT2 band also corresponded to the ~17 kDa phosphotyrosine band seen in Figure 18A, suggesting that tyrosine-phosphorylated MUC1 was identified at ~17 kDa. The identified molecular weight of the MUC1 phosphorylation was also consistent with those found in Figure 16. Therefore, the data from section 3.2.2 suggested that putative MUC1 tyrosine phosphorylation at ~17 kDa was detected in the MDA-MB-468 cell line upon EGF stimulation. This experimental condition would be a feasible positive control for MUC1 phosphorylation in subsequent experiments. However, the molecular weight of MUC1 phosphorylation found here was different than those found by Schroeder *et al.* (2001), which were ~30 kDa and 25 kDa[41]. The fact that they found two different molecular weights of phosphorylated MUC1 was already very puzzling and no explanations were presented. Moreover, appropriate positive and negative controls were absent in the EGF-stimulation experiments, and the phosphotyrosine blots obtained from their experiments were not re-probed for MUC1. Hence, the data from Schroeder *et al.* (2001) was very difficult to interpret[41]. Other studies done on MUC1 phosphorylation shared similar problems, such that experimental controls and MUC1 reprobes were frequently

missing. As a result, it was difficult to compare the data that we have with those in the literature.

Rahn *et al.* (unpublished observations) from our lab discovered that MUC1-ICAM-1 interaction was crucial in mediating tumor cell transendothelial migration in a Transwell model[37]. Furthermore, the presence of fibroblasts and cytokines resulted in a significantly greater extent of tumor cell transmigration than in the absence of these variables[37]. Cytokines like TNF-α and IL-1β are known to increase ICAM-1 expression on HUVECs[129], while fibroblasts could secrete soluble factors and proteolytic enzymes into the cellular microenvironment. Therefore, the importance of ICAM-1 and factors in the cellular microenvironment in promoting tumor cell transmigration was implicated. Based on the Transwell data from Rahn *et al.* (unpublished observations)[37], we were interested to know whether experimental conditions known to promote tumor cell transendothelial migration would affect the status of tumor MUC1 tyrosine phosphorylation. This question was investigated with an *in vitro* co-culturing system that simulated the conditions used in the Transwell experiments. The MCF-7s were used as the experimental model because they were more physiologically relevant than the GZ.Hi and 410.4 mouse cell lines. To mimic the Transwell experimental conditions, MCF-7 cells were cultured on gelatin-coated tissue culture plates and co-cultured with either NIH3T3/ICAM-1 or NIH3T3/Mock transfectants for 10 minutes, with or without sodium orthovanadate. Being a tyrosine phosphatase inhibitor, the purpose of using

sodium orthovanadate was to preserve tyrosine phosphorylations of proteins. All culturing was done with fibroblast-conditioned media that had been supplemented with TNF-α and Il-1β cytokines. Western blotting with PY99 antibody revealed a unique phosphotyrosine band at ~17 kDa exclusively in the MUC-1 positive MCF-7 samples (Figures 16A, C and E). The same membranes were re-probed with CT2 antibody, and a unique MUC1/CT2 band at ~17 kDa was detected exclusively in the MCF-7s (Figures 16B, D and F). Interestingly, this MUC1/CT2 band also matched with the unique phosphotyrosine band detected earlier in Figures 16A, C and E when the film images were overlaid. The phosphotyrosine and MUC1 levels in each experimental condition were quantified using the Scion Image computer software. The ratio of phosphotyrosine/CT2 quantities in each condition were calculated and compared on a bar graph (Figure 17). The ratios were then analyzed with ANOVA test using a p value of 0.01. There was no statistical difference in MUC1 phosphorylation among any of the experimental conditions. Therefore, the data in section 3.2.1 suggested that putative MUC1 tyrosine phosphorylation was identified at ~17 kDa. However, the presence of ICAM-1 and/or sodium orthovanadate had no significant effect on MUC1 tyrosine phosphorylation under Transwell experimental conditions known to induce tumor cell transendothelial migration. However, it has been suggested in the literature that MUC1 tyrosine phosphorylation is only a transient event[41, 83, 132]. It has been suggested in the literature that only a very small subpopulation of MUC1 would complex and subsequently become phosphorylated by kinases like EGFR[41]. Therefore, any

changes in MUC1 tyrosine phosphorylation would likely be very subtle, and hence, difficult to identify. Consequently, the use of more sensitive techniques for detecting MUC1 phosphorylation, such as radioactive labeling, may be considered for future experiments.

In addition to promoting tumor cell transendothelial migration, we have recently discovered that MUC1-ICAM-1 interaction could also trigger calcium ion (Ca^{2+}) oscillations in tumor cells[38]. Calcium ion oscillations and protein tyrosine phosphorylations are often key components of cellular signalling events. Therefore, the effect of ICAM-1 stimulation on MUC1 tyrosine phosphorylation under experimental conditions known to induce tumor cell Ca^{2+} oscillations was investigated. MCF-7s were cultured on FBS-coated tissue culture plates and co-cultured with NIH3T3/ICAM-1 or NIH3T3/Mock transfectants for 1 and 4 min. These time points were chosen because Ca^{2+} oscillations in tumor cells were observed within the initial 3 min of ICAM-1 stimulation[38]. Therefore, it was of interest to see whether MUC1 tyrosine phosphorylation would also occur within the time frame of calcium ion oscillations. Upon Western blotting with PY99, a unique phosphotyrosine band at ~17 kDa was most readily detected when MCF-7 cells were stimulated with NIH3T3/ICAM-1 or NIH3T3/Mock for 1 min, but was noticeably less detectable at 4 min (Figures 19A, C and E). However, the band was absent in the non-stimulated MCF-7s that were incubated with Imaging Buffer for 1 min and 4 min (Figures 19A, C and E). These conditions were included to ensure that the Imaging Buffer itself was not inducing MUC1

phosphorylation. Upon re-probing with CT2 antibody, a unique MUC1/CT2 band at ~17 kDa was detected exclusively in all of the MUC1-positive samples (Figures 19B, D and F). The band also mactched with the ~17 kDa phosphotyrosine band found in Figures 19A, C and E when the film images were overlaid. The phosphotyrosine and MUC1 levels in each experimental condition were quantified using the Scion Image computer software. The ratio of phosphotyrosine/CT2 quantities in each condition were calculated and compared on a bar graph (Figure 20). The ratios were then analyzed with the ANOVA and Newman-Keuls tests using a p value of 0.05. It was found that ICAM-1 and Mock stimulation for 1 min significantly increased the extent of MUC1 tyrosine phosphorylation (Figure 20). However, phosphorylation was attenuated to basal levels after 4 min of co-culturing with the NIH3T3 transfectants. Therefore, the data in section 3.2.3 suggested that putative MUC1 tyrosine phosphorylation was identified at ~17 kDa, which was consistent with the earlier findings (Figures 16 and 18). However, significant changes in MUC1 phosphorylation was only observed after 1 min of stimulation with either ICAM-1 or Mock under experimental conditions known to induce Ca^{2+} oscillations in tumor cells. Furthermore, the extent of MUC1 tyrosine phosphorylation induced by ICAM-1 and Mock transfectants for 1 min was not significantly different from each other.

It appeared that under experimental conditions where ICAM-1 is known to induce tumor cell Ca^{2+} oscillations[38], significant inductions of MUC1 phosphorylation were observed only after 1 min of co-culturing regardless of the presence of

ICAM-1 (Figure 20). Therefore, it was possible that mechanical stimulation alone was sufficient to induce MUC1 tyrosine phosphorylation. Changes in cellular signalling in response to mechanical stresses have been well-established in the literature. For instance, changes in cellular Ca^{2+} concentrations due to prodding or stretching of cells have previously been reported for cardiocytes[137] and endothelial cells[138, 139]. Similarly, mechanical force induced-alterations of kinase activities have also been shown in lung[140], endothelial[141], cardiac[142], and bone[143, 144] cells. For example, pressurization of vascular smooth muscle cells has been transiently correlated with ERK1/2 activation, in a PKC-independent and Src-family tyrosine kinase-dependent mechanism[145]. Similar type of ERK activation in endothelial cells has also been reported by Azuma *et al.* (2000)[146]. Therefore, alterations of Ca^{2+} and kinase-related activities/signalling by mechanical stimuli are common phenomena observed in many cell types. However, further experiments are required to verify the "mechanical stimulation" theory. For instance, the use of non-cellular materials such as agarose beads can replace the NIH3T3 transfectants in the co-culturing experiments. If the induction of MUC1 tyrosine phosphorylation is observed, then it would further suggest the importance of mechanical stimulation in modulating MUC1 phosphorylation.

Even more interestingly, mechanical stimulation of rat endothelial cells for 1 min has been demonstrated to induce a 2.4-fold increase in Src phosphorylation[147]. In addition, Kawata *et al.* (1998) have found that mechanical stresses on

mesangial cells rapidly increased the phosphorylation and activation of MAPK which peaked at 1 minute[148]. Therefore, it is evident that kinase activities can be modulated by mechanical stimuli within a one-minute time frame. Based on the literature data, it is hypothesized here that perhaps Src in tumor cells was activated after 1 minute of simple mechanical stimulation with either the ICAM-1 or Mock transfectants. Since Src is a kinase known to phosphorylate MUC1[81], its activation could increase MUC1 tyrosine phosphorylation as observed with the 1 min of co-culturing (Figure 20). However, both the initiation and termination of signalling activities must be well controlled. For instance, prolonged EGFR stimulation would eventually result in endocytosis of the receptor from cellular membrane, resulting in signalling termination (review article by Salcini et al., 1999)[149]. Hence, the reduced MUC1 phosphorylation after 4 minutes of co-culturing (Figure 20) could indicate the shutdown of certain kinases or MUC1 itself due to prolonged activation. These termination processes may be endocytosis-mediated, paralleling those for EGFR since MUC1 is known to undergo the lysosomal degradative pathway via clathrin-mediated endocytosis at cellular membranes[150]. Alternatively, the prominent decrease in MUC1 phosphorylation within the first 4 minutes of co-culturing could be due to rapid activation of *in vivo* tyrosine phosphatases as suggested in the literature[83], although the specific enzyme(s) responsible for MUC1 de-phosphorylation is still unknown. Moreover, the technical issue of finding a more sensitive detection method for MUC1 phosphorylation may be further investigated. Therefore, although Rahn *et al.* (2004) have found that ICAM-1 was able to induce

significantly higher tumor cell Ca^{2+} oscillations than with Mock stimulation[38], it was found in section 3.2.3 that both ICAM-1 and Mock stimulations for 1 min resulted in significant inductions of MUC1 tyrosine phosphorylation under the same experimental conditions. Hence, the mechanisms regulating MUC1 tyrosine phosphorylation and Ca^{2+} oscillation of tumor cells appeared to be differentially modulated by ICAM-1.

Another interesting observation was that there seemed to be higher basal levels of MUC1 tyrosine phosphorylation when tumor cells were grown on gelatin than FBS matrices. There is increasing evidence that the cellular microenvironment can affect various cellular properties. For instance, it has been found that the proliferation and differentiation of endothelial cells were optimal when cultured on different matrices, such as type I collagen and fibronectin, respectively. Furthermore, previous studies have also supported the importance of cellular microenvironment in modulating the malignant behavior of tumor cells[151]. Therefore, it was possible that gelatin and FBS matrices had different effects on regulating MUC1 phosphorylation. Perhaps the gelatin matrix provided a microenvironment that supported more constitutive activation of kinases (or less phosphatase suppression), and consequently, higher basal levels of MUC1 phosphorylation. In contrast, the FBS matrix might have a more suppressive effect on kinase activities (or greater kinase activation), and thus, MUC1 phosphorylation was absent until mechanical induction with the NIH3T3 transfectants. However, analyses of kinase and phosphatase activities under the

co-culturing conditions (i.e. different matrices) used in this project would be necessary to verify this theory. It would also be interesting to see if there is a relationship between integrin activation and MUC1 phosphorylation in the gelatin and FBS microenvironments.

Although the appropriate MUC1-positive and negative controls were included in the Western blots that tested for MUC1 phosphorylation in section 2.2.3, an additional test was employed in attempt to validate the phosphorylation status of the protein bands. This was accomplished by treating Western blot membranes from the MUC1-ICAM-1 co-culturing experiments with alkaline phosphatase. Three samples from section 2.2.3 were analyzed again by Western blotting. A distinct phosphotyrosine band at ~17 kDa (red asterisks) was detected exclusively in the MDA-MB-468/EGF 1 min and MCF-7/ICAM-1 1 min conditions (lanes 1 and 3, Figure 21). The molecular weight of this band was previously found to be tyrosine-phosphorylated MUC1 in earlier experiments (Figures 16, 18 and 19). However, alkaline phosphatase treatment on sections of the membrane containing these two samples (halves of lanes 1 and 3) was unable to prevent the subsequent detection of phosphotyrosine signals. Therefore, the preliminary results suggested that the alkaline phosphatase used in this experiment was ineffective in abolishing the detection of the putative tyrosine-phosphorylated MUC1 on the Western blot. Although this might imply that the ~17 kDa protein band was not a phosphorylated protein, the apparent ineffectiveness of the alkaline phosphatase could also stem from the protocol. For instance, the protocol used here was

obtained from Ahmad and Huang (1981)[152], which was not intended for treating Western blot membranes. In fact, it was originally designed for *in vitro* dephosphorylation of I-form glycogen synthase of rabbit skeletal muscle. However, it was used here since alternative protocols specifically designed for dephosphorylating Western blot membranes were unavailable in the literature. Although a higher phosphatase activity (hydrolysis of 6700 nmol versus 10 nmol of phosphate/min) and longer treatment duration (6 h versus 1 h) were employed in this experiment, we postulate that it was still unable to remove the putative tyrosine phosphorylated protein bands on the Western Blot (lanes 1 and 3, Figure 21). Perhaps phosphatase dilution and time course experiments would be required to determine the optimal units of phosphatase activity and duration of treatment necessary to dephosphorylate the protein bands on Western blot membranes.

4.3. Conclusion

Through Western blot analyses of crude and immunoprecipitated lysates of various cell lines, the molecular weights of full-length and cytoplasmic domain of MUC1 were found to be greater than 200 kDa and ~13-30 kDa, respectively. Contrary to our hypothesis, ICAM-1 did not induce MUC1 tyrosine phosphorylation under the experimental conditions where tumor cell transmigration and Ca^{2+} oscillation were observed. By using the *in vitro* co-culturing system designed in this project, it was found that the ICAM-1 and/or sodium orthovanadate had no significant effect on MUC1 tyrosine phosphorylation under Transwell conditions. In contrast, both ICAM-1 and mock stimulations for 1 min resulted in significant inductions of MUC1 tyrosine phosphorylation (at ~17 kDa, which was consistent with the EGF-stimulated MDA-MB-468s positive control) under the experimental conditions known to induce Ca^{2+} oscillations in tumor cells. However, MUC1 phosphorylation reverted back to basal levels after 4 min of co-culturing, suggesting that MUC1 tyrosine phosphorylation events are transient. The induction of MUC1 phosphorylation by ICAM-1 and Mock transfectants could possibly be a result of simple mechanical stimulation of tumor cells, which will need further investigation. In contrast, only ICAM-1 could trigger significant Ca^{2+} oscillations in tumor cells under the same experimental conditions used here[38]. Therefore, it appeared the mechanisms regulating MUC1 tyrosine phosphorylation and Ca^{2+} oscillation of tumor cells could be differentially modulated by ICAM-1, although further investigation is necessary for confirmation.

Bibliography

1. Rennie J, Rusting R: **Making headway against cancer**. *Sci Am* 1996, **275**(3):56-59.
2. Lodish H, Berk, A., Zipursky, S. L., Matsudaira, P., Baltimore, D., Darnell, J.: **Molecular Cell Biology**, Fourth edn. New York: W. H. Freeman and Company; 2000.
3. Hanahan D, Weinberg RA: **The hallmarks of cancer**. *Cell* 2000, **100**(1):57-70.
4. **Canadian Cancer Statistics** [www.cancer.ca]
5. Liotta LA: **An attractive force in metastasis**. *Nature* 2001, **410**(6824):24-25.
6. Morgan-Parkes JH: **Metastases: mechanisms, pathways, and cascades**. *AJR Am J Roentgenol* 1995, **164**(5):1075-1082.
7. Kurschat P, Mauch C: **Mechanisms of metastasis**. *ClinExpDermatol* 2000, **25**(6):482-489.
8. Tannock IFH, R. P.: **The Basic Science of Oncology**, Third edn. Toronto: McGraw-Hill Health Professions Division; 1998.
9. Meyer T, Hart IR: **Mechanisms of tumour metastasis**. *Eur J Cancer* 1998, **34**(2):214-221.
10. Berquin IM, Sloane BF: **Cathepsin B expression in human tumors**. *Adv Exp Med Biol* 1996, **389**:281-294.
11. Koliopanos A, Friess H, Kleeff J, Shi X, Liao Q, Pecker I, Vlodavsky I, Zimmermann A, Buchler MW: **Heparanase expression in primary and metastatic pancreatic cancer**. *Cancer Res* 2001, **61**(12):4655-4659.
12. Brakebusch C, Bouvard D, Stanchi F, Sakai T, Fassler R: **Integrins in invasive growth**. *J Clin Invest* 2002, **109**(8):999-1006.
13. Felding-Habermann B, Mueller BM, Romerdahl CA, Cheresh DA: **Involvement of integrin alpha V gene expression in human melanoma tumorigenicity**. *J Clin Invest* 1992, **89**(6):2018-2022.
14. Weaver VM, Petersen OW, Wang F, Larabell CA, Briand P, Damsky C, Bissell MJ: **Reversion of the malignant phenotype of human breast cells in three- dimensional culture and in vivo by integrin blocking antibodies**. *J Cell Biol* 1997, **137**(1):231-245.
15. Vogetseder W, Feichtinger H, Schulz TF, Schwaeble W, Tabaczewski P, Mitterer M, Bock G, Marth C, Dapunt O, Mikuz G *et al*: **Expression of 7F7-antigen, a human adhesion molecule identical to intercellular adhesion molecule-1 (ICAM-1) in human carcinomas and their stromal fibroblasts**. *Int J Cancer* 1989, **43**(5):768-773.
16. Weiss L: **Comments on hematogenous metastatic patterns in humans as revealed by autopsy**. *Clin Exp Metastasis* 1992, **10**(3):191-199.
17. Orr FW, Wang HH, Lafrenie RM, Scherbarth S, Nance DM: **Interactions between cancer cells and the endothelium in metastasis**. *J Pathol* 2000, **190**(3):310-329.
18. Bianchi E, Bender JR, Blasi F, Pardi R: **Through and beyond the wall: late steps in leukocyte transendothelial migration**. *ImmunolToday* 1997, **18**(12):586-591.
19. Bradley JR, Pober JS: **Prolonged cytokine exposure causes a dynamic redistribution of endothelial cell adhesion molecules to intercellular junctions**. *Lab Invest* 1996, **75**(4):463-472.
20. Burns AR, Walker DC, Brown ES, Thurmon LT, Bowden RA, Keese CR, Simon SI, Entman ML, Smith CW: **Neutrophil transendothelial migration is independent of tight junctions and occurs preferentially at tricellular corners**. *J Immunol* 1997, **159**(6):2893-2903.
21. Clayton A, Evans RA, Pettit E, Hallett M, Williams JD, Steadman R: **Cellular activation through the ligation of intercellular adhesion molecule-1**. *J Cell Sci* 1998, **111 (Pt . 4)**:443-453.
22. Lorenzon P, Vecile E, Nardon E, Ferrero E, Harlan JM, Tedesco F, Dobrina A: **Endothelial cell E- and P-selectin and vascular cell adhesion molecule-1 function as signaling receptors**. *J Cell Biol* 1998, **142**(5):1381-1391.
23. Price EA, Coombe DR, Murray JC: **beta-1 Integrins mediate tumour cell adhesion to quiescent endothelial cells in vitro**. *BrJ Cancer* 1996, **74**(11):1762-1766.

24. Sandig M, Negrou E, Rogers KA: **Changes in the distribution of LFA-1, catenins, and F-actin during transendothelial migration of monocytes in culture**. *J Cell Sci* 1997, **110 (Pt 22)**:2807-2818.
25. Tsang YT, Neelamegham S, Hu Y, Berg EL, Burns AR, Smith CW, Simon SI: **Synergy between L-selectin signaling and chemotactic activation during neutrophil adhesion and transmigration**. *J Immunol* 1997, **159**(9):4566-4577.
26. Ozaki H, Ishii K, Horiuchi H, Arai H, Kawamoto T, Okawa K, Iwamatsu A, Kita T: **Cutting edge: combined treatment of TNF-alpha and IFN-gamma causes redistribution of junctional adhesion molecule in human endothelial cells**. *J Immunol* 1999, **163**(2):553-557.
27. Gopalan PK, Burns AR, Simon SI, Sparks S, McIntire LV, Smith CW: **Preferential sites for stationary adhesion of neutrophils to cytokine-stimulated HUVEC under flow conditions**. *J Leukoc Biol* 2000, **68**(1):47-57.
28. Tozawa K, Sakurada S, Kohri K, Okamoto T: **Effects of anti-nuclear factor kappa B reagents in blocking adhesion of human cancer cells to vascular endothelial cells**. *Cancer Res* 1995, **55**(18):4162-4167.
29. Ye C, Kiriyama K, Mistuoka C, Kannagi R, Ito K, Watanabe T, Kondo K, Akiyama S, Takagi H: **Expression of E-selectin on endothelial cells of small veins in human colorectal cancer**. *Int J Cancer* 1995, **61**(4):455-460.
30. Steinbach F, Tanabe K, Alexander J, Edinger M, Tubbs R, Brenner W, Stockle M, Novick AC, Klein EA: **The influence of cytokines on the adhesion of renal cancer cells to endothelium**. *J Urol* 1996, **155**(2):743-748.
31. Lafrenie RM, Gallo S, Podor TJ, Buchanan MR, Orr FW: **The relative roles of vitronectin receptor, E-selectin and alpha 4 beta 1 in cancer cell adhesion to interleukin-1-treated endothelial cells**. *Eur J Cancer* 1994, **30A**(14):2151-2158.
32. Majuri ML, Niemela R, Tiisala S, Renkonen O, Renkonen R: **Expression and function of alpha 2,3-sialyl- and alpha 1,3/1,4-fucosyltransferases in colon adenocarcinoma cell lines: role in synthesis of E-selectin counter-receptors**. *Int J Cancer* 1995, **63**(4):551-559.
33. Tarin D, Matsumura Y: **Recent advances in the study of tumour invasion and metastasis**. *J Clin Pathol* 1994, **47**(5):385-390.
34. Regimbald LH, Pilarski LM, Longenecker BM, Reddish MA, Zimmermann G, Hugh JC: **The breast mucin MUC1 as a novel adhesion ligand for endothelial intercellular adhesion molecule 1 in breast cancer**. *Cancer Res* 1996, **56**(18):4244-4249.
35. Kam JL, Regimbald LH, Hilgers JH, Hoffman P, Krantz MJ, Longenecker BM, Hugh JC: **MUC1 synthetic peptide inhibition of intercellular adhesion molecule-1 and MUC1 binding requires six tandem repeats**. *Cancer Res* 1998, **58**(23):5577-5581.
36. Horne G: **The role of breast cancer associated MCU1 in tumor cell recruitment to vascular endothelium during physiological fluid flow**. *Master's Degree*. Edmonton: University of Alberta; 1999.
37. Rahn JJ, Horne, G.J., Latif, D.A., Mah, K.M., Hoffman, P. & Hugh, J.C.: **MUC1/ICAM-1 interactions can significantly increase transendothelial migration of MCF-7 human breast cancer cells**. Pending.
38. Rahn JJ, Shen, Q., Mah, B.K. & Hugh, J.C.: **MUC1 initiates a calcium signal after ligation by intercellular adhesion molecule-1**. *J Biol Chem* 2004, **279**(28):29386-90.
39. Kobylka D, Carraway KL: **Proteins and glycoproteins of the milk fat globule membrane**. *Biochim Biophys Acta* 1972, **288**(2):282-295.
40. Mather IH, Keenan TW: **Studies on the structure of milk fat globule membrane**. *J Membr Biol* 1975, **21**(1-2):65-85.
41. Schroeder JA, Thompson MC, Gardner MM, Gendler SJ: **Transgenic MUC1 interacts with epidermal growth factor receptor and correlates with mitogen-activated protein kinase activation in the mouse mammary gland**. *J Biol Chem* 2001, **276**(16):13057-13064.

42. Patton S, Gendler SJ, Spicer AP: **The epithelial mucin, MUC1, of milk, mammary gland and other tissues**. *BiochimBiophysActa* 1995, **1241**(3):407-423.
43. Zrihan-Licht S, Baruch A, Elroy-Stein O, Keydar I, Wreschner DH: **Tyrosine phosphorylation of the MUC1 breast cancer membrane proteins. Cytokine receptor-like molecules**. *FEBS Lett* 1994, **356**(1):130-136.
44. Bieche I, Lidereau R: **A gene dosage effect is responsible for high overexpression of the MUC1 gene observed in human breast tumors**. *Cancer Genet Cytogenet* 1997, **98**(1):75-80.
45. Burchell J, Wang D, Taylor-Papadimitriou J: **Detection of the tumour-associated antigens recognized by the monoclonal antibodies HMFG-1 and 2 in serum from patients with breast cancer**. *Int J Cancer* 1984, **34**(6):763-768.
46. McGuckin MA, Ramm LE, Joy GJ, Devine PL, Ward BG: **Circulating tumour-associated mucin concentrations, determined by the CASA assay, in healthy women**. *Clin Chim Acta* 1993, **214**(2):139-151.
47. Boshell M, Lalani EN, Pemberton L, Burchell J, Gendler S, Taylor-Papadimitriou J: **The product of the human MUC1 gene when secreted by mouse cells transfected with the full-length cDNA lacks the cytoplasmic tail**. *Biochem Biophys Res Commun* 1992, **185**(1):1-8.
48. Williams CJ, Wreschner DH, Tanaka A, Tsarfaty I, Keydar I, Dion AS: **Multiple protein forms of the human breast tumor-associated epithelial membrane antigen (EMA) are generated by alternative splicing and induced by hormonal stimulation**. *Biochem Biophys Res Commun* 1990, **170**(3):1331-1338.
49. Ligtenberg MJ, Kruijshaar L, Buijs F, van Meijer M, Litvinov SV, Hilkens J: **Cell-associated episialin is a complex containing two proteins derived from a common precursor**. *J Biol Chem* 1992, **267**(9):6171-6177.
50. Zotter S, Hageman PC, Lossnitzer A, van den Tweel J, Hilkens J, Mooi WJ, Hilgers J: **Monoclonal antibodies to epithelial sialomucins recognize epitopes at different cellular sites in adenolymphomas of the parotid gland**. *Int J Cancer Suppl* 1988, **3**:38-44.
51. MacLean GD, Longenecker BM: **New possibilities for cancer therapy with advances in cancer immunology**. *Can J Oncol* 1994, **4**(2):249-254.
52. Gendler S, Taylor-Papadimitriou J, Duhig T, Rothbard J, Burchell J: **A highly immunogenic region of a human polymorphic epithelial mucin expressed by carcinomas is made up of tandem repeats**. *J Biol Chem* 1988, **263**(26):12820-12823.
53. Fukuda T, Kamishima T, Ohnishi Y, Suzuki T: **Sarcomatoid carcinoma of the small intestine: histologic, immunohistochemical and ultrastructural features of three cases and its differential diagnosis**. *Pathol Int* 1996, **46**(9):682-688.
54. Fukuda M: **Possible roles of tumor-associated carbohydrate antigens**. *Cancer Res* 1996, **56**(10):2237-2244.
55. Rahn JJ, Dabbagh L, Pasdar M, Hugh JC: **The importance of MUC1 cellular localization in patients with breast carcinoma: an immunohistologic study of 71 patients and review of the literature**. *Cancer* 2001, **91**(11):1973-1982.
56. Swallow DM, Gendler S, Griffiths B, Kearney A, Povey S, Sheer D, Palmer RW, Taylor-Papadimitriou J: **The hypervariable gene locus PUM, which codes for the tumour associated epithelial mucins, is located on chromosome 1, within the region 1q21-24**. *Ann Hum Genet* 1987, **51 (Pt 4)**:289-294.
57. Spicer AP, Parry G, Patton S, Gendler SJ: **Molecular cloning and analysis of the mouse homologue of the tumor-associated mucin, MUC1, reveals conservation of potential O-glycosylation sites, transmembrane, and cytoplasmic domains and a loss of minisatellite-like polymorphism**. *J Biol Chem* 1991, **266**(23):15099-15109.
58. Ligtenberg MJ, Vos HL, Gennissen AM, Hilkens J: **Episialin, a carcinoma-associated mucin, is generated by a polymorphic gene encoding splice variants with alternative amino termini**. *J Biol Chem* 1990, **265**(10):5573-5578.

59. Wreschner DH, Hareuveni M, Tsarfaty I, Smorodinsky N, Horev J, Zaretsky J, Kotkes P, Weiss M, Lathe R, Dion A *et al*: **Human epithelial tumor antigen cDNA sequences. Differential splicing may generate multiple protein forms**. *Eur J Biochem* 1990, **189**(3):463-473.
60. Hareuveni M, Tsarfaty I, Zaretsky J, Kotkes P, Horev J, Zrihan S, Weiss M, Green S, Lathe R, Keydar I *et al*: **A transcribed gene, containing a variable number of tandem repeats, codes for a human epithelial tumor antigen. cDNA cloning, expression of the transfected gene and over-expression in breast cancer tissue**. *Eur J Biochem* 1990, **189**(3):475-486.
61. Lan MS, Batra SK, Qi WN, Metzgar RS, Hollingsworth MA: **Cloning and sequencing of a human pancreatic tumor mucin cDNA**. *J Biol Chem* 1990, **265**(25):15294-15299.
62. Lancaster CA, Peat N, Duhig T, Wilson D, Taylor-Papadimitriou J, Gendler SJ: **Structure and expression of the human polymorphic epithelial mucin gene: an expressed VNTR unit**. *Biochem Biophys Res Commun* 1990, **173**(3):1019-1029.
63. Gendler SJ, Spicer AP: **Epithelial mucin genes**. *Annu Rev Physiol* 1995, **57**:607-634.
64. Wesseling J, van der Valk SW, Vos HL, Sonnenberg A, Hilkens J: **Episialin (MUC1) overexpression inhibits integrin-mediated cell adhesion to extracellular matrix components**. *J Cell Biol* 1995, **129**(1):255-265.
65. Fontenot JD, Tjandra N, Bu D, Ho C, Montelaro RC, Finn OJ: **Biophysical characterization of one-, two-, and three-tandem repeats of human mucin (muc-1) protein core**. *Cancer Res* 1993, **53**(22):5386-5394.
66. Jentoft N: **Why are proteins O-glycosylated?** *Trends Biochem Sci* 1990, **15**(8):291-294.
67. Gendler SJ, Lancaster CA, Taylor-Papadimitriou J, Duhig T, Peat N, Burchell J, Pemberton L, Lalani EN, Wilson D: **Molecular cloning and expression of human tumor-associated polymorphic epithelial mucin**. *J Biol Chem* 1990, **265**(25):15286-15293.
68. Abe M, Kufe DW: **Identification of a family of high molecular weight tumor-associated glycoproteins**. *J Immunol* 1987, **139**(1):257-261.
69. Abe M, Kufe D: **Structural analysis of the DF3 human breast carcinoma-associated protein**. *Cancer Res* 1989, **49**(11):2834-2839.
70. Bork P, Patthy L: **The SEA module: a new extracellular domain associated with O-glycosylation**. *Protein Sci* 1995, **4**(7):1421-1425.
71. Wreschner DH, McGuckin MA, Williams SJ, Baruch A, Yoeli M, Ziv R, Okun L, Zaretsky J, Smorodinsky N, Keydar I *et al*: **Generation of ligand-receptor alliances by "SEA" module-mediated cleavage of membrane-associated mucin proteins**. *Protein Sci* 2002, **11**(3):698-706.
72. Apostolopoulos V, Xing PX, McKenzie IF: **Murine immune response to cells transfected with human MUC1: immunization with cellular and synthetic antigens**. *Cancer Res* 1994, **54**(19):5186-5193.
73. Hinoda Y, Takahashi T, Hayashi T, Suwa T, Makiguchi Y, Itoh F, Adachi M, Imai K: **Enhancement of reactivity of anti-MUC1 core protein antibody and killing activity of anti-MUC1 cytotoxic T cells by deglycosylation of target tissues or cells**. *J Gastroenterol* 1998, **33**(2):164-171.
74. Chan AK, Lockhart DC, von Bernstorff W, Spanjaard RA, Joo HG, Eberlein TJ, Goedegebuure PS: **Soluble MUC1 secreted by human epithelial cancer cells mediates immune suppression by blocking T-cell activation**. *Int J Cancer* 1999, **82**(5):721-726.
75. Barnd DL, Lan MS, Metzgar RS, Finn OJ: **Specific, major histocompatibility complex-unrestricted recognition of tumor-associated mucins by human cytotoxic T cells**. *Proc Natl Acad Sci U S A* 1989, **86**(18):7159-7163.
76. Hayes DF, Silberstein DS, Rodrique SW, Kufe DW: **DF3 antigen, a human epithelial cell mucin, inhibits adhesion of eosinophils to antibody-coated targets**. *J Immunol* 1990, **145**(3):962-970.

77. Agrawal B, Krantz MJ, Reddish MA, Longenecker BM: **Cancer-associated MUC1 mucin inhibits human T-cell proliferation, which is reversible by IL-2**. *Nat Med* 1998, **4**(1):43-49.
78. Hilkens J, Wesseling J, Vos HL, Storm J, Boer B, van der Valk SW, Maas MC: **Involvement of the cell surface-bound mucin, episialin/MUC1, in progression of human carcinomas**. *Biochem Soc Trans* 1995, **23**(4):822-826.
79. Hilkens J, Vos HL, Wesseling J, Boer M, Storm J, van der Valk S, Calafat J, Patriarca C: **Is episialin/MUC1 involved in breast cancer progression?** *Cancer Lett* 1995, **90**(1):27-33.
80. Lillehoj EP, Han F, Kim KC: **Mutagenesis of a Gly-Ser cleavage site in MUC1 inhibits ectodomain shedding**. *Biochem Biophys Res Commun* 2003, **307**(3):743-749.
81. Li Y, Kuwahara H, Ren J, Wen G, Kufe D: **The c-Src tyrosine kinase regulates signaling of the human DF3/MUC1 carcinoma-associated antigen with GSK3 beta and beta-catenin**. *J BiolChem* 2001, **276**(9):6061-6064.
82. Ren J, Li Y, Kufe D: **Protein kinase C delta regulates function of the DF3/MUC1 carcinoma antigen in beta-catenin signaling**. *J Biol Chem* 2002, **277**(20):17616-17622.
83. Schroeder JA, Adriance MC, Thompson MC, Camenisch TD, Gendler SJ: **MUC1 alters beta-catenin-dependent tumor formation and promotes cellular invasion**. *Oncogene* 2003, **22**(9):1324-1332.
84. Meerzaman D, Shapiro PS, Kim KC: **Involvement of the MAP kinase ERK2 in MUC1 mucin signaling**. *Am J Physiol Lung Cell Mol Physiol* 2001, **281**(1):L86-91.
85. Pandey P, Kharbanda S, Kufe D: **Association of the DF3/MUC1 breast cancer antigen with Grb2 and the Sos/Ras exchange protein**. *Cancer Res* 1995, **55**(18):4000-4003.
86. Wang H, Lillehoj EP, Kim KC.: **Identification of four sites of stimulated tyrosine phosphorylation in the MUC1 cytoplasmic tail.** *Biochem Biophys Res Commun* 2003, **310**(2):341-6.
87. Li Y, Bharti A, Chen D, Gong J, Kufe D: **Interaction of glycogen synthase kinase 3beta with the DF3/MUC1 carcinoma-associated antigen and beta-catenin**. *MolCell Biol* 1998, **18**(12):7216-7224.
88. Kondo K, Kohno N, Yokoyama A, Hiwada K: **Decreased MUC1 expression induces E-cadherin-mediated cell adhesion of breast cancer cell lines**. *Cancer Res* 1998, **58**(9):2014-2019.
89. Chen Y, Lu Q, Schneeberger EE, Goodenough DA: **Restoration of tight junction structure and barrier function by down-regulation of the mitogen-activated protein kinase pathway in ras-transformed Madin-Darby canine kidney cells**. *Mol Biol Cell* 2000, **11**(3):849-862.
90. Feldner JC, Brandt BH: **Cancer cell motility--on the road from c-erbB-2 receptor steered signaling to actin reorganization**. *Exp Cell Res* 2002, **272**(2):93-108.
91. Meerzaman D, Xing PX, Kim KC: **Construction and characterization of a chimeric receptor containing the cytoplasmic domain of MUC1 mucin**. *Am J Physiol Lung Cell MolPhysiol* 2000, **278**(3):L625-L629.
92. van de Stolpe A, van der Saag PT: **Intercellular adhesion molecule-1**. *J MolMed* 1996, **74**(1):13-33.
93. Fawcett J, Holness CL, Needham LA, Turley H, Gatter KC, Mason DY, Simmons DL: **Molecular cloning of ICAM-3, a third ligand for LFA-1, constitutively expressed on resting leukocytes**. *Nature* 1992, **360**(6403):481-484.
94. Ledebur HC, Parks TP: **Transcriptional regulation of the intercellular adhesion molecule-1 gene by inflammatory cytokines in human endothelial cells. Essential roles of a variant NF-kappa B site and p65 homodimers**. *J Biol Chem* 1995, **270**(2):933-943.

95. van de Stolpe A, Caldenhoven E, Stade BG, Koenderman L, Raaijmakers JA, Johnson JP, van der Saag PT: **12-O-tetradecanoylphorbol-13-acetate- and tumor necrosis factor alpha-mediated induction of intercellular adhesion molecule-1 is inhibited by dexamethasone. Functional analysis of the human intercellular adhesion molecular-1 promoter**. *J Biol Chem* 1994, **269**(8):6185-6192.

96. Bacus SS, Zelnick CR, Chin DM, Yarden Y, Kaminsky DB, Bennington J, Wen D, Marcus JN, Page DL: **Medullary carcinoma is associated with expression of intercellular adhesion molecule-1. Implication to its morphology and its clinical behavior**. *Am J Pathol* 1994, **145**(6):1337-1348.

97. Dustin ML, Rothlein R, Bhan AK, Dinarello CA, Springer TA: **Induction by IL 1 and interferon-gamma: tissue distribution, biochemistry, and function of a natural adherence molecule (ICAM-1)**. *J Immunol* 1986, **137**(1):245-254.

98. Ohh M, Smith CA, Carpenito C, Takei F: **Regulation of intercellular adhesion molecule-1 gene expression involves multiple mRNA stabilization mechanisms: effects of interferon-gamma and phorbol myristate acetate**. *Blood* 1994, **84**(8):2632-2639.

99. van de Stolpe A, Caldenhoven E, Raaijmakers JA, van der Saag PT, Koenderman L: **Glucocorticoid-mediated repression of intercellular adhesion molecule-1 expression in human monocytic and bronchial epithelial cell lines**. *Am J Respir Cell Mol Biol* 1993, **8**(3):340-347.

100. Griffioen AW, Damen CA, Martinotti S, Blijham GH, Groenewegen G: **Endothelial intercellular adhesion molecule-1 expression is suppressed in human malignancies: the role of angiogenic factors**. *Cancer Res* 1996, **56**(5):1111-1117.

101. Bouillon M, Fortier MA, Boulianne R, Audette M: **Biphasic effect of cAMP-elevating agents on ICAM-1 expression stimulated by retinoic acid and interferon gamma**. *Int J Cancer* 1992, **50**(2):281-288.

102. Pober JS, Slowik MR, De Luca LG, Ritchie AJ: **Elevated cyclic AMP inhibits endothelial cell synthesis and expression of TNF-induced endothelial leukocyte adhesion molecule-1, and vascular cell adhesion molecule-1, but not intercellular adhesion molecule-1**. *J Immunol* 1993, **150**(11):5114-5123.

103. Renkonen R, Mennander A, Ustinov J, Mattila P: **Activation of protein kinase C is crucial in the regulation of ICAM-1 expression on endothelial cells by interferon-gamma**. *Int Immunol* 1990, **2**(8):719-724.

104. Dean NM, McKay R, Condon TP, Bennett CF: **Inhibition of protein kinase C-alpha expression in human A549 cells by antisense oligonucleotides inhibits induction of intercellular adhesion molecule 1 (ICAM-1) mRNA by phorbol esters**. *J Biol Chem* 1994, **269**(23):16416-16424.

105. Morisaki N, Takahashi K, Shiina R, Zenibayashi M, Otabe M, Yoshida S, Saito Y: **Platelet-derived growth factor is a potent stimulator of expression of intercellular adhesion molecule-1 in human arterial smooth muscle cells**. *Biochem Biophys Res Commun* 1994, **200**(1):612-618.

106. Kurose I, Kubes P, Wolf R, Anderson DC, Paulson J, Miyasaka M, Granger DN: **Inhibition of nitric oxide production. Mechanisms of vascular albumin leakage**. *Circ Res* 1993, **73**(1):164-171.

107. Tiisala S, Majuri ML, Carpen O, Renkonen R: **Genistein enhances the ICAM-mediated adhesion by inducing the expression of ICAM-1 and its counter-receptors**. *Biochem Biophys Res Commun* 1994, **203**(1):443-449.

108. Voraberger G, Schafer R, Stratowa C: **Cloning of the human gene for intercellular adhesion molecule 1 and analysis of its 5'-regulatory region. Induction by cytokines and phorbol ester**. *J Immunol* 1991, **147**(8):2777-2786.

109. Diamond MS, Staunton DE, Marlin SD, Springer TA: **Binding of the integrin Mac-1 (CD11b/CD18) to the third immunoglobulin-like domain of ICAM-1 (CD54) and its regulation by glycosylation**. *Cell* 1991, **65**(6):961-971.

110. Staunton DE, Marlin SD, Stratowa C, Dustin ML, Springer TA: **Primary structure of ICAM-1 demonstrates interaction between members of the immunoglobulin and integrin supergene families**. *Cell* 1988, **52**(6):925-933.
111. Staunton DE, Dustin ML, Erickson HP, Springer TA: **The arrangement of the immunoglobulin-like domains of ICAM-1 and the binding sites for LFA-1 and rhinovirus**. *Cell* 1990, **61**(2):243-254.
112. Rothlein R, Dustin ML, Marlin SD, Springer TA: **A human intercellular adhesion molecule (ICAM-1) distinct from LFA-1**. *J Immunol* 1986, **137**(4):1270-1274.
113. Manning AM, Lu HF, Kukielka GL, Oliver MG, Ty T, Toman CA, Drong RF, Slightom JL, Ballantyne CM, Entman ML *et al*: **Cloning and comparative sequence analysis of the gene encoding canine intercellular adhesion molecule-1 (ICAM-1)**. *Gene* 1995, **156**(2):291-295.
114. Almenar-Queralt A, Duperray A, Miles LA, Felez J, Altieri DC: **Apical topography and modulation of ICAM-1 expression on activated endothelium**. *Am J Pathol* 1995, **147**(5):1278-1288.
115. Geissler D, Gaggl S, Most J, Greil R, Herold M, Dietrich M: **A monoclonal antibody directed against the human intercellular adhesion molecule (ICAM-1) modulates the release of tumor necrosis factor-alpha, interferon-gamma and interleukin 1**. *Eur J Immunol* 1990, **20**(12):2591-2596.
116. Rothlein R, Kishimoto TK, Mainolfi E: **Cross-linking of ICAM-1 induces co-signaling of an oxidative burst from mononuclear leukocytes**. *J Immunol* 1994, **152**(5):2488-2495.
117. Fischer H, Gjorloff A, Hedlund G, Hedman H, Lundgren E, Kalland T, Sjogren HO, Dohlsten M: **Stimulation of human naive and memory T helper cells with bacterial superantigen. Naive CD4+45RA+ T cells require a costimulatory signal mediated through the LFA-1/ICAM-1 pathway**. *J Immunol* 1992, **148**(7):1993-1998.
118. Damle NK, Klussman K, Linsley PS, Aruffo A: **Differential costimulatory effects of adhesion molecules B7, ICAM-1, LFA-3, and VCAM-1 on resting and antigen-primed CD4+ T lymphocytes**. *J Immunol* 1992, **148**(7):1985-1992.
119. Maio M, Tessitori G, Pinto A, Temponi M, Colombatti A, Ferrone S: **Differential role of distinct determinants of intercellular adhesion molecule-1 in immunologic phenomena**. *J Immunol* 1989, **143**(1):181-188.
120. Makgoba MW, Sanders ME, Ginther Luce GE, Dustin ML, Springer TA, Clark EA, Mannoni P, Shaw S: **ICAM-1 a ligand for LFA-1-dependent adhesion of B, T and myeloid cells**. *Nature* 1988, **331**(6151):86-88.
121. Marlin SD, Springer TA: **Purified intercellular adhesion molecule-1 (ICAM-1) is a ligand for lymphocyte function-associated antigen 1 (LFA-1)**. *Cell* 1987, **51**(5):813-819.
122. Remold-O'Donnell E, Zimmerman C, Kenney D, Rosen FS: **Expression on blood cells of sialophorin, the surface glycoprotein that is defective in Wiskott-Aldrich syndrome**. *Blood* 1987, **70**(1):104-109.
123. Rosenstein Y, Park JK, Hahn WC, Rosen FS, Bierer BE, Burakoff SJ: **CD43, a molecule defective in Wiskott-Aldrich syndrome, binds ICAM-1**. *Nature* 1991, **354**(6350):233-235.
124. Dustin ML, Garcia-Aguilar J, Hibbs ML, Larson RS, Stacker SA, Staunton DE, Wardlaw AJ, Springer TA: **Structure and regulation of the leukocyte adhesion receptor LFA-1 and its counterreceptors, ICAM-1 and ICAM-2**. *Cold Spring Harb Symp Quant Biol* 1989, **54 Pt 2**:753-765.
125. Diamond MS, Garcia-Aguilar J, Bickford JK, Corbi AL, Springer TA: **The I domain is a major recognition site on the leukocyte integrin Mac-1 (CD11b/CD18) for four distinct adhesion ligands**. *J Cell Biol* 1993, **120**(4):1031-1043.
126. van Kooyk Y, van de Wiel-van Kemenade P, Weder P, Kuijpers TW, Figdor CG: **Enhancement of LFA-1-mediated cell adhesion by triggering through CD2 or CD3 on T lymphocytes**. *Nature* 1989, **342**(6251):811-813.

127. Li Y, Liu D, Chen D, Kharbanda S, Kufe D: **Human DF3/MUC1 carcinoma-associated protein functions as an oncogene**. *Oncogene* 2003, **22**(38):6107-6110.
128. Alpaugh ML, Tomlinson JS, Kasraeian S, Barsky SH: **Cooperative role of E-cadherin and sialyl-Lewis X/A-deficient MUC1 in the passive dissemination of tumor emboli in inflammatory breast carcinoma**. *Oncogene* 2002, **21**(22):3631-3643.
129. Lane TA, Lamkin GE, Wancewicz EV: **Protein kinase C inhibitors block the enhanced expression of intercellular adhesion molecule-1 on endothelial cells activated by interleukin-1, lipopolysaccharide and tumor necrosis factor**. *Biochem Biophys Res Commun* 1990, **172**(3):1273-1281.
130. Gonzalez-Guerrico AM, Cafferata EG, Radrizzani M, Marcucci F, Gruenert D, Pivetta OH, Favaloro RR, Laguens R, Perrone SV, Gallo GC *et al*: **Tyrosine kinase c-Src constitutes a bridge between cystic fibrosis transmembrane regulator channel failure and MUC1 overexpression in cystic fibrosis**. *J Biol Chem* 2002, **277**(19):17239-17247.
131. Ciborowski P, Konitzki WM, Blander JM, Finn OJ: **Screening of anti-MUC1 antibodies for reactivity with native (ascites) and recombinant (baculovirus) MUC1 and for blocking MUC1 specific cytotoxic T-lymphocytes**. *Tumour Biol* 1998, **19 Suppl 1**:147-151.
132. Quin RJ, McGuckin MA: **Phosphorylation of the cytoplasmic domain of the MUC1 mucin correlates with changes in cell-cell adhesion**. *IntJ Cancer* 2000, **87**(4):499-506.
133. Laemmli UK: **Cleavage of structural proteins during the assembly of the head of bacteriophage T4**. *Nature* 1970, **227**(259):680-685.
134. Oosawa Y, Imada C, Furuya K: **Temperature dependency of calcium responses in mammary tumour cells**. *Cell Biochem Funct* 1997, **15**(2):113-117.
135. Li Y, Hively WP, Varmus HE: **Use of MMTV-Wnt-1 transgenic mice for studying the genetic basis of breast cancer**. *Oncogene* 2000, **19**(8):1002-1009.
136. Harlow EL, D.: **Antibodies: A Laboratory Manual**. In: *Cold Spring Harbor Laboratory Press*. NY; 1988.
137. Ruwhof C, van Wamel JT, Noordzij LA, Aydin S, Harper JC, van der Laarse A: **Mechanical stress stimulates phospholipase C activity and intracellular calcium ion levels in neonatal rat cardiomyocytes**. *Cell Calcium* 2001, **29**(2):73-83.
138. Mocrenhout M, Vereecke J, Himpens B: **Mechanism of intracellular Ca(2+)-wave propagation elicited by mechanical stimulation in cultured endothelial CPAE cells**. *Cell Calcium* 2001, **29**(2):117-123.
139. Yamamoto K, Korenaga R, Kamiya A, Ando J: **Fluid shear stress activates Ca(2+) influx into human endothelial cells via P2X4 purinoceptors**. *Circ Res* 2000, **87**(5):385-391.
140. Liu M, Qin Y, Liu J, Tanswell AK, Post M: **Mechanical strain induces pp60src activation and translocation to cytoskeleton in fetal rat lung cells**. *J Biol Chem* 1996, **271**(12):7066-7071.
141. Boo YC, Jo H: **Flow-dependent regulation of endothelial nitric oxide synthase: role of protein kinases**. *Am J Physiol Cell Physiol* 2003, **285**(3):C499-508.
142. Torsoni AS, Constancio SS, Nadruz W, Jr., Hanks SK, Franchini KG: **Focal adhesion kinase is activated and mediates the early hypertrophic response to stretch in cardiac myocytes**. *Circ Res* 2003, **93**(2):140-147.
143. Hatton JP, Pooran M, Li CF, Luzzio C, Hughes-Fulford M: **A short pulse of mechanical force induces gene expression and growth in MC3T3-E1 osteoblasts via an ERK 1/2 pathway**. *J Bone Miner Res* 2003, **18**(1):58-66.
144. Weyts FA, Li YS, van Leeuwen J, Weinans H, Chien S: **ERK activation and alpha v beta 3 integrin signaling through Shc recruitment in response to mechanical stimulation in human osteoblasts**. *J Cell Biochem* 2002, **87**(1):85-92.

145. Birukov KG, Lehoux S, Birukova AA, Merval R, Tkachuk VA, Tedgui A: **Increased pressure induces sustained protein kinase C-independent herbimycin A-sensitive activation of extracellular signal-related kinase 1/2 in the rabbit aorta in organ culture**. *Circ Res* 1997, **81**(6):895-903.
146. Azuma N, Duzgun SA, Ikeda M, Kito H, Akasaka N, Sasajima T, Sumpio BE: **Endothelial cell response to different mechanical forces**. *J Vasc Surg* 2000, **32**(4):789-794.
147. Rice DC, Dobrian AD, Schriver SD, Prewitt RL: **Src autophosphorylation is an early event in pressure-mediated signaling pathways in isolated resistance arteries**. *Hypertension* 2002, **39**(2 Pt 2):502-507.
148. Kawata Y, Mizukami Y, Fujii Z, Sakumura T, Yoshida K, Matsuzaki M: **Applied pressure enhances cell proliferation through mitogen-activated protein kinase activation in mesangial cells**. *J Biol Chem* 1998, **273**(27):16905-16912.
149. Salcini AE, Chen H, Iannolo G, De Camilli P, Di Fiore PP: **Epidermal growth factor pathway substrate 15, Eps15**. *Int J Biochem Cell Biol* 1999, **31**(8):805-809.
150. Altschuler Y, Kinlough CL, Poland PA, Bruns JB, Apodaca G, Weisz OA, Hughey RP: **Clathrin-mediated endocytosis of MUC1 is modulated by its glycosylation state**. *Mol Biol Cell* 2000, **11**(3):819-831.
151. Bissell MJ, Weaver VM, Lelievre SA, Wang F, Petersen OW, Schmeichel KL: **Tissue structure, nuclear organization, and gene expression in normal and malignant breast**. *Cancer Res* 1999, **59**(7 Suppl):1757-1763s.
152. Ahmad Z, Huang KP: **Dephosphorylation of rabbit skeletal muscle glycogen synthase (phosphorylated by cyclic AMP-independent synthase kinase 1) by phosphatases**. *J Biol Chem* 1981, **256**(2):757-760.
153. Walker DC, MacKenzie A, Hosford S: **The structure of the tricellular region of endothelial tight junctions of pulmonary capillaries analyzed by freeze-fracture**. *Microvasc Res* 1994, **48**(3):259-281.
154. Bazzoni G, Martinez Estrada O, Dejana E: **Molecular structure and functional role of vascular tight junctions**. *Trends Cardiovasc Med* 1999, **9**(6):147-152.
155. Del Maschio A, Zanetti A, Corada M, Rival Y, Ruco L, Lampugnani MG, Dejana E: **Polymorphonuclear leukocyte adhesion triggers the disorganization of endothelial cell-to-cell adherens junctions**. *J Cell Biol* 1996, **135**(2):497-510.
156. Burns AR, Bowden RA, MacDonell SD, Walker DC, Odebunmi TO, Donnachie EM, Simon SI, Entman ML, Smith CW: **Analysis of tight junctions during neutrophil transendothelial migration**. *J Cell Sci* 2000, **113 (Pt 1)**:45-57.
157. Reiss Y, Hoch G, Deutsch U, Engelhardt B: **T cell interaction with ICAM-1-deficient endothelium in vitro: essential role for ICAM-1 and ICAM-2 in transendothelial migration of T cells**. *Eur J Immunol* 1998, **28**(10):3086-3099.
158. Hayashi T, Takahashi T, Motoya S, Ishida T, Itoh F, Adachi M, Hinoda Y, Imai K. **MUC1 mucin core protein binds to the domain 1 of ICAM-1.** *Digestion* 2001, 63 (Suppl 1):87-92.
159. O'Byrne K. J., A. G. Dalgleish. **Chronic immune activation and inflammation as the cause of malignancy.** *Br J Cancer* 2001, **85**(4):473-83.
160. Leandro M. J., D. A. Isenberg. **Rheumatic diseases and malignancy--is there an association?** *Scand J Rheumatol* 2001, **30**(4):185-8.

APPENDIX A

Comparison of RIPA and Brij-97 Lysis Buffers

APPENDIX A

Comparison of RIPA and Brij-97 Lysis Buffers

A.1. Objective

The extraction of MUC1 from cellular samples with lysis buffer was required for many of the experiments in this project. Interestingly, it has been reported that the efficiency of MUC1 extraction could differ depending on the type of lysis buffer detergent used[132]. In 2000, Quin and McGuckin compared the RIPA and Brij-97 (consisted mainly of NP40 and Brij-97 detergents, respectively) lysis buffers and found that they had unique MUC1-extraction properties[132]. Since MUC1 extraction was a crucial part of most experiments in this project, we were interested to determine the capabilities of RIPA and Brij-97 lysis buffers to extract MUC1 from cell lines MCF-7 and GZ.Hi.

A.2. Materials and Methods

Antibodies

Monoclonal mouse β-tubulin antibody was purchased from BD Biosciences (Mississauga, ON, Canada). Monoclonal anti-CT2, HRP-conjugated goat anti-Armenian hamster, and HRP-conjugated goat anti-mouse were previously described in section 2.1.1.

Cells and Reagents

Cell lines and culturing conditions for MCF-7, GZ.Hi, and NIH3T3 were previously described in sections 2.1.1 and 2.1.3. All cell lines were cultured at 37°C in a humidified incubator containing 5% CO_2.

Reagents used were previously described in sections 2.1- 2.2.

Experimental Conditions and Cell Extraction

Cell lines were cultured and extracted with either 80 µl of RIPA or Brij-97 lysis buffers as described in section 2.1.1. Crude samples were boiled in Laemmli Buffer, then either analyzed immediately or stored at -20°C.

SDS-PAGE and Western Blotting

Samples were analyzed with Bio-Rad *DC* Protein Assay and Bio-Rad Mini-PROTEAN II gel (12% (w/v acrylamide) with 4% (w/v acrylamide) stacking) electrophoresis as described in section 2.1.1. Proteins were then transferred to 0.45 micron Immobilon-P membranes as described in section 2.1.1.

Immunoblotting procedures with the anti-CT2 antibody, in addition to image development with ECL Plus were previously described in section 2.1.1.

A.3. Results

Cell lines MCF-7 and GZ.Hi were lysed with either RIPA or Brij-97 lysis buffers and subsequently Western blotted for the cytoplasmic domain of MUC1 with CT2 antibody. The NIH3T3 cell line was used as a MUC1-negative control as it was determined to lack MUC1 expression in section 3.1.1. Reactive protein smears at ~25 kDa and ~13 kDa were readily detected in the MCF-7 and GZ.Hi cell lines that were extracted with the RIPA lysis buffer (lanes 2 and 4, Figure A.1A). These protein bands were also detected when the same cell lines were lysed with Brij-97 lysis buffer (lanes 3 and 5, Figure A.1A). However, they were much less intense than the RIPA buffer-lysed counterparts. An additional protein band at ~17 kDa was found almost exclusively in the RIPA buffer-lysed samples (red arrows, Figure A.1A). This band was only barely detectable in the GZ.Hi's and MCF-7s when these cells lines were lysed with the Brij-97 buffer. The protein bands at ~25 kDa, 17 kDa, and 13 kDa described above were not found in the NIH3T3 samples, suggesting that they were most likely specific CT2 bands. When the membrane was re-probed with β-tubulin antibody, a protein band at ~50 kDa of similar intensity was detected in all lanes (Figure A.1B).

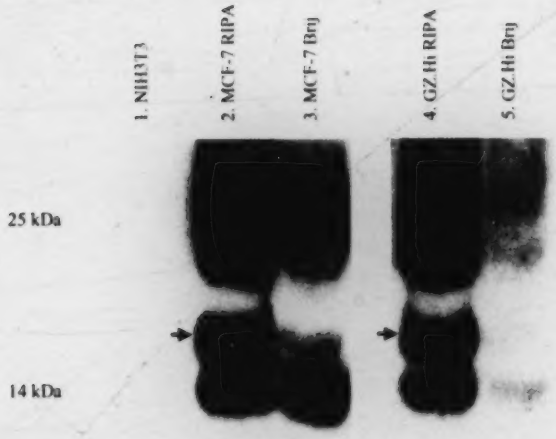

Figure A.1A. The RIPA lysis buffer was more efficient in MUC1 extraction. Upon immunoblotting with CT2 antibody, a reactive protein smear at ~25 kDa and a band at ~13 kDa were readily detected in the MCF-7 and GZ.Hi cell lines extracted with RIPA lysis buffer. These bands were also detected when the same cell lines were lysed with Brij-97 lysis buffer, but of much less intensities. An additional protein band at ~17 kDa was found almost exclusively in the RIPA buffer-lysed samples (red arrows). This band was only barely detectable in the Brij-97 buffer-lysed counterparts. The protein bands at ~25 kDa, 17 kDa, and 13 kDa were not found in the NIH3T3 samples.

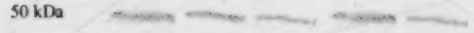

Figure A.1B. β-tubulin detected in all experimental conditions. The same membrane was re-probed with β-tubulin antibody, a protein band at ~50 kDa of similar intensity was detected in all lanes.

A.4. Discussion and Conclusion

Detergents in lysis buffers have amphipathic properties and function to disrupt cellular membranes by intercalating into phospholipid bilayers[2]. An additional role of detergents is to solubilize transmembrane proteins by coating, and consequently preventing interactions of their hydrophobic regions[2]. Otherwise, transmembrane protein molecules can aggregate and precipitate from aqueous solutions[2]. Quin and McGuckin (2000) have shown that the RIPA and Brij-97 lysis buffers had different MUC1 extraction efficiencies[132]. The RIPA buffer contained NP40 (also known as Nonidet P 40 or Imbentin-N/52) as the major detergent, which is stronger than the Brij-97 detergent[132]. Therefore, it was reported that the RIPA buffer could extract higher levels of total MUC1 from breast and ovarian cancer cell lines[132]. We investigated the MUC1-extracting capabilities of the two lysis buffers. It was found that the RIPA and Brij-97 buffers were able to extract MUC1 of molecular weights ~25 kDa and 13 kDa (Figure A.1A). These values were consistent with the molecular weights of MUC1's cytoplasmic domains found in earlier experiments (Figures 15-17) and the literature[43, 132]. However, the RIPA buffer had consistently extracted higher levels of these proteins than the Brij-97 buffer (Figure A.1A), which was consistent with the fact that NP40 is a stronger detergent than Brij-97. These findings were also in agreement with those from Quin and McGuckin (2000)[132]. Interestingly, the ~17 kDa MUC1/CT2 band was found almost exclusively in the RIPA buffer-lysed MCF-7 and GZ.Hi samples (Figure A.1A). This band was consistent with the molecular weight of MUC1's cytoplasmic

domain found in earlier experiments (Figures 15-21) and the literature[43, 132]. Based on these preliminary results, it appeared that the RIPA buffer has two advantages over the Brij-97 buffer. First, it was able to extract greater amounts of MUC1 from membranes of MCF-7 and GZ.Hi cell lines. Moreover, the RIPA buffer extracted an additional MUC1 cytoplasmic domain isoform at ~17 kDa that the Brij-97 buffer could not accomplish. Therefore, the RIPA lysis buffer was selected for MUC1 extraction in this project in order to maximize the MUC1 extraction yield, and to reduce the risk of losing MUC1 isoforms.

APPENDIX B

Differential Cell Density and MUC1 Detection

APPENDIX B

Differential Cell Density and MUC1 Detection

B.1. Objective

It was previously reported by Quin and McGuckin (2000) that the extent of MUC1 tyrosine phosphorylation was inversely related to the density of cancer cell culture[132]. Our lab suspected the reason for this phenomenon was due to the possible dependency of MUC1 expression on cell confluence. This theory was investigated with the MCF-7 cell line, where the extent of MUC1 expression was compared at three different cell culturing densities corresponding to 20%, 80% and 160% confluences.

B.2. Materials and Methods

Antibodies

Monoclonal mouse β-tubulin antibody was previously described in Appendix A. Monoclonal anti-CT2, HRP-conjugated goat anti-Armenian Hamster, and HRP-conjugated goat anti-mouse were previously described in section 2.1.1.

Cells and Reagents

Cell lines and culturing conditions of MCF-7 and NIH3T3/Mock were previously described in section 2.1.1. All cell lines were cultured at 37°C in a humidified incubator containing 5% CO_2.

Reagents used were previously described in sections 2.1-2.2.

Experimental Conditions and Cell Extraction

Cell number of either 8.4 x 10^5, 6.72 x 10^6 or 1.34 x 10^7 MCF-7s was plated on 100 mm x 20 mm tissue culture plates for overnight under the conditions described in section 2.1.1. These cell densities corresponded to approximately 20%, 80% and 160% confluence, respectively. The NIH3T3/Mock cell line was cultured to 70-80% confluence. Cell extraction procedures were previously described in section 2.1.1. Supernatants were boiled in Laemmli Buffer, then either analyzed immediately or stored at -20°C.

SDS-PAGE and Western Blotting

Samples were analyzed with Bio-Rad *DC* Protein Assay and Bio-Rad Mini-PROTEAN II gel (10-15% (w/v acrylamide) with 4% (w/v acrylamide) stacking). Detailed procedures for electrophoresis can be found in section 2.1.1. Proteins were then transferred to 0.45 micron Immobilon-P membranes as described in section 2.1.1.

Detailed procedures of CT2 and β-tubulin immunoblotting, in addition to image development with ECL Plus were previously described in Appendix A and section 2.1.1, respectively. The membranes were first immunoblotted for CT2, followed by β-tubulin, without stripping off the membrane-bound CT2 antibodies. Detailed procedures were previously described in section 2.2.1.

The levels of CT2 and β-tubulin expressions in each experimental condition were quantified using the Scion Image computer software. The CT2 level in each condition was then taken as a ratio to the corresponding amount of β-tubulin and compared. The ANOVA (analysis of variance) test with a p value of 0.01 was performed to statistically test the null hypothesis that the CT2/β-tubulin ratio of each experimental condition was indifferent from each other.

B.3. Results

The levels of MUC1 expression was compared in the MCF-7 cell line grown at three different cell culturing densities: $8.4x10^5$ (designated as 20% confluence), $6.72x10^6$ (80% confluence) and $1.34x10^7$ (160% confluence). The crude lysates were then analyzed on a 10-15% polyacrylamide gel and immunoblotted with anti-CT2 (Figure B.1A). Distinct protein smears at ~17-25 kDa and ~13-15 kDa were detected in MCF-7 exclusively, but not in the MUC1-negative control NIH3T3/Mock. The molecular weights of these protein smears were consistent with the bands determined to be MUC1 from Figures 14B and 15, and hence, were most likely the cytoplasmic domains of MUC1.

The same membrane from Figure B.1A was blocked with 5% milk TBS-T for at least 24 h at 4°C, and subsequently re-probed with monoclonal β-tubulin antibody without stripping. Membrane-stripping was not performed due to reasons previously discussed in section 3.2.1. A distinct protein band representing β-

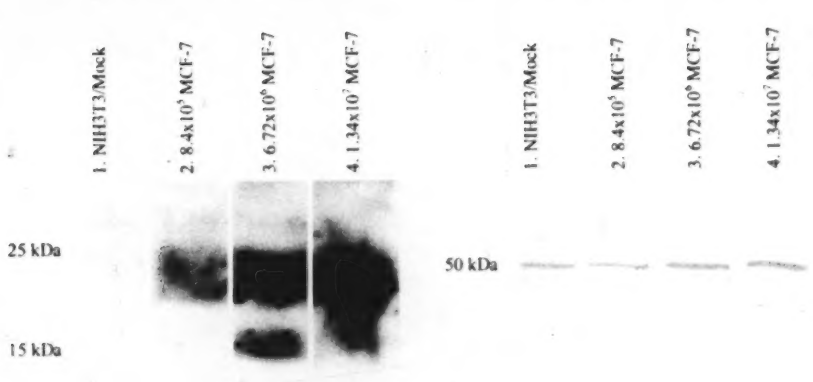

(A) IB: CT2 **(B)** IB: β-Tubulin

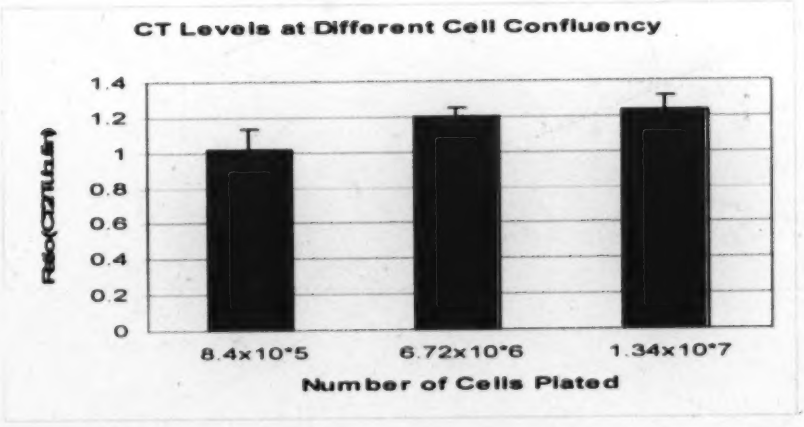

(C) Corrected CT2 levels at different cell confluences

Figure B.1. **(A)** Western blot of MCF-7 crude samples for MUC1's cytoplasmic domain with monoclonal CT2 antibody on a 10-15% (w/v) polyacrylamide gel. MCF-7 was plated at densities $8.4x10^5$ (20% confluence), $6.72x10^6$ (80% confluence) and $1.34x10^7$ (160% confluence) cells and cultured overnight. Distinct protein smears at ~17-25 kDa and ~13-15 kDa detected in MCF-7 exclusively. **(B)** The same membrane from **(A)** was re-probed with monoclonal β-tubulin antibody. A distinct protein band at 50 kDa was detected in all lanes. **(C)** The ratio of CT2/β-tubulin expressions at each cell density was calculated and analyzed with the ANOVA test using p value of 0.01. No significant difference in MUC1 expression was found in between the three cellular densities.

tubulin at 50 kDa was detected in all lanes (Figure B.1B). The levels of CT2 and β-tubulin expressions in each lane were quantified using the Scion Image computer software. The CT2 level in each lane was then taken as a ratio to the corresponding amount of β-tubulin and compared on a bar graph (Figure B.1C). Subsequently, the test of ANOVA with a p value of 0.01 was performed on the data for statistical analysis, and the null hypothesis was accepted. The levels of MUC1 expression did not significantly differ in between the different cell culturing densities. Therefore, the data suggested that MUC1 expression in MCF-7 cells was not dependent on cell confluence. This would mean the inverse relationship between cell confluence and the extent of MUC1 tyrosine phosphorylation observed by Quin and McGuckin (2000) was not attributed to variations in the levels of MUC1 expression[132].

B.4. Discussion and Conclusion

Quin and McGuckin (2000) previously reported that the extent of MUC1 tyrosine phosphorylation was inversely related to the density of cancer cell culture[132]. In fact, they found that MUC1 phosphorylation was at least six-fold higher in sub-confluent cultures than in confluent or over-confluent cultures[132]. Although no explanation was given for this phenomenon, our lab suspected it could be due to the dependence of MUC1 expression on culturing confluence. To test out this theory, the extent of MUC1 expression in MCF-7 cells was compared between the arbitrary 20%, 80% and 160% confluences. The cytoplasmic domains of MUC1 were detected at ~17-25 kDa and ~13-15 kDa (Figure B.1A), which were

consistent with the findings from Figures 14B and 15, and also the literature[43, 83, 132]. In addition, β-tubulin was detected at ~50 kDa upon re-probing the membranes with monoclonal β-tubulin antibody. The extent of MUC1 and β-tubulin (Figure B.1B) expressions in each condition were quantified with Scion Image computer software, and the CT2/β-tubulin ratio was then calculated. The ratios were analyzed with the ANOVA test using a p value of 0.01. There was no statistical difference in MUC1 expression under the three cell culturing densities tested (Figure B.1C). Hence, the data from Appendix B suggested that there was no significant relationship between MUC1 expression and cell confluence in the MCF-7s. Therefore, the inverse relationship between cell confluence and the extent of MUC1 tyrosine phosphorylation observed by Quin and McGuckin (2000) was unlikely due to variations in the levels of MUC1 expression[132]. However, other factors such as the adherent status[132] and agents in the microenvironment[41] of tumor cells have also been reported to affect MUC1 phosphorylation.

APPENDIX C

Sodium Orthovanadate Treatment on MCF-7 Cell Line

APPENDIX C

Sodium Orthovanadate Treatment on MCF-7 Cell Line

C.1. Objective

The ability to detect tyrosine-phosphorylated MUC1 through Western blotting was one of the crucial prerequisites for analyzing results in this project. The literature molecular weight values of MUC1 cytoplasmic domain phosphorylation ranged anywhere from ~30 kDa[132] to ~15 kDa[81]. These inconsistencies have made data interpretation extremely difficult. Therefore, it was attempted here to determine the molecular weight of MUC1 tyrosine phosphorylation by Western blots. This was accomplished by analyzing the effects on phosphotyrosine detection after treatment of the MCF-7 cell line with sodium orthovanadate (a tyrosine phosphatase inhibitor that functions to preserve tyrosine phosphorylations of proteins) for various durations.

C.2. Materials and Methods

Antibodies

Monoclonal anti-phosphotyrosine PY99, monoclonal anti-CT2, HRP-conjugated goat anti-mouse, and HRP-conjugated goat anti-Armenian hamster were previously described in sections 2.1.1 and 2.2.1.

Cells and Reagents

Cell lines and culturing conditions of MCF-7 and NIH3T3/ICAM-1 were previously described in section 2.1.1. They were cultured at 37°C in a humidified incubator containing 5% CO_2.

Reagents used were previously described in sections 2.1- 2.2.

Experimental Conditions and Cell Extraction

Cell lines were cultured on 100 mm x 20 mm tissue culture plates until 70-80% confluent. Plates of cells were washed twice with sterile PBS and incubated with 2 ml of FBS-free DMEM media for 6 h. Starved MCF-7 cells were subsequently incubated with 1 mM Na_3VO_4 for durations: 2 min, 5 min, 10 min and 30 min. MCF-7 and NIH3T3/ICAM-1 cells not treated with Na_3VO_4 were used as controls.

All cell extraction procedures were performed at 4°C or on ice. Cultured cells were washed twice with cold PBS, and the washes were collected in 15 milliliter centrifuge tubes. The washes were discarded after centrifugation at 1500 RPM and 4°C for 5 min. Cell pellets were re-suspended in 50 µl of RIPA lysis buffer and collected in 1.5 ml Eppendorf tubes. Cells that remained on culture plates were scraped into 80 µl of RIPA lysis buffer with a Teflon policeman. Subsequently, samples were collected in the 1.5 ml Eppendorf tube containing the

washed pellet counterpart obtained earlier, and lysed with 26 gauge needles. Lysates were centrifuged at 10,000 x g for 10 minutes, and supernatants were subjected to immunoprecipitation (via CT2 antibody) immediately. The crude lysates were boiled in Laemmli Buffer for 10 min, which were either analyzed immediately or stored at -20°C.

Immunoprecipitation of MUC1

Supernatants were immunoprecipitated for MUC1 with monoclonal CT2 antibody at 4°C or on ice. Detailed procedures were previously described in section 2.1.2. Furthermore, the experimental condition called Mock IP (consisted of RIPA lysis buffer, CT2 antibody and protein G-agarose) was also included to identify the non-specific bands associated with the IP procedure.

SDS-PAGE and Western Blotting

Samples were analyzed with Bio-Rad *DC* Protein Assay and Bio-Rad Mini-PROTEAN II gel (10-15% (w/v acrylamide) with 4% (w/v acrylamide) stacking) electrophoresis. Detailed procedures for electrophoresis can be found in section 2.1.1. Proteins were then transferred to 0.45 micron Immobilon-P membranes as described in section 2.1.1.

Detailed procedures for phosphotyrosine and CT2 immunoblotting, in addition to image development with ECL Plus were previously described in section 2.2.1.

C.3. Results

Following the treatment of MCF-7s with Na_3VO_4 for durations ranging from zero to 30 minutes, lysates were immunoprecipitated with monoclonal CT2 antibody. The samples were subsequently analyzed on a 10-15% polyacrylamide gel and Western blotted for phosphotyrosines with monoclonal PY99 antibody. Non-specific protein bands were identified with the Mock IP condition, which consisted of RIPA lysis buffer and IP reagents (i.e. anti-CT2 and protein G-agarose) (lane 8, Figure C.1A). Two distinctive phosphotyrosine bands at ~14 kDa and 15 kDa were detected in the MCF-7 and NIH3T3/ICAM-1 samples (red arrows in lanes 3-7, Figure C.1A), but absent in the Mock IP (lane 8, Figure C.1A). Due to the presence of the two phosphotyrosine bands in the MUC1-negative control (NIH3T3/ICAM-1), they were unlikely to be phosphorylated MUC1.

In order to verify the identities of the ~14 kDa and 15 kDa phosphotyrosine bands seen in Figure C.1A, the same membrane was re-probed for MUC1 cytoplasmic domain using CT2 antibody after at least 24 h from the initial phosphotyrosine detection. The membrane was not stripped in between consecutive Western blotting for reasons previously discussed in section 3.2.1. Again, non-specific protein bands were identified with the Mock IP condition (lane 8, Figure C.1B). As can be seen, two distinct protein bands at moelcular weights of ~14 kDa and 15 kDa were identified in the MCF-7 and NIH3T3/ICAM-1 samples (indicated by

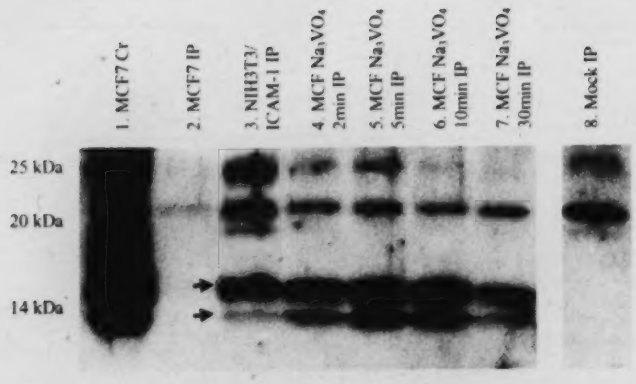

(A) IB: Anti-Phosphotyrosine

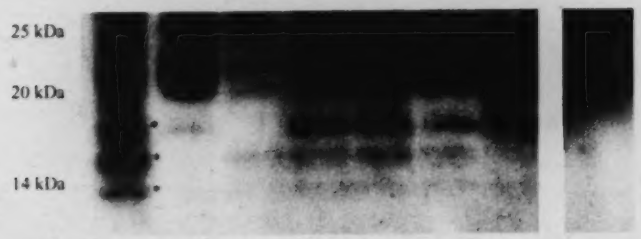

(B) IB: Anti-CT2

Figure C.1. MUC1 tyrosine phosphorylation was not detected upon treating MCF-7 cells with sodium orthovanadate for various durations. **(A)** Western blot with PY99 antibody on a 10-15% (w/v) polyacrylamide gel. Non-specific phosphotyrosine bands at ~15 kDa and 14 kDa detected (red arrows). **(B)** The same membrane from **(A)** re-probed for MUC1's cytoplasmic domain with CT2 antibody. The two non-specific protein bands that matched the two phosphotyrosine bands in **(A)** are indicated by the red asterisks. The specific MUC1/CT2 band at ~17 kDa (blue asterisk) did not correspond to any phosphotyrosine bands in **(A)**.

the red asteriks, Figure C.1B). These bands corresponded in molecular weights to the two phosphotyrosine bands seen earlier in Figure C.1A, as determined by overlaying the film images of both blots. However, the two protein bands were unlikley to be MUC1 due to their presence in the NIH3T3/ICAM-1 samples. Interestingly, a third protein band at ~17 kDa was found exclusively in the MCF-7 samples (indicated by the blue asterisk in lanes 1-2 and 4-7, Figure C.1B). This was most likely a specific MUC1/CT2 band since it was not detected in the two MUC1-negative controls, NIH3T3/ICAM-1 IP and Mock IP. Moreover, the molecular weight of this band was consistent with the MUC1 cytoplasmic domain found in earlier experiments (Figures 14B and 15) and the literature[41, 43, 132]. However, the ~17 kDa MUC1/CT2 band did not correspond to any phosphotyrosine bands detected in Figure C.1A.

C.4. Discussion and Conclusion

MUC1 cytoplasmic domain phosphorylations have been reported to range anywhere from ~15 kDa to 30 kDa in the literature[81, 132]. These inconsistencies have made data interpretation extremely difficult. Therefore, it was attempted here to determine the molecular weight of MUC1 tyrosine phosphorylation by Western blots. The MCF-7 cell line was treated with sodium orthovanadate, a tyrosine phosphatase inhibitor that functions to preserve tyrosine phosphorylations of proteins. Although two very distinctive phosphotyrosine bands at ~14 kDa and 15 kDa were detected in the MCF-7s, they were also present in the MUC1-negative control NIH3T3/ICAM-1 (Figure C.1A). Upon re-

probing for MUC1's cytoplasmic domain, two bands at ~14 kDa and 15 kDa were found in the MCF-7 and NIH3T3/ICAM-1 samples (Figure C.1B), which also overlapped with the phosphotyrosine bands detected in Figure C.1A. Based on the observation that NIH3T3/ICAM-1 and MCF-7 samples shared these same bands, the ~14 kDa and 15 kDa bands were unlikely to be phosphorylated MUC1. The detection of non-specfic protein bands in the NIH3T3/ICAM-1 samples and Mock IP could possibly be due to cross-reactivity of the HRP-conjugated secondary antibodies. This theory can be tested by Western blotting the same samples with only the HRP-conjugated antibodies in the absence of any primary antibodies of interest (Appendix D). Such experiment would indicate non-specificity of the secondary antibodies if the same non-specific protein bands as found in Figures C.1A and C.1B are obtained.

Interestingly, a third CT2 band at ~17 kDa was found exclusively in the MCF-7s (Figure C.1B), and hence, was most likely MUC1. However, it did not correspond to any phosphotyrosine bands identified in Figure C.1A. Therefore, the preliminary data from Appendix C suggested that tyrosine-phosphorylated MUC1 at ~17 kDa was not detected upon treating MCF-7 cells with sodium orthovanadate for up to 30 minutes.

Tyrosine phosphorylation of full-length MUC1 upon treating MCF-7s with sodium pervanadate for 30 min have been previously shown by Pandey *et al.* (1995)[85]. However, their protocol differed from the one used in this experiment

in two major ways. First of all, they used anti-DF3, an antibody specific for the extracellular domain of MUC1 for immunoprecipitation. In contrast, the CT2 antibody was chosen as the immunoprecipitating antibody here. This was because the presence of SDS in the lysis buffer could present the risk of dissociation of the two MUC1 (extracellular and cytoplasmic) segments[132]. Hence, the use of CT2 antibody would prevent the loss of MUC1's cytoplasmic domain during the immunoprecipitation process. Secondly, Pandey *et al.* (1995) used the Brij-96 detergent for cell lysing as opposed to the NP40 detergent used here[85]. The reason why NP40 was selected for cell lysing in this experiment was because of its ability to extract more MUC1 isoforms in greater concentrations, as shown in Appendix A. However, other groups have previously used anti-CT2 as the immunoprecipitation antibody and NP40 as the cell lysis detergent, and were successful in finding MUC1 tyrosine phosphorylation under other experimental conditions[43, 81]. Therefore, perhaps a longer Na_3VO_4 incubation time would be sufficient for more effective detection of MUC1 phosphorylation when the CT2 antibody and NP40 detergent are used. Furthermore, it appeared that the Mock IP condition was not effective in identifiying certain non-specific protein bands. Consequently, it would be crucial to include a MUC1-negative cell line as controls in order to identify certain non-specific protein bands that could easily be mistaken as MUC1 due to similarities in molecular weights.

APPENDIX D

Test Specificity of HRP-Goat Anti-Mouse and HRP-Goat Anti-Armenian Hamster Monoclonal Antibodies

APPENDIX D

Test Specificity of HRP-Goat Anti-Mouse and HRP-Goat Anti-Armenian Hamster Monoclonal Antibodies

D.1. Objective

The detection of non-specific protein bands for MUC1-negative samples on Western blots was a common problem encountered in Appendix C, which made data interpretation extremely difficult. This phenomenon could be due to cross-reactivity of the HRP-goat anti-mouse and HRP-goat anti-Armenian hamster antibodies used in Western blotting. To test this theory, cell lines (1) MCF-7, (2) MDA-MB-468, (3) NIH3T3/ICAM-1 and (4) NIH3T3/Mock were analyzed by Western blots in the absence of any primary antibodies of interest, and with only the HRP-conjugated secondary antibodies.

D.2. Materials and Methods

Antibodies

Monoclonal anti-CT2, HRP-conjugated goat anti-mouse, and HRP-conjugated goat anti-Armenian Hamster were previously described in sections 2.1.1 and 2.2.1.

Cells and Reagents

Cell lines and culturing conditions for MCF-7, MDA-MB-468, NIH3T3/ICAM-1, and NIH3T3/Mock were previously described in section 2.1.1. All cell lines were cultured at 37°C in a humidified incubator containing 5% CO_2.

Reagents used were previously described in sections 2.1- 2.2.

Experimental Conditions and Cell Extraction

Cells were cultured and extracted with RIPA lysis buffer as previously described in section 2.1.1. Supernatants were subjected to immunoprecipitation (via CT2 antibody) immediately. Crude samples were boiled in Laemmli Buffer, then either analyzed immediately or stored at minus 20°C.

Immunoprecipitation of MUC1

Supernatants were immunoprecipitated for MUC1 with monoclonal CT2 antibody at 4°C or on ice. Detailed procedures were previously described in section 2.1.2. Furthermore, the experimental condition called Mock IP (consisted of RIPA lysis buffer, CT2 antibody and protein G-agarose) was also included to identify the non-specific bands associated with the IP procedure.

SDS-PAGE and Western Blotting

Samples were analyzed with Bio-Rad *DC* Protein Assay and Bio-Rad Mini-PROTEAN II gel (10-15% (w/v acrylamide) with 4% (w/v acrylamide) stacking) electrophoresis. Detailed procedures for electrophoresis can be found in section 2.1.1. Proteins were then transferred to 0.45 micron Immobilon-P membranes as previously described in section 2.1.1.

Membranes were blocked with 2% BSA in TBS-T overnight at 4°C or 1 h at room temperature, and then incubated with 120 ng/ml of HRP-conjugated goat anti-mouse for 1 h at room temperature. This was followed by three 10 min washes in TBS-T. ECL Plus was used for detection of reactive bands by exposing the membranes to imaging films from 10 s to 5 min, until the desired image intensity was obtained. Without stripping, the same membranes were then blocked with 5% commercial milk in TBS-T at 4°C for at least 24 h. This served to allow sufficient time for the previous ECL Plus signals (which have a duration of 24 h) to diminish before commencing the next round of Western blotting. Membranes were subsequently incubated with 120 ng/ml of HRP-conjugated goat anti-Armenian Hamster for 1 h at room temperature, followed by 3 washes with TBS-T. Finally, reactive bands were detected with ECL Plus on imaging films.

D.3. Results

Crude and immunoprecipitated samples of two MUC1-positive cell lines MCF-7 and MDA-MB-468, and two MUC1-negative cell lines NIH3T3/ICAM-1 and

NIH3T3/Mock were analyzed on a 10-15% (w/v) polyacrylamide gel. The samples were Western blotted directly with HRP-goat anti-mouse antibody. As it can be seen from Figure D.1A, many non-specific protein bands in from ~15-50 kDa were detected in all of the crude samples regardless of MUC1 expression (lanes 1, 3, 5 and 7). The number of non-specific bands decreased greatly upon immunoprecipitation with the CT2 antibody (lanes 2, 4, 6 and 8, Figure D.1A). The three major non-specific bands at ~50 kDa, 30 kDa and 14 kDa were particularly evident in the NIH3T3/ICAM-1 IP and NIH3T3/Mock IP samples (lanes 4 and 8, Figure D.1A). Therefore, the data suggested the HRP-conjugated goat anti-mouse bound to many non-specific proteins in crude samples regardless of MUC1 expression. However, MUC1 immunoprecipitation with anti-CT2 antibody was effective in reducing the non-specific binding of this antibody.

The same membrane from Figure D.1A was blocked in 5% milk Tween-TBS for at least 24 hours at 4°C. The purpose was not only to reduce background levels of the blot, but also to allow sufficient time for the ECL Plus signals to die down before the round of protein detection began. The membrane was then incubated with HRP-conjugated goat anti-Armenian Hamster, again in the absence of prior probing with any primary antibody. There were relatively more non-specific binding in the IP samples (lanes 2, 4, 6 and 8, Figure D.1B) than their crude counterparts, ranging from ~15-50 kDa. Therefore, the data suggested the HRP-

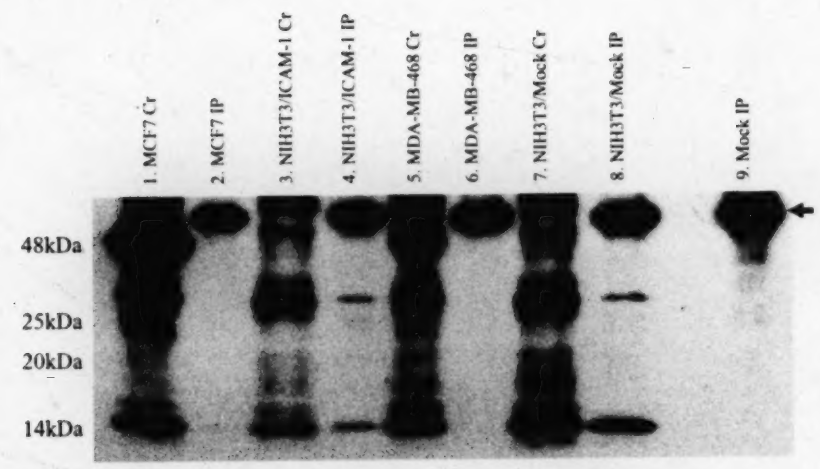

(A) IB: HRP-goat anti-mouse

(B) IB: HRP-goat anti-Armenian Hamster

Figure D.1. The HRP-conjugated secondary antibodies have inherent non-specific binding properties. **(A)** Western blot of crude and IP samples with HRP-conjugated goat anti-mouse antibody without any primary antibody of interest on a 10-15% (w/v) polyacrylamide gel. More non-specific protein bands were detected in the crude samples than their corresponding IP counterparts. A common band at ~50 KDa detected in all IP samples (blue arrow). **(B)** The same membrane from **(A)** was re-probed with HRP-conjugated goat anti-Armenian Hamster antibody in the absence of any primary antibody incubation. In contrast to **(A)**, relatively more non-specific protein bands were observed with the IP than crude samples. Two common bands at ~27 kDa and 50 kDa detected in all IP samples (red arrows).

conjugated goat anti-Armenian Hamster bound to many non-specific proteins in the IP samples regardless of MUC1 expression. The non-specific protein bands identified in Figures D.1A and D.1B will be taken into consideration for subsequent Western blot analyses.

D.4. Discussion and Conclusion

The detection of non-specific protein bands for MUC1-negative samples on Western blots was a common problem encountered in Appendix C, which made data interpretation extremely difficult. This phenomenon could be due to cross-reactivity of the HRP-goat anti-mouse and HRP-goat anti-Armenian hamster antibodies used in Western blotting. The MCF-7, MDA-MB-468, NIH3T3/ICAM-1 and NIH3T3/Mock cell lines were first analyzed by Western blots with only the HRP-conjugated goat anti-mouse, the secondary antibody normally used for phosphotyrosine immunoblotting. A whole range of non-specific protein bands from ~15-50 kDa were detected in all of the crude samples regardless of MUC1 expression (Figure D.1A). In contrast, only the ~50 kDa non-specific band was present in every IP sample, which was most likely the heavy chain of the CT2 antibody (blue arrow in Figure D.1A). Moreover, the non-specific ~30 and 15 kDa bands of unknown identities were apparently exclusive to the NIH3T3/ICAM-1 and NIH3T3/Mock IP samples (Figure D.1A). Therefore, the HRP-conjugated goat anti-mouse antibody was shown to bind non-specifically in Western blotting. However, MUC1 immunoprecipitation with

anti-CT2 antibody was effective in reducing the extent of non-specific antibody-protein associations.

The same membrane from Figure D.1A was then re-probed with HRP-conjugated goat anti-Armenian Hamster, the secondary antibody normally used for CT2 immunoblotting. In contrary to the findings from Figure D.1A, relatively more non-specific binding was found in the IP samples than their crude counterparts (Figure D.1B). Again, the molecular weights of the non-specific protein bands ranged from ~15-50 kDa, with the ~50 and 27 kDa bands most likely corresponding to the heavy and light chains of the CT2 antibody, respectively (red arrows in Figure D.1B). However, the remaining bands were of unknown identities, and would be interpreted as non-specific proteins in subsequent Western blots. Therefore, the HRP-conjugated goat anti-Armenian Hamster antibody was shown to bind non-specifically in Western blotting. The preliminary data from Appendix D suggested that both HRP-conjugated goat anti-mouse and goat anti-Armenian Hamster antibodies had some inherent non-specific binding properties. The non-specific protein bands identified were taken into consideration for the remaining Western blots obtained in this project. In addition, the non-specific phosphotyrosine and CT2 bands at ~14 KDa and 15 kDa found in Appendix C could possibly be due to the non-specificities of the HRP-conjugated secondary antibodies as shown in Figures D.1A and D.1B.

APPENDIX E

rhICAM-1 Stimulation on GZ.Hi and 410.4 Cell Lines

APPENDIX E

rhICAM-1 Stimulation on GZ.Hi and 410.4 Cell Lines

E.1. Objective

The main objective of the project was to determine the effect of ICAM-1 stimulation on MUC1 tyrosine phosphorylation in tumor cells. Therefore, a source of ICAM-1 stimulation was necessary to investigate this question. The first approach taken was to use rhICAM-1, a dimeric recombinant human immunoglobulin fusion protein as the source of ICAM-1 stimulation. Its effect on MUC1 tyrosine phosphorylation was tested on two cell lines, GZ.Hi and 410.4 via an *in vitro* binding system. GZ.Hi is the mouse mammary adenocarcinoma (410.4) transfected with the human MUC1. Therefore, it expresses both the mouse and human MUC1 proteins. In contrast, 410.4 cell line expresses only the mouse MUC1, which lacks the human MUC1 tandem repeats that bind to ICAM-1. As a result, any effect on MUC1 tyrosine phosphorylation attributed to MUC1-ICAM-1 ligation should theoretically be absent in 410.4.

E.2. Materials and Methods

Antibodies

Monoclonal anti-ICAM-1 was kindly donated by ICOS Corp. (Bothell, WA, USA). Monoclonal anti-phosphotyrosine PY99, monoclonal anti-CT2, monoclonal B27.29, HRP-conjugated goat anti-mouse, and HRP-conjugated goat anti-Armenian hamster were previously described in sections 2.1.1 and 2.2.1.

Cells and Reagents

Cell lines 410.4 and GZ.Hi were previously described in sections 2.1.1 and 2.1.3, respectively. They were maintained in RPMI 1640 supplemented with 10% FBS and 2 mM L-glutamine at 37°C in a humidified incubator containing 5% CO_2.

rhICAM-1 is a dimeric recombinant human immunoglobulin fusion protein of human ICAM-1 and IgG molecule (a gift from ICOS Corp). Other reagents used were previously described in sections 2.1-2.2.

Experimental Conditions and Cell Extraction

Cell lines were cultured on 100 mm x 20 mm tissue culture plates until 70-80% confluent. Prior to incubation with rhICAM-1, plates were washed twice with sterile PBS, and then incubated with 2 ml of sterile 60 μg/ml rhICAM-1 in PBS, with or without sodium orthovanadate. Incubation occurred at 37°C and 5% CO_2 for 10 min and 90 min. Subsequently, plates were held on ice and the rhICAM-1/PBS was recollected under sterile conditions for future use. GZ.Hi and 410.4 cells not stimulated with rhICAM-1 were used as controls.

All cell extraction procedures with Brij-97 lysis buffer were performed at 4°C or on ice, as previously described in section 2.1.1. Supernatants were subjected to immunoprecipitation (via B27.29 antibody) immediately. The crude lysates were

boiled in Laemmli Buffer for 10 min, which were either analyzed immediately or stored at -20°C.

Immunoprecipitation of MUC1

Immunoprecipitation procedures with monoclonal B27.29 antibody were previously described in section 2.1.2. The modification used in this experiment was that all of the washes were done with Brij-97 instead of RIPA lysis buffer. Furthermore, the experimental condition called Mock IP (consisted of Brij-97 lysis buffer, B27.29 antibody and protein G-agarose) was also included to identify the non-specific bands associated with the IP procedure.

SDS-PAGE and Western Blotting

Samples were analyzed with Bio-Rad *DC* Protein Assay and Bio-Rad Mini-PROTEAN II gel (10-15% (w/v acrylamide) with 4% (w/v acrylamide) stacking) electrophoresis. Detailed procedures for electrophoresis can be found in section 2.1.1. Proteins were then transferred to 0.45 micron Immobilon-P membranes, as previously described in section 2.1.1.

Detailed procedures for phosphotyrosine and CT2 immunoblotting, in addition to image development with ECL Plus were previously described in section 2.2.1. The membranes were first immunoblotted for phosphotyrosine, followed by CT2 without any membrane stripping (refer to section 2.2.1).

The levels of phosphotyrosine and CT2 expressions in each experimental condition were quantified using the Scion Image computer software. The phosphotyrosine level in each condition was then taken as a ratio to the corresponding amount of CT2 and compared. The ANOVA test with a p value of 0.01 was performed to statistically test the null hypothesis that the phosphotyrosine/CT2 ratio of each experimental condition was indifferent from each other.

E.3. Results

GZ.Hi and 410.4 cells were incubated with rhICAM-1 for 10 min and 90 min either with or without sodium orthovanadate. The samples were immunoprecipitated for MUC1 with monoclonal B27.29 antibody and analyzed on 10-15% (w/v) polyacrylamide gels. The membranes were first immunoblotted for phosphotyrosines with PY99 antibody. Non-specific protein bands were identified with the Mock IP (lane 11, Figure E.1A), a condition that consisted of Brij-97 lysis buffer, B27.29 antibody and protein G-agarose. A phosphotyrosine band at ~15 kDa was detected in the GZ.Hi and 410.4 samples (red asterisks in lanes 1-10, Figure E.1A). However, the same band was also detected in the Mock IP (red asterisk in lane 11 Figure E.1A).

In order to determine the identity of the ~15 kDa phosphotyrosine band seen in Figure E.1A, the same membranes were re-probed for MUC1's cytoplasmic domain with monoclonal CT2 antibody after at least 24 h from the initial

Trial 1

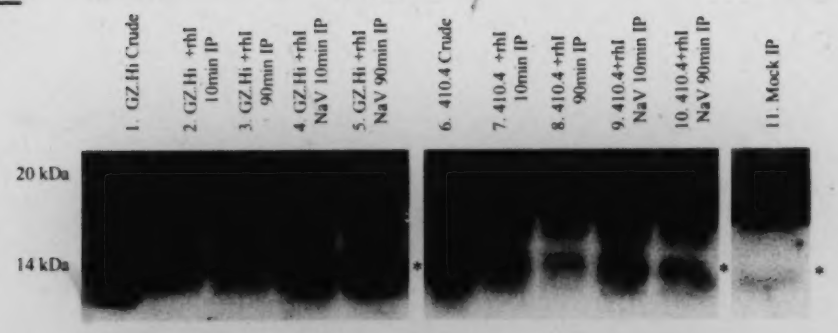
1. GZ.Hi Crude
2. GZ.Hi +rhI 10min IP
3. GZ.Hi +rhI 90min IP
4. GZ.Hi +rhI NaV 10min IP
5. GZ.Hi +rhI NaV 90min IP
6. 410.4 Crude
7. 410.4 +rhI 10min IP
8. 410.4 +rhI 90min IP
9. 410.4+rhI NaV 10min IP
10. 410.4+rhI NaV 90min IP
11. Mock IP
20 kDa
14 kDa

(A) IB: PY99

(B) IB: Anti-CT2

Trial 2

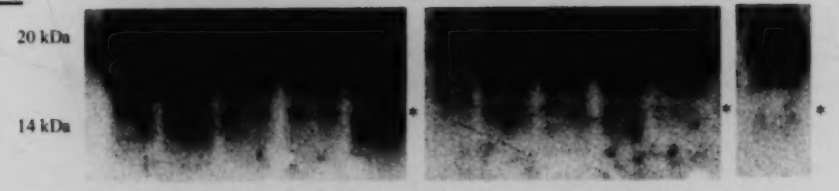

(C) IB: PY99

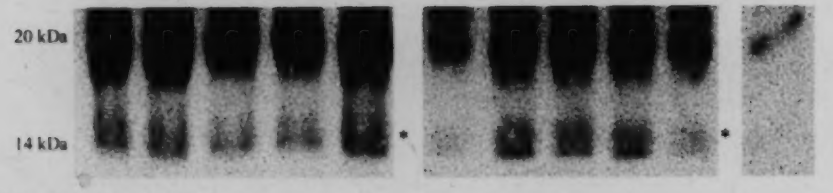

(D) IB: Anti-CT2

Figure E.1. (To be continued on next page)

Trial 3

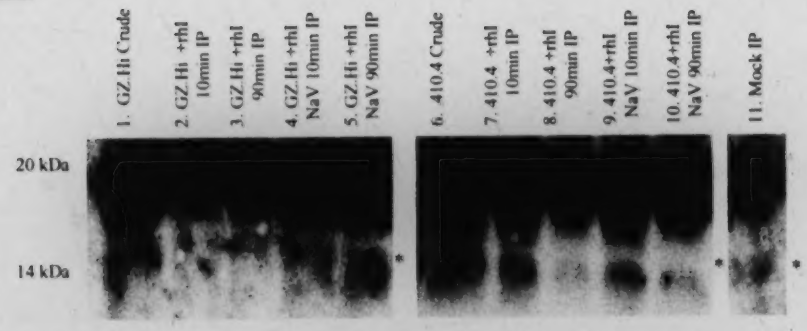
1. GZ.Hi Crude
2. GZ.Hi +rhI 10min IP
3. GZ.Hi +rhI 90min IP
4. GZ.Hi +rhI NaV 10min IP
5. GZ.Hi +rhI NaV 90min IP
6. 410.4 Crude
7. 410.4 +rhI 10min IP
8. 410.4 +rhI 90min IP
9. 410.4+rhI NaV 10min IP
10. 410.4+rhI NaV 90min IP
11. Mock IP
20 kDa
14 kDa

(E) IB: PY99

(F) IB: Anti-CT2

Figure E.1. Putative MUC1 tyrosine phosphorylation was unaffected by the presence of rhICAM-1 and/or sodium orthovanadate in GZ.Hi and 410.4 cells. **(A)** Western blotting for phosphotyrosines with PY99 antibody in GZ.Hi and 410.4 cells incubated with ±rh-ICAM-1 (I) and ±sodium orthovanadate (NaV) for 10 min and 90 min. Samples were immunoprecipitated (IP) with B27.29 and analyzed on a 10-15% (w/v) polyacrylamide gel. Phosphotyrosine band at ~15 kDa (red asterisk) detected in the GZ.Hi and 410.4 samples, but also in Mock IP. **(B)** The same membrane from **(A)** re-probed for MUC1's cytoplasmic domain with CT2 antibody. A distinct CT2 band at ~15 kDa found exclusively in the GZ.Hi and 410.4 samples (blue asteriks), but absent in the Mock IP. This band also matched with the molecular weight of the ~15 kDa phosphotyrosine band detected in **(A)**.

phosphotyrosine detection. The membranes were not stripped in between consecutive Western blotting for reasons previously discussed in section 3.2.1. A specific CT2 band at ~15 kDa was found exclusively in the GZ.Hi and 410.4 samples (blue asterisks in lanes 1-10, Figure E.1B). The same band was absent in the Mock IP (lane 11, Figure E.1B). Interestingly, the ~15 kDa CT2 band matched up with the ~15 kDa phosphotyrosine band detected earlier in Figure E.1A when the film images were overlaid.

The phosphotyrosine and MUC1 levels in each experimental condition were quantified using the Scion Image computer software. The phosphotyrosine level in each lane was then taken as a ratio to the corresponding amount of CT2 and compared on a bar graph (Figure E.2). Subsequently, the ANOVA test with a p value of 0.01 was performed on the data for statistical analysis. No significant statistical differences in the putative MUC1 phosphorylation between each of the experimental conditions. Therefore, the data suggested that the levels of putative MUC1 phosphorylation were not significantly altered by the presence of rhICAM-1 and/or sodium orthovanadate.

E.4. Discussion

The main objective of the project was to investigate the effect of ICAM-1 stimulation on MUC1 tyrosine phosphorylation in tumor cells. Therefore, a source of ICAM-1 stimulation was necessary to investigate this question. The first approach taken was to use rhICAM-1, a dimeric recombinant human

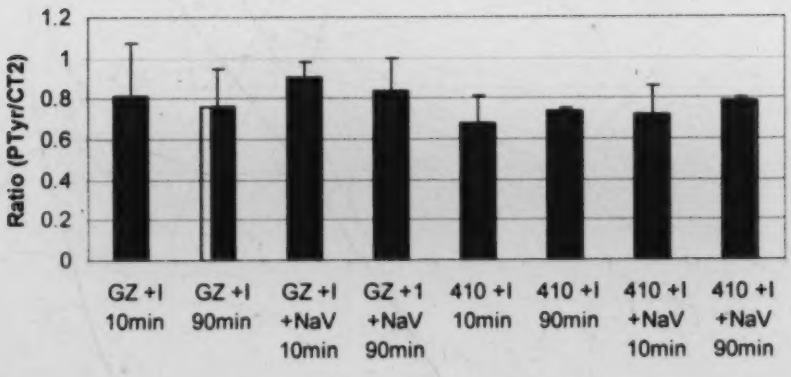

Figure E.2. Levels of MUC1 tyrosine phosphorylation was not affected by the presence of ICAM-1 and/or sodium orthovanadate. GZ.Hi and 410.4 cells were stimulated ±rhICAM-1 (I) and ±sodium orthovanadate (NaV) for 10 minutes and 90 minutes. The ratio of phosphotyrosine/CT2 expressions in each experimental condition was calculated. ANOVA Test with p value of 0.01 revealed no significant difference in levels of putative MUC1 tyrosine phosphorylation in the experimental conditions tested.

immunoglobulin fusion protein as the source of ICAM-1 stimulation. The reason for the choice of rhICAM-1 was because Kam *et al.* (1998) have demonstrated that it could bind to the human MUC1 on the surface of GZ.Hi cells[35]. Its effect on MUC1 tyrosine phosphorylation was tested on two cell lines, GZ.Hi and 410.4. GZ.Hi is the mouse mammary adenocarcinoma (410.4) transfected with the human MUC1. Therefore, it expresses both the mouse and human MUC1 proteins. In contrast, 410.4 cells express only the mouse MUC1, which lacks the human MUC1 tandem repeats that bind to ICAM-1. Therefore, effect on MUC1 tyrosine phosphorylation attributed to MUC1-ICAM-1 ligation should theoretically be absent in the 410.4 cells. The GZ.Hi and 410.4 cells were incubated with rhICAM-1 for 10 min and 90 minutes either with or without sodium orthovanadate. As demonstrated in Appendix E, a phosphotyrosine band at ~15 kDa was detected in the GZ.Hi, 410.4 and Mock IP (Figure E.1A). The same membranes were then re-probed with CT2 antibody, and a specific CT2 band at ~15 kDa was found exclusively in the GZ.Hi and 410.4 samples (Figure E.1B). The specific CT2 band also matched with the ~15 kDa phosphotyrosine band detected earlier in Figure E.1A when the film images were overlaid. However, the ~15 kDa phosphotyrosine band was unlikely to be phosphorylated MUC1 due to its presence in the Mock IP (lane 11, Figure E.1A). Perhaps a MUC1-negative cell line and a MUC1-phosphorylated sample as controls would help to identify this protein band.

Although the ~15 kDa phosphotyrosine band was unlikely to be MUC1, further analysis was carried out for verification. As was mentioned earlier, the 410.4 cell line expresses the mouse MUC1 that lacks the extracellular tandem repeats found with the human MUC1. Therefore, the MUC1 phoshorylation status in 410.4 should have been unaffected by the presence of rhICAM-1 stimulation. However, the same putative MUC1 phsophorylation at ~15 kDa was detected in both GZ.Hi and 410.4 cells (Figure E.1A). A possible explanation for this observation could be the band seen in the 410.4s represented the tyrosine-phosphorylated mouse MUC1. In contrast, the phosphotyrosine band detected in GZ.Hi cells comprised of both human and mouse MUC1 phosphorylations. Based this assumption, the phosphotyrosine levels in 410.4s should indicate the basal phosphorylation levels of mouse MUC1. Any phosphorylation in the GZ.Hi cells above those seen with the 410.4s could be attributed to human MUC1 tyrosine phosphorylation. In order to verify this theory, the phosphotyrosine and MUC1 levels in each experimental condition were quantified using the Scion Image computer software. The ratio of phosphotyrosine/CT2 quantities in each condition was calculated and compared on a bar graph (Figure E.2). The ratios were then analyzed with the test of ANOVA using a p value of 0.01 and the null hypothesis was accepted. Therefore, the data from Appendix E suggested a phosphotyrosine band at ~15 kDa was detected in both GZ.Hi and 410.4 cells that could possibly be MUC1, although more experimental controls (i.e. MUC1-negative cell line and a positive control for MUC1 phosphorylation) would be required for verification. Even if the ~15 kDa phosphotyrosine bands were MUC1, their phosphorylation statuses

were not significantly altered upon rhICAM-1 induction or Na_3VO_4 treatment. Hence, perhaps an alternative source of ICAM-1 stimulation should be employed to investigate the role of MUC1-ICAM-1 ligation on tumor cell MUC1 phosphorylation.

APPENDIX F

Localization of Tumor Cells at Tri-Endothelial Cellular Corners

APPENDIX F

Localization of Tumor Cells at Tri-Endothelial Cellular Corners

F.1. Objective

There is evidence that the steps involved in leukocyte and metastatic extravasations share some common characteristics[17, 18]. In an acute inflammatory reaction, circulating leukocytes "roll" along and subsequently firmly attach to the endothelium that lines the site of tissue injury[19, 21, 27]. Arrested leukocytes will then preferentially localize to tri-endothelial cellular junctions, sites where borders of three endothelial cells meet[18]. These are also the main locations for leukocyte transendothelial migration[18]. Similarly, circulating tumor cells also commence extravasation by first binding weakly, followed by firmly attaching to the endothelium[17]. However, it is not known in the literature whether tumor cells also localize to tri-endothelial cell corners for transendothelial migration. Therefore, it was of interest to determine whether tumor cells would preferentially localize to tri-endothelial cellular junctions, a mechanism that is used by leukocytes during inflammatory extravasation.

F.2. Materials and Methods

Antibodies

Monoclonal mouse β-catenin antibody was purchased from Zymed Laboratories Inc. (Markham, Ontario, Canada). Monoclonal rabbit Cy3-conjugated goat anti-rabbit were purchased from Jackson Immunoresearch Laboratories.

Cells and Reagents

EAhy-926 is a hybrid of HUVEC (human umbilical vein endothelial cell) and the human bronchial carcinoma cell line A549. It was a gift from Dr. C. Edgell (Immuno-Rheumatology Laboratory and Xavier Bichat University of Medicine, Paris, France). It was maintained in RPMI 1640 supplemented with 10% FBS and 2 mM L-glutamine. Human breast carcinoma cell line MDA-MB-231 and culturing conditions were previously described in section 2.1.1. All cell lines were cultured at 37°C in a humidified incubator containing 5% CO_2.

CellTracker™ Green BODIPY (8-chloromethyl-4,4-difluoro-1,3,5,7- tetramethyl-4-bora-3a,4a-diaza-*s*- indacene), a green fluorescent cell dye was purchased from Molecular Probes (Burlington, Ontario, Canada). Formaldehyde aqueous solution and glycerol gelatin were purchased from Sigma. Other reagents used were previously described in sections 2.1-2.2.

Tri-Endothelial Cellular Corner Localization Assay

75mm x 25 mm microscope slides (J. Melvin Freed Brand, U.S.A.) were shortened by 1 cm with a diamond pencil, and about 80% of the remaining area was encircled with a hydrophobic slide marker (Kiyota International Inc., Elk Grove Village, IL., U.S.A.). The slides were then UV-sterilized overnight. The EAhy-926 cell line was cultured in T-75 tissue culture flasks until fully confluent. Cells were detached with Trypsin (0.5%)-EDTA, and $5.0x10^5$ of detached cells were re-seeded within the encircled regions on the microscope slides with final

volumes of 500 µl culturing media. Subsequently, the slides were placed into 100 mm x 20 mm tissue culture plates and incubated at 37°C and 5% CO_2 until confluent monolayers were formed, as determined by light microscopy.

MDA-MB-231 cell line was cultured in T-75 tissue culture flasks until fully confluent. The cells were washed twice with sterile PBS, and subsequently incubated with 10 µM CellTracker™ Green in 10 ml of serum-free DMEM media for 30 minutes at 37°C and 5% CO_2. Flasks were then washed once with sterile PBS and re-incubated with 10 ml of pre-warmed, serum-containing media at 37°C and 5% CO_2 for another 30 min. Cells were then detached from the flasks with Trypsin (0.5%)-EDTA. A count of $7.0x10^4$ detached cells was incubated with each slide of EAhy-926 monolayer in 200 µl final volume of media at 37°C + 5% CO_2 for 3 h. The slides were then fixed with 2% formaldehyde for 15 min at room temperature, followed by 3 brief washes with 0.05% Tween PBS (PBS-T). Slides were stored at room temperature for future analysis or subjected to fluorescent staining immediately.

Fluorescent Staining and Confocal Microscopy:

Fluorescent staining procedures were performed in a hydrated chamber at room temperature. Slides were permeabilized with 500 µl of 0.5% Triton in PBS for 15 min. Subsequently, the slides were blocked with 2% BSA in PBS-T for 1 h, followed by 1 h incubation with 0.4 µg/ml β-catenin antibody. The slides were

subjected to three 15 min washes with PBS-T, followed by an hour of incubation with 10 μg/ml Cy3-conjugated goat anti-rabbit. Another three 15 min washes with PBS-T took place. A piece of 24 mm x 30 mm glass coverslip (thickness 1; Fisher Scientific Co.) was adhered to each microscope slide with a small drop of warm glycerol gelatin and let air-dried for overnight. Digital images were recorded on a Zeiss Axiovert confocal microscope.

F.3. Results

The EAhy-926 cell line was grown to confluent monolayers on microscope slides to simulate the endothelium lining of blood vessels. It is a hybrid of HUVEC and human lung carcinoma cell lines, and thus, it was likely to be less physiologically relevant experimental model than the HUVEC line. However, EAhy-926 cell line was chosen as the pilot model mainly because it was much easier to cultivate than the HUVECs. CellTracker™ Green-labeled MDA-MB-231s were incubated with EAhy-926 monolayers for 3 h, which were subsequently fixed and fluorescently stained for β-catenin. The 3 hour time point was chosen because our previous lab data (not shown) indicated that it was sufficient amount of time for ensuring the detached tumor cells had firmly adhered to the endothelium. The confocal microscopy image (Figure F.1A) showed the presence of β-catenin (stained red) in the membranes of EAhy-926s, which had formed a confluent monolayer. In addition, the localization of MDA-MB-231 tumor cells (stained green) to tricellular corners of the monolayer was also observed (white arrows, Figure

Figure F.1A. Tumor cell localization at tri-endothelial cellular junctions. CellTracker™ Green-labeled MDA-MB-231s were incubated with EAhy-926 monolayers for 3 h. A confluent monolayer of EAhy-926s was formed as indicated by β-catenin (stained red) in the cellular membranes. The localization of MDA-MB-231 tumor cells (stained green) to tricellular corners of the monolayer was observed (white arrows).

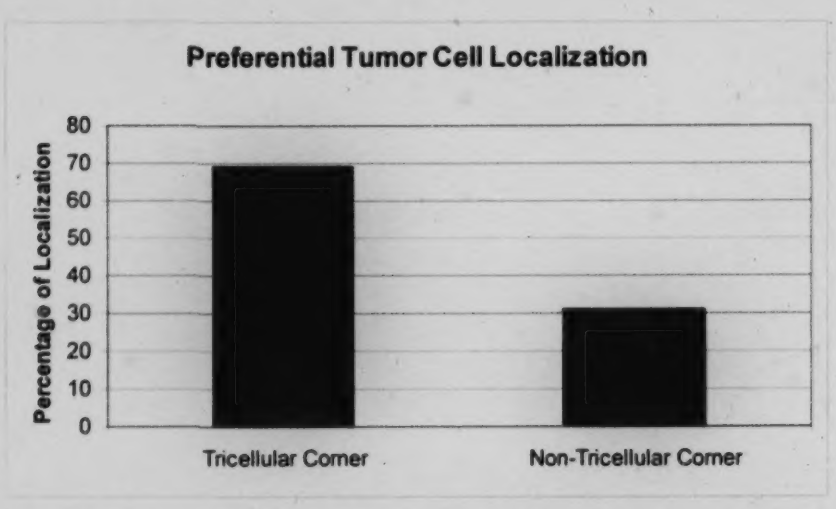

Figure F.1B. Preferential localization of tumor cells to tri-endothelial cellular junctions. Several microscopic fields were quantified for the extent of tricellular corner localization of tumor cells. Out of the total 384 tumor cells analyzed in those fields, 264 (69%) of them were localized to tricellular corners.

F.1A). Several microscopic fields were quantified for the extent of tricellular corner localization of tumor cells. Out of the total 384 tumor cells analyzed in those fields, 264 (69%) of them were localized to tricellular corners (Figure F.1B).

F.4. Discussion and Conclusion

It has been suggested that inflammatory processes may help to establish a favorable environment for malignancy development[159]. For example, inflammatory mediators (i.e. cyclo-oxygenase-2) and cytokines (i.e. prostaglandins) are up-regulated during inflammation, which can consequently suppress cell-mediated immune responses and promote angiogenesis[159]. Furthermore, chronic inflammation may lead to the production of reactive oxygen species and metabolites within affected cells[159]. These conditions can induce DNA damage, which may result in carcinogenesis[159]. In fact, correlations between inflammatory diseases and malignancy have been documented in various settings[160]. For instance, patients with rheumatoid arthritis or Sjogren's syndrome (systemic sclerosis with pulmonary fibrosis) may have increased risk of cancer and malignancy developments[160]. Therefore, there seems to be some relationship between inflammation and cancer.

Interestingly, the steps involved in metastatic extravasation seem to parallel those for leukocyte extravasation during inflammation (Figure 6A)[17, 18]. In an acute inflammatory reaction, circulating leukocytes first loosely adhere to and "roll"

along the endothelium that lines the site of tissue injury[19]. As leukocytes slow down within the circulation, they can interact with endothelial ICAM-1 to help establish firm contacts between the two cell types[21, 24, 27]. Arrested leukocytes will then preferentially localize to tri-endothelial cellular junctions, sites where borders of three endothelial cells meet[18]. A distinctive characteristic of tricellular corners is their absence or discontinuous nature of tight junctions (TJ) and adherens junctions (AJ)[153]. Therefore, there is increased focal permeability at these locations[20]. Tight junctions are not only involved in macromolecular permeability regulation, they are also the first barriers that transmigrating leukocytes must pass through[154, 155]. As a result, previous studies have shown that leukocyte transmigration occurs mainly at tricellular corners (~75%), while only a minority of them (~25%) will travel through tight junctions in between two endothelial cells[20]. Even more interestingly, the preference for migration at these corners persists (70%) under *in vitro* fluid-flow conditions resembling physiological blood flow[156]. Although the precise signal that directs leukocytes to tricellular corners is unknown, it has been suggested that adhesion molecules or chemotactic factors of endothelial cells are involved[20]. For example, *in vitro* immunofluorescence studies have revealed the redistribution of ICAM-1 on endothelial cells from the apical surfaces to intercellular junctions after prolonged TNF-α cytokine treatment[20]. The increased ICAM-1 density at intercellular junctions may serve to attract leukocytes to, and subsequently facilitate their transendothelial migration at these sites[20, 26, 157].

In molecular mimicry to leukocyte extravasation, it was first demonstrated by our lab that the extracellular domain of MUC1 on tumor cell surfaces could bind to ICAM-1[34, 35]. In subsequent work, we have found that MUC1 can mediate breast tumor cell adhesion to a simulated blood vessel wall under shear flow conditions equivalent to physiological blood flow[36]. The process of tumor cells firmly attaching to the endothelium has also been suggested to be mediated, at least in part, by ICAM-1 expressed on endothelial cells[17]. Based on the parallels found between the early steps in leukocyte and tumor extravasation, we were interested to determine whether tumor cells would also localize to tri-endothelial cellular junctions for subsequent transendothelial migration as seen with the leukocyte transmigration model. MDA-MB-231 cells incubated with EAhy-926 monolayers that were grown on microscope slides were analyzed via confocal microscopy (Figure F.1A). Tumor cells (stained green as indicated by white arrows, Figure F.1A) were seen to be capable of localizing to junctions where three endothelial cell membranes (stained red) meet. In fact, it was found that the majority of tumor cells (69%) were localized to tricellular corners upon quantification (Figure F.1B). Therefore, the preliminary results suggested that tumor cells had preferentially localized to tri-endothelial cellular corners following firm attachments to EAhy-926 monolayers. This would further indicate the resemblance of metastatic tumor cell extravasation to the leukocyte inflammatory transmigration model. However, more experimental trials, as well as replicating the experimental conditions with HUVEC monolayers would be required to validate these early findings.